

NUMERICAL MODELING OF COLD-FORMED STEEL SHEATHED SHEAR
WALLS UNDER LATERAL LOADING

A THESIS SUBMITTED TO
THE GRADUATE SCHOOL OF NATURAL AND APPLIED SCIENCES
OF
MIDDLE EAST TECHNICAL UNIVERSITY

BY

YAĞMUR TOPÇUOĞLUGİL

IN PARTIAL FULFILLMENT OF THE REQUIREMENTS
FOR
THE DEGREE OF MASTER OF SCIENCE
IN
CIVIL ENGINEERING

NOVEMBER 2019

Approval of the thesis:

**NUMERICAL MODELING OF COLD-FORMED STEEL SHEATHED
SHEAR WALLS UNDER LATERAL LOADING**

submitted by **YAĞMUR TOPÇUOĞLUGİL** in partial fulfillment of the requirements for the degree of **Master of Science in Civil Engineering Department, Middle East Technical University** by,

Prof. Dr. Halil Kalıpçılar
Dean, Graduate School of **Natural and Applied Sciences**

Prof. Dr. Ahmet Türer
Head of Department, **Civil Engineering**

Prof. Dr. Eray Baran
Supervisor, **Civil Engineering, METU**

Examining Committee Members:

Prof. Dr. Cem Topkaya
Civil Engineering, METU

Prof. Dr. Eray Baran
Civil Engineering, METU

Prof. Dr. Kağan Tuncay
Civil Engineering, METU

Prof. Dr. Özgür Kurç
Civil Engineering, METU

Assoc. Prof. Dr. Saeid Kazemzadeh Azad
Atılım University

Date: 27.11.2019

I hereby declare that all information in this document has been obtained and presented in accordance with academic rules and ethical conduct. I also declare that, as required by these rules and conduct, I have fully cited and referenced all material and results that are not original to this work.

Name, Surname: Yağmur Topçuoğlugil

Signature:

ABSTRACT

NUMERICAL MODELING OF COLD-FORMED STEEL SHEATHED SHEAR WALLS UNDER LATERAL LOADING

Topçuoğlugil , Yağmur
Master of Science, Civil Engineering
Supervisor: Prof. Dr. Eray Baran

November 2019, 123 pages

Cold-formed steel (CFS) structural systems have been used increasingly in seismically active regions. Shear walls consisting of CFS framing and sheathing panels constitute one type of lateral force resisting system for such CFS framed buildings. The purpose of this study is to develop an efficient numerical model to predict the lateral load response of shear walls that are framed with CFS profiles and sheathed with oriented strand board (OSB) panels. Numerical modeling of shear walls was conducted in OpenSees platform. Fastener-based approach incorporating nonlinear fastener model for screw connections was adopted. Screw connections were modeled by using a special hysteretic material model capable of softening, strength degradation, and cyclic pinching called as Pinching4. Parameters required to define this hysteretic model were based on a series of monotonic and cyclic loading tests conducted on OSB-to-CFS screw connections. Additionally, a complementary test program was carried out on OSB specimens to determine the in-plane shear properties of OSB sheathing panels. Shear wall model was verified with full-scale experimental data in terms of strength, stiffness and pinching characteristics. Then, a parametric study by utilizing the verified model was conducted in order to investigate the influence of various parameters such as local fastener behavior, fastener spacing, rigidity of stud-track connection, stiffness of CFS framing members, stiffness of hold-down members

and the level of gravity loading on overall wall response. Seismic force modification (R) factors, including ductility related force modification factor (R_{μ}) and overstrength related force modification factor (R_{Ω}), were calculated by using the bilinear force-displacement response determined from the numerically determined hysteretic response of several shear walls following the Equivalent Energy Elastic-Plastic (EEEP) approach.

Keywords: Cold-Formed Steel, CFS Shear Wall, Thin-Walled Structures, Cyclic Response, Fastener-Based Approach

ÖZ

HAFİF ÇELİK PROFİLLERDEN OLUŞTURULMUŞ KAPLAMALI DUVAR PANELLERİNİN NUMERİK OLARAK MODELLENMESİ

Topçuoğlugil , Yağmur
Yüksek Lisans, İnşaat Mühendisliği
Tez Danışmanı: Prof. Dr. Eray Baran

Kasım 2019, 123 sayfa

Hafif çelik yapısal sistemlerin sismik olarak aktif bölgelerde kullanımı günden güne artmaktadır. Hafif çelik çerçeve elemanları ve kaplama panellerinden oluşan perde duvarlar, bu tür yapılarda kullanılan yatay yük taşıyıcı sistemlerden bir tanesidir. Bu çalışmanın amacı, hafif çelik profillerle çerçevelenmiş ve yonga levha plakalarla kaplanmış olan perde duvarların yatay yük altındaki davranışını belirlemek için bir sayısal model geliştirmektir. Duvar numunelerinin monotonik ve tersinir tekrarlı yüklemeler altında gösterdiği karmaşık davranışın sayısal olarak modellenmesi için OpenSees platformu kullanılmıştır. Duvar deneylerinde gözlemlenen deformasyon ve göçme mekanizmalarının çoğunlukla yonga levha plaka ile hafif çelik profiller arasında kullanılan bağlantı vidalarında meydana gelmesi üzerine, yatay duvar davranışının büyük ölçüde bu vidalar tarafından kontrol edildiği sonucuna varılmıştır. Bağlantı vidalarının duvar davranışı üzerindeki etkisi sayısal model oluşturulurken de dikkate alınmıştır. Sayısal duvar modelinin perde duvar elemanlarının davranışını doğru bir şekilde temsil edebilmesi için en önemli hususlardan bir tanesi bağlantı vidalarında kullanılan malzeme modelinin vidaların tekil davranışını gerçekçi olarak yansıtır olmasıdır. Vida bağlantılarının modellenmesinde Pinching4 isimli özel bir histeretik malzeme modeli kullanılmıştır. Bu histeretik modeli tanımlamak için gereken parametreler, yonga levha ile hafif çelik

vida bağlantıları üzerinde yapılan bir dizi monotonik ve tekrarlı yükleme testlerinden elde edilmiştir. Ayrıca yonga levha plakaların düzlem için kesme dayanımını belirlemek amacıyla ilave bir test programı yürütülmüştür. Duvar modeli sonuçları duvar teslerinden elde edilmiş sonuçlarla karşılaştırılarak doğrulanmıştır. Daha sonra OpenSees modeli vida aralığı, çerçeve bağlantılarının rijitliği, hafif çelik profillerin kalınlığı, çekme tutucu elemanların rijitliği ve uygulanan düşey yük miktarı gibi parametrelerin genel duvar modeli davranışına etkisini anlamak amacıyla kullanılmıştır. Duvar sayısal modellerinden elde edilen çevrimsel yük-deformasyon eğrileri Eşdeğer Enerji Elastik-Plastik (EEEP) yaklaşımı kullanılarak çift doğrusal davranışa dönüştürülmüş ve bu davranış kullanılarak duvarların taşıyıcı sistem davranış katsayıları belirlenmiştir.

Anahtar Kelimeler: Hafif Çelik, Hafif Çelik Duvar Panelleri, İnce Cidarlı Yapılar, Tersinir Tekrarlı Yükleme Davranışı, Bağlantı Elamanı Bazlı Model Yaklaşımı

To my beloved mom, Münevver Semen...

ACKNOWLEDGEMENTS

I would like to express my sincere gratitude to my supervisor Prof. Dr. Eray Baran for his endless support, patience and encouragement throughout this study. He was always there when I need and helped me a lot with his broad knowledge and experience. It was a great opportunity to work with him.

I would like to thank to my Prof. Dr. Cem Topkaya for his suggestions and contributions. His recommendations were very valuable and they made this study much better.

I would like to express my special thanks to my dearest instructors, Dr. Engin Karaesmen and Dr. Erhan Karaesmen. I feel lucky to have met them who have an amazing teaching spirit. They taught me something more than engineering. I am also grateful to Prof. Dr. Ayşegül Askan Gündoğan for her motivations and contributions on my engineering background.

One of the biggest thanks belongs to my dearest colleague and beloved husband, Gökberk Işık. We have been always a strong team together from the very first day of this journey. All the memories we shared were extremely beautiful and his contributions in my collage life were inestimable.

I would like to thank my sister Özge Topçuoğlugil for her encouragements and friendship. I also would like to thank my second family, Gökçen Işık and Orhan Işık for their support.

I am grateful to my friends; Ece Döner, Ezgi Çınar, Bengi Alp, Çisil Torgay and Ezgi Dağdeviren for their presence in my life. Their friendship means a lot.

I would also like to thank Destek Engineering Ankara Team for their support and being such a great team! They made a large part of a day in the office very enjoyable.

I would like to thank my beloved cat and sweetest family member, Bıcırık. We have grown together and shared 14 years together. While everyone was sleeping, he was the only one staying awake with me in my sleepless nights before exams. If he was still here, he would be the happiest about my graduation and the end of those boring nights.

Even if I put all elegant words here, I can't sufficiently express my gratitude to my well-beloved mom, Münevver Semen. She became not only a mother but also a father and best friend to me with her unconditional love and endless support. I owe everything to her and she is the best thing that ever happened to me.

This research is supported by the Scientific and Technological Research Council of Turkey (TÜBİTAK) under grant number 115M234.

TABLE OF CONTENTS

ABSTRACT	v
ÖZ	vii
ACKNOWLEDGEMENTS.....	x
TABLE OF CONTENTS	xii
LIST OF TABLES.....	xv
LIST OF FIGURES	xvi
CHAPTERS	
1. INTRODUCTION.....	1
1.1. General Overview	1
1.2. Research Aim and Scope	3
1.3. Thesis Outline	4
2. LITERATURE SURVEY	7
2.1. Overview of Stud-Sheathing Connection Behavior.....	7
2.2. Overview of the Numerical Modeling of CFS Shear Walls	11
3. SUMMARY OF CFS SHEAR WALL EXPERIMENTS	19
3.1. Introduction.....	19
3.2. Wall Panel Tests.....	19
3.2.1. Test Specimens, Test Setup and Instrumentation.....	19
3.2.2. Observed Deformation Modes	24
3.2.3. Discussion of Test Results	25
3.3. Hold Down Tests	27
4. FASTENER TEST PROGRAM	31

4.1. Introduction	31
4.2. Test Specimens, Test Setup and Instrumentation.....	32
4.3. Test Results	36
4.3.1. Test Group 1	37
4.3.2. Test Group 2	40
4.3.3. Comparison with Previous Tests in Literature	42
5. OSB TEST PROGRAM	45
5.1. Introduction	45
5.2. Test Setup and Instrumentation.....	46
5.3. Calculation of Shear Properties	47
5.4. Test Results and Discussion	49
6. NUMERICAL MODELING OF SHEAR WALLS	55
6.1. Introduction	55
6.2. Description of Shear Wall Numerical Model.....	58
6.2.1. Hold-Down Material Model	60
6.2.2. Fastener Material Model.....	61
6.2.3. Multi-Panel Wall Models.....	66
6.3. Wall Model Results	68
6.3.1. Investigation of Local Fastener Response	68
6.3.2. Comparison of Numerically Predicted and Measured Wall Response	74
Wall Model 3.....	74
Wall Model 4.....	77
Wall Model 8.....	81
Wall Model 18.....	83

Wall Model 24	87
Wall Model 37	89
7. PARAMETRIC STUDY	93
7.1. Effect of Local Fastener Behavior	93
7.2. Effect of Fastener Spacing	95
7.3. Effect of Hold-Down Stiffness	99
7.4. Effect of CFS Framing Member Stiffness	100
7.5. Effect of Stud-Track Connection Rigidity	103
7.6. Effect of Gravity Load Level	104
7.7. Effect of Modeling Approach of OSB Panels.....	105
8. SEISMIC EVALUATION OF CFS SHEAR WALLS	109
8.1. Conceptual Background and Definitions	109
8.2. Idealization of Capacity Curve	111
8.3. Determination of Seismic Response Modification Factor	113
9. CONCLUSION	117
REFERENCES	119

LIST OF TABLES

TABLES

Table 4.1 Basic fastener test matrix	33
Table 4.2 Monotonic test results of Test Group 1	38
Table 4.3 Cyclic test results of Test Group 1	40
Table 4.4 Monotonic test results of Test Group 2.....	41
Table 4.5 Cyclic test results of Test Group 2.....	42
Table 4.6 Parameters of screw tests from this study, Fiorino et al. (2007) and Peterman and Schafer (2013)	42
Table 5.1 Parameters used in OSB test specimens	46
Table 5.2 Calculated in-plane shear strength values	52
Table 5.3 Calculated in-plane shear modulus values	52
Table 5.4 Test results for edgewise shear of wood sheathing panels (Boudreault, 2005)	53
Table 5.5 OSB test results (Iuorio et al., 2014).....	53
Table 6.1 CFS shear wall model matrix.....	56
Table 6.2 Material and geometric properties assigned to framing members in shear wall numerical models	60
Table 6.3 Hold-down tension stiffness values used in shear wall numerical models	61
Table 6.4 Pinching4 backbone parameters for monotonic material model.....	63
Table 6.5 Pinching4 backbone parameters for cyclic material model	64
Table 8.1 Response modification factors for wall models.....	116
Table 8.2 Statistical properties of response modification factors	116
Table 8.3 R factor values proposed by different building codes.....	117

LIST OF FIGURES

FIGURES

Figure 1.1 CFS structural systems	1
Figure 1.2 Components of a typical CFS shear wall	2
Figure 2.1 Wallboard-fastener connection test setup used by Miller and Pekoz (1994)	8
Figure 2.2 Test specimen details used by Okasha (2004)	9
Figure 2.3 Specimen details used by Fiorino et al. (2007): (a) test setup; (b) displacement transducers	10
Figure 2.4 (a) Comparison of experimental and numerical results (b) comparison of experimental and numerical results in terms of shear strength (c) comparison of experimental and numerical results in terms of energy dissipation.....	13
Figure 2.5 Numerical models developed in Opensees by (Shamim et al., 2013): (a) original model; (b) model modified based on experimental data	14
Figure 2.6 Implementation of fastener-based model response into equivalent brace model (Leng et al., 2017).....	15
Figure 2.7 Details of shear wall numerical model by Buonopane et al. (2015): (a) details of fasteners and support; (b) general layout of shear wall	17
Figure 2.8 Details of shear wall modeling by Padillo (2015): (a) shear wall model layout and fastener material model; (b) comparison of shear wall model results with and without stud buckling; (c) comparison of predicted response and experimental data.....	18
Figure 3.1 Cold-formed steel profile used in shear wall test specimens	20
Figure 3.2 Details of a single panel shear wall specimen.....	20
Figure 3.3 Details of wall panel setup (Pehlivan et al., 2018).....	21
Figure 3.4 Displacement history of CUREE cyclic loading protocol	22
Figure 3.5 Two- and four-panel shear wall specimens.....	23

Figure 3.6 Hold down elements used in shear wall numerical models.....	24
Figure 3.7 Deformation modes observed in wall panel tests: (a) Tilting of screws and uplift of the base; (b) Stud buckling.....	25
Figure 3.8 Load-displacement response of Wall Test 3.....	26
Figure 3.9 Details of hold down specimens: (a) relation between shear wall and hold down specimen; (b) hold down specimen dimensions; (c) position of hold down element in specimen (Pehlivan et al., 2018)	27
Figure 3.10 Setup used for testing of hold down specimens (Pehlivan et al., 2018)	28
Figure 3.11 Load-deformation response of various hold down devices (Pehlivan et al., 2018).....	29
Figure 4.1 Difference in deformation modes of OSB sheathing and CFS frame	32
Figure 4.2 Details of fastener test specimens and test setup.....	34
Figure 4.3 Displacement history of CUREE cyclic loading protocol.....	35
Figure 4.4 Calculation of reference displacement based on monotonic load-displacement response.....	36
Figure 4.5 (a) Undeformed screws before load testing, (b) Tilting of screws, (c) Screw pull-through, (d) Breaking of sheathing edge	37
Figure 4.6 Load-displacement curves of Test 1-5.....	38
Figure 4.7 Load-displacement curves of Test 6-8.....	39
Figure 4.8 Load-displacement curves of Test 9-13.....	40
Figure 4.9 Load-displacement curves of Test 14-16.....	41
Figure 4.10 Load-displacement curves of Test Group 1 from this study and tests conducted by Fioriono et al. (2006) and Peterman and Schafer (2013).....	44
Figure 5.1 OSB test setup	47
Figure 5.2 Dimensions of OSB panel test specimens	48
Figure 5.3 Deformed OSB panel specimen.....	49
Figure 5.4 Load-displacement results of all 22 specimens	50
Figure 6.1 Displacement history of CUREE cyclic loading protocol.....	57
Figure 6.2 General layout of the OpenSees CFS shear wall model.....	58

Figure 6.3 Load-displacement results of hold down devices HD-4, HD-7 and HD-8	61
Figure 6.4 OpenSees Pinching4 model definition	62
Figure 6.5 Fastener material models for monotonic loading.....	63
Figure 6.6 Cyclic fastener material model based on experimental data	64
Figure 6.7 Cyclic fastener model calibration.....	66
Figure 6.8 General layout of two- and four-panel shear walls	68
Figure 6.9 Similarity between fastener material model and overall shear wall response	69
Figure 6.10 (a) Screw material model (mono-5) showing Stages 1-4 (b) Wall model response divided into 20 time steps (c) Stage of fasteners at each time step	71
Figure 6.11 Vector plot of forces on fasteners at three different levels: (a) elastic range; (b) peak lateral load; (c) maximum drift.....	74
Figure 6.12 Axial forces in studs at peak lateral load.....	74
Figure 6.13 Load-displacement responses of shear wall test 3 and model 3	76
Figure 6.14 Comparison of test 3 and model 3 results through main cycles.....	77
Figure 6.15 Comparison of test 3 and model 3 results through stiffness curves	78
Figure 6.16 Comparison of test 3 and model 3 results through energy curves	78
Figure 6.17 Load-displacement responses of shear wall test 4 and model 4	79
Figure 6.18 Comparison of test 4 and model 4 results through main cycles.....	80
Figure 6.19 Comparison of test 4 and model 4 results through stiffness curves	81
Figure 6.20 Comparison of test 4 and model 4 results through energy curves	81
Figure 6.21 Load-displacement responses of shear wall test 8 and model 8	82
Figure 6.22 Comparison of test 8 and model 8 results through main cycles.....	83
Figure 6.23 Comparison of test 8 and model 8 results through stiffness curves.	84
Figure 6.24 Comparison of test 8 and model 8 results through energy curves	84
Figure 6.25 Load-displacement responses of shear wall test 18 and model 18	85
Figure 6.26 Comparison of test 18 and model 18 results through main cycles.....	86
Figure 6.27 Comparison of test 18 and model 18 results through stiffness curves ...	87
Figure 6.28 Comparison of test 18 and model 18 results through energy curves	87

Figure 6.29 Load-displacement responses of shear wall test 24 and model 24	88
Figure 6.30 Comparison of test 24 and model 24 results through main cycles	89
Figure 6.31 Comparison of test 24 and model 24 results through stiffness curves ...	90
Figure 6.32 Comparison of test 24 and model 24 results through energy curves.....	90
Figure 6.33 Load-displacement responses of shear wall test 37 and model 37	91
Figure 6.34 Comparison of test 37 and model 37 results through main cycles	92
Figure 6.35 Comparison of test 37 and model 37 results through stiffness curves ...	93
Figure 6.36 Comparison of test 37 and model 37 results through energy curves.....	93
Figure 7.1 Selected fastener tests and their material models	96
Figure 7.2 Comparison of wall model responses including different material models	96
Figure 7.3 Load-displacement response of wall models having various fastener spacing	98
Figure 7.4 Relationship between number of fasteners and load capacity of wall panel	98
Figure 7.5 (a) Screw material model (mono-5) showing Stage 1-4 (b)Wall model responses divided into 20 time steps (c)Stages of fasteners at each step.....	101
Figure 7.6 Load-displacement response of wall models having various hold-downs	103
Figure 7.7 Load-displacement response of wall models having CFS with various thicknesses	104
Figure 7.8 Effect of CFS thickness on fastener response (Peterman and Schafer, 2013)	105
Figure 7.9 Load-displacement responses of wall models with various stud-track connections.....	106
Figure 7.10 Load-displacement response of wall models applied various gravity load	107
Figure 7.11 CFS shear wall model layout with shell elements for OSB sheathing .	109
Figure 7.12 Load-displacement response of wall models having various OSB sheathing stiffnesses.....	110

Figure 8.1 Determination of design force by using ductility and overstrength factors 112

Figure 8.2 Backbone pushover curve of a cyclic model response..... 114

Figure 8.3 EEEP curve obtained from pushover curve of Wall Model 6..... 115

CHAPTER 1

INTRODUCTION

1.1. General Overview

The use of Cold-Formed Steel (CFS) structural systems has been gaining global popularity especially for low and mid-rise buildings during recent years (Figure 1.1). This type of structural systems offer the major advantages of high strength-to-weight ratio and reduced construction time. As a result of off-site production and on-site installation of CFS members, this method of construction takes advantage of controlled production and rapid construction. Thanks to the controlled environment of a factory, higher accuracy in dimensioning and flexibility in forming various cross-section shapes can be achieved. CFS members are also considered as environmental friendly products due to the recyclable nature of steel and reduced material waste in their manufacturing process.



Figure 1.1 CFS structural systems

CFS shear walls sheathed with panels are one of the main lateral load resisting components used in structural system. An example of a typical sheathed CFS wall panel is shown in Figure 1.2. Various material types can be used as a sheathing material for CFS shear walls. Oriented Strand Board (OSB), gypsum board, and steel sheets are the most common sheathing materials. Among these different sheathing materials, OSB panels are the most popular type due to their relatively low cost and favorable mechanical properties.

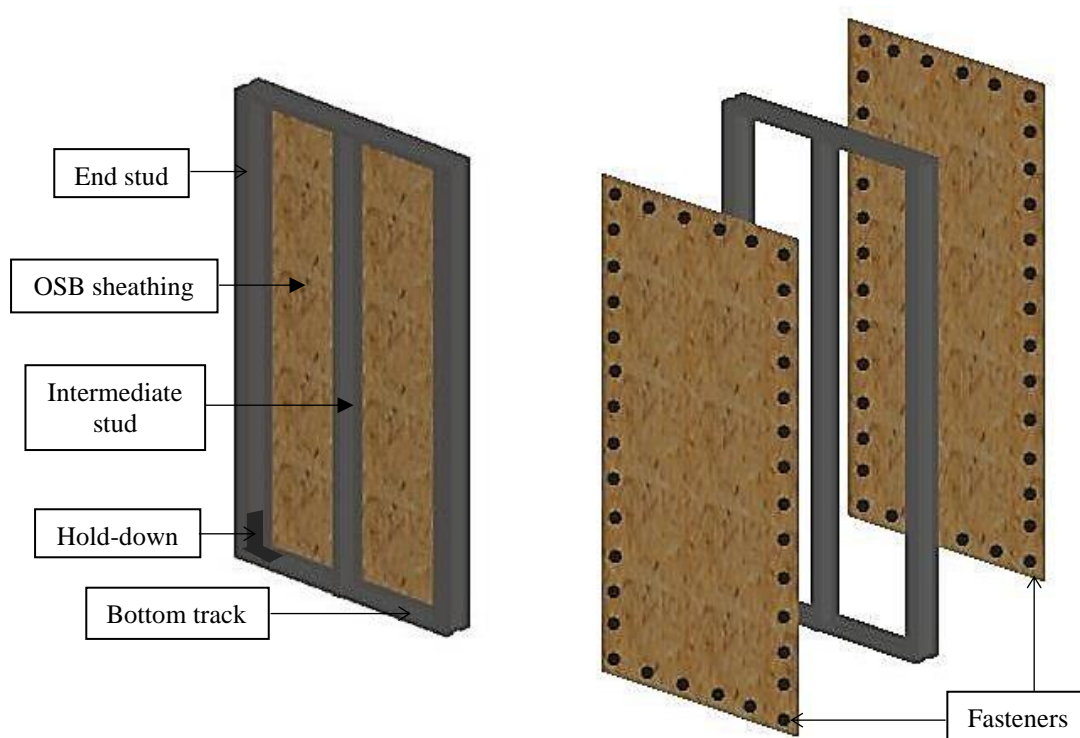


Figure 1.2 Components of a typical CFS shear wall

A typical CFS shear wall panel consists of CFS framing members, sheathing panels, and fasteners that provide connection between the sheathing panels and framing members. Vertical CFS framing members are called studs, while the horizontal members are called tracks. In a single CFS shear wall usually an intermediate stud is

placed between two end studs. End studs and intermediate studs are typically placed at 120 cm spacing. Stud-to-track connections are usually achieved by rivets or self-tapping screws. Depending on the lateral force demand exerted on wall panels single-sided or double-sided sheathing is provided. In conventional CFS shear walls sheathing panels are connected to the CFS framing members with self-tapping screws. Spacing of these screws is usually dictated by the lateral force demand on wall panels. Hold down devices are typically provided at the base of wall panels to transfer the tensile force developed in end studs as a result of lateral loading. These devices resist the uplift between the wall panel and the foundation. Additional shear anchors are provided between the bottom track and the foundation system along the wall length for the transfer of horizontal shear force.

1.2. Research Aim and Scope

Since the use of CFS structural systems in seismically active regions has been gaining popularity, there is a need for additional research about seismic performance of such systems. Seismic performance of this type of structures was overlooked until quite recently, but latest experimental studies provide insights into the response of such systems under seismic effects. The purpose of the current study is to develop an efficient numerical model to predict the lateral load response of shear walls that are framed by CFS profiles and sheathed with OSB panels. Numerical modeling of shear walls was conducted in OpenSees platform because of its high performance for simulating the seismic response of these type of structures.

Studies in literature indicate that fasteners used for CFS-to-OSB connections are the main energy dissipating elements and the behavior of CFS shear walls are highly influenced by the shear response of these fasteners (Henriques, 2017). Based on this observation, a fastener-based approach was adopted when creating the numerical model in the current study. In order to understand the behavior of these connections

and provide experimental data for modeling the local fastener response, fastener tests were conducted under monotonic and cyclic loading.

In an attempt to accurately predict the shear wall response, realistic fastener material models were constructed based on the measured fastener response. A special hysteretic material model capable of softening, strength degradation, and cyclic pinching available in OpenSees was utilized for modeling of screw connections. Rigid diaphragm assumption was used for the OSB panels in the numerical model developed for predicting the shear wall response. In order to investigate the validity of this assumption a complementary test program also was carried out. As part of this testing program in-plane strength and shear modulus of OSB panels were determined.

Results obtained from the numerical CFS shear wall model were validated by full-scale shear wall experiments in terms of strength, stiffness, and pinching characteristics. The verified numerical model was then used in a parametric study to further investigate the effect of fastener material model, stiffness of CFS frame members, number of fasteners, gravity loading on wall panel, rigidity of stud-track connection and stiffness of hold-down members.

1.3. Thesis Outline

This thesis is divided into nine chapters. The present chapter provides a brief information about CFS structural systems, shear walls utilized in these systems and general description of the current research.

In Chapter 2, a comprehensive literature review on various approaches of numerical modeling of CFS shear walls is provided. Moreover, related experimental studies on screw connections and OSB panels are summarized.

Chapter 3 summarizes the recently conducted experimental study on seismic performance of CFS shear walls at Middle East Technical University. Results of these

experiments were used to verify the numerical model developed as part of the current study.

Chapter 4 contains a description of the testing program on fasteners used between OSB panels and CFS framing members. The chapter includes information about test setup, instrumentation, loading protocol and testing program, as well as the obtained results.

Chapter 5 summarizes the complementary test program on in-plane shear behavior of OSB panels. The chapter includes information about test setup, instrumentation, loading protocol and testing program, followed by the method utilized to compute the shear strength and shear modulus using the measured data.

Chapter 6 describes the fastener-based numerical modeling of CFS shear walls in OpenSees platform. The adopted modeling approach and the details of element types and materials models are provided. A comparison of the predicted shear wall response with the response measured from full-scale CFS shear wall experiments is presented in terms of strength, stiffness, and pinching characteristics.

In Chapter 7, effects of various parameters such as the local fastener behavior, fastener spacing, rigidity of stud-track connection, stiffness of CFS framing members, stiffness of hold-down members and the level of gravity loading on overall wall response are discussed in detail.

Chapter 8 provides a seismic evaluation of CFS shear walls by proposing seismic force modification factors.

Chapter 9 concludes the thesis by providing highlights of the study and future recommendations.

CHAPTER 2

LITERATURE SURVEY

In this chapter previous experimental and numerical studies on CFS shear walls were reviewed. Firstly, stud-sheathing connection behavior was investigated through both experimental and numerical studies in literature. Since the fasteners providing connection between the CFS framing members and the OSB sheathing are the main energy dissipating elements, the wall response under lateral loading is highly influenced by the local response of these fasteners (Henriques 2017). For this reason an extensive literature review was provided on fastener response in order to thoroughly understand the connection behavior. Following the local fastener response, the studies available on the current literature on CFS shear wall numerical modeling was reviewed in detail.

Because timber framing has conventionally been used extensively for sheathed shear walls, majority of the earlier studies focused on timber framed shear walls with a wood-based sheathing material. This type of construction is similar to the CFS framed shear walls in terms of stud-sheathing connection behavior. Therefore, studies on light framed shear walls with timber studs form the foundation of the later studies investigating the behavior of CFS framed shear walls.

2.1. Overview of Stud-Sheathing Connection Behavior

There are numerous studies on local behavior of screw connections focusing on the analytical, experimental and numerical aspects. Early studies were aiming to determine racking strength of shear walls, which mainly depends on nail-wood connection behavior. Tuomi and McCutcheon (1978) developed a closed-form racking strength equation for light-frame plywood shear walls. The proposed equation

was validated by full-scale and small-scale shear wall experiments. McCutcheon (1985) presented a new theory in order to predict racking deformations in light framed and wood sheathed shear walls by using a method similar to the one developed by Tuomi and McCutcheon (1978). The method utilizes a nonlinear connection behavior in order to predict racking performance of wood sheathed shear walls.

Stewart (1987) was one of the pioneering researchers who worked on the investigation of seismic performance of plywood sheathed shear walls. The approach adopted in this study includes analytical modeling as well as an experimental program on full-scale plywood sheathed shear walls. Sheathing nails were considered as energy dissipating elements and a complementary experimental study was conducted on nailed joints under reverse cyclic loading. Analytical models validated with experimental findings demonstrated that shear wall strength and stiffness are directly affected by local response of nailed connections.

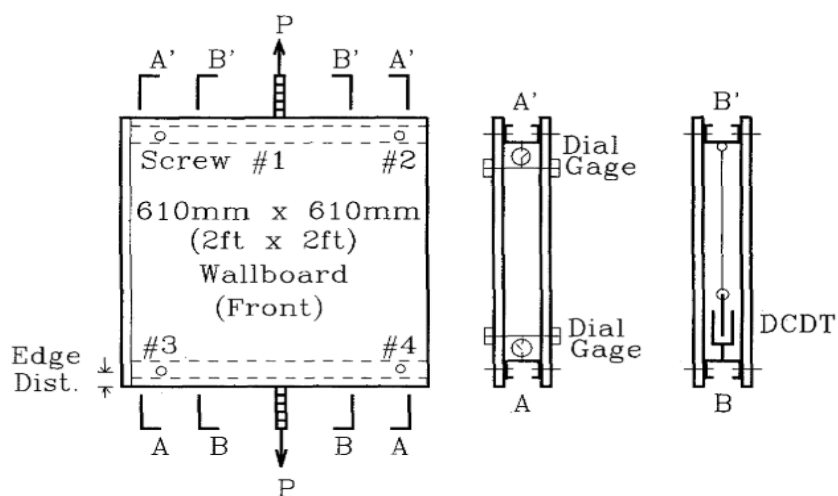


Figure 2.1 Wallboard-fastener connection test setup used by Miller and Pekoz (1994)

Miller and Pekoz (1994) tested connections between fasteners and gypsum boards by using a test setup including eight screws as shown in Figure 2.1. Test results revealed that fastener strength increases with wallboard thickness and screw edge distance.

Chui et al. (1998) presented a sophisticated finite element model including pinching behavior of nailed wood joints. The model results were verified with single-nailed joint tests under reversed cyclic loading. Fastener characteristics such as strength degradation, energy absorption and ductility were included in the finite element model.

Salenikovich (2000) carried out a detailed experimental study and analytical modeling in order to determine performance characteristics of light framed shear walls under lateral loading. In addition to full-scale shear wall tests, a series of tests were conducted on sheathing connections under monotonic loading using a test setup that is similar to previously used test setups.

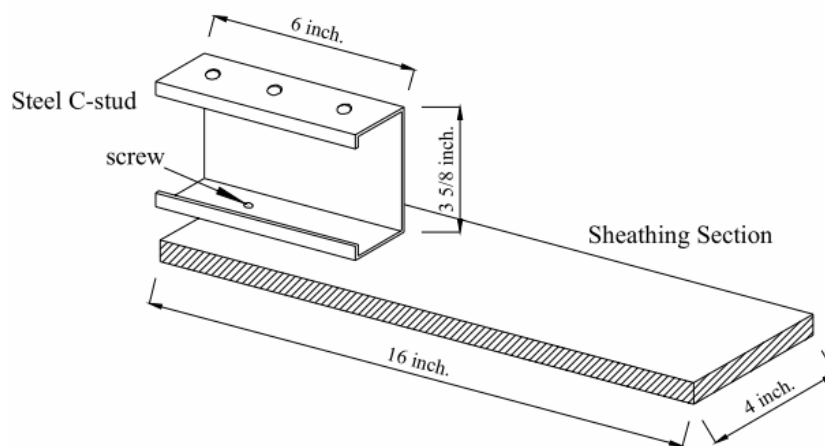


Figure 2.2 Test specimen details used by Okasha (2004)

To build a better understanding of the screw connection between steel frame and wood panel shear walls, Okasha (2004) performed monotonic and cyclic loading tests on 216 connection specimens similar to the one shown in Figure 2.2. For cyclic tests, the loading protocol proposed by the Consortium of Universities for Research in Earthquake Engineering (CUREE) (Krawinkler et al., 2000) was used. Test results showed that an increase in sheathing thickness and screw edge distance enhances the

connection capacity, stiffness and energy absorption. Sheathing orientation with respect to grains was found effective as well. It was also highlighted that a single screw behavior may differ from the behavior of a group of screw connections.

Fulop and Dubina (2004) focused on the local behavior of sheathing-framing screw connections. A series of tests was conducted on connections as well as on full-scale wall panels. Additional finite element analyses were also conducted in order to predict the wall panel response under lateral loading. The setup used for steel-to-steel and steel-to-OSB connection tests conducted in this study was similar to the setups previously used by other researchers.

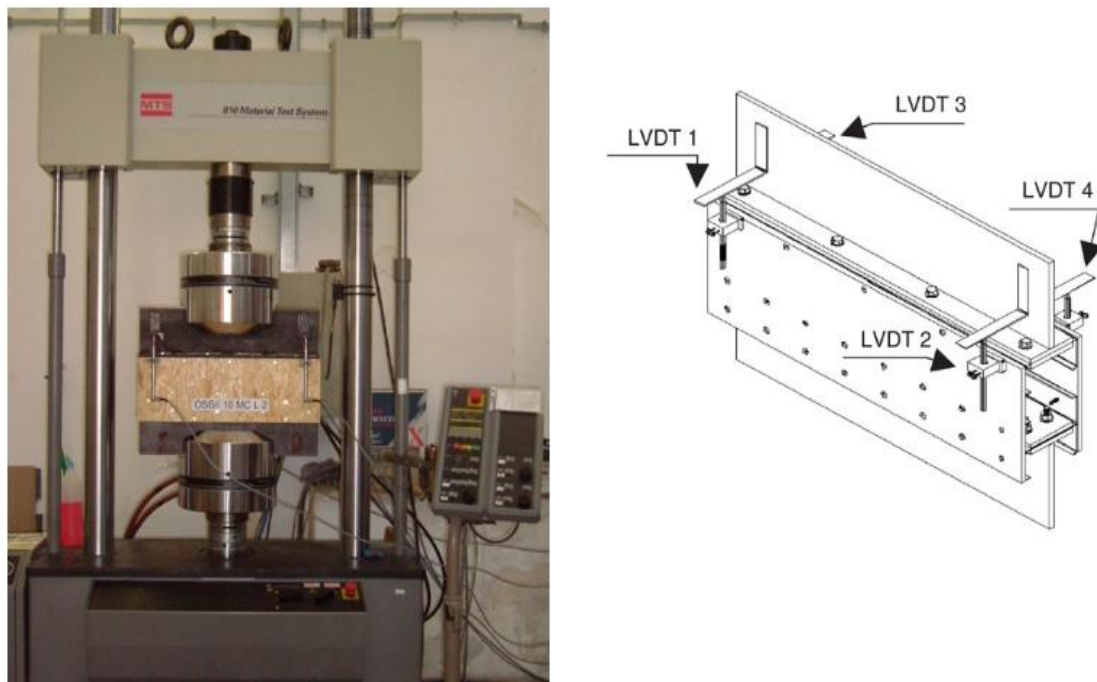


Figure 2.3 Specimen details used by Fiorino et al. (2007): (a) test setup; (b) displacement transducers

Fiorino et al. (2007) utilized an improved test setup for screw connection tests. As shown in Figure 2.3, their test setup included a group of screws instead of one single screw so that group effect can be incorporated. The authors demonstrated that

sheathing type has an important effect on screw connection behavior. They compared the local response of screws when used with OSB and GWB (Gypsum Wall Board) sheathings was compared and it was reported that OSB sheathing provides higher strength and absorbed more energy. Test results indicated that edge distance around screws has a direct effect on connection capacity. It was also reported that OSB orientation affects the screw response. Another finding from this study is that there is a significant reduction in connection capacity under cyclic loading when compared to monotonic loading. As part of another study the same researchers investigated the screw response with CP (Cement-based Panel) as sheathing material utilizing the same testing procedure (2008). The test results indicated that CP screw connections show higher stiffness compared to OSB but performed poorly terms of strength and energy absorption.

Vieira and Schafer (2009) conducted a series of connection experiments by using OSB and gypsum board as sheathing. Their test setup was similar to the ones used by Miller and Pekoz (1994) and Fiorino (2007). Effects of sheathing type, fastener spacing, edge distance, humidity and fastener overdriving were investigated under monotonic loading. Test results showed that OSB provides a higher shear capacity than gypsum boards by a wide margin. Authors stated that humidity decreases stiffness and strength. Overdriving of fasteners into the sheathing material resulted in an increase in stiffness and a decrease in strength. Edge distance was found to be an influential parameter in both strength and stiffness while fastener spacing has no significant effect on results. Similar conclusions were later reported by Peterman and Schafer (2013).

2.2. Overview of the Numerical Modeling of CFS Shear Walls

Numerical simulation of CFS shear walls has become an essential research subject in order to understand the behavior of these structural elements under lateral loading. A large number of numerical models have been developed throughout the past few decades. Usefi et al. (2019) divided the existing numerical modeling techniques into

two groups: micro modeling and macro modeling. In literature, macro modeling studies focused on efficient modeling which provides reduced computation time and effort while micro modeling aimed to provide a detailed analysis of local responses and more accurate results with FE methods. A comprehensive review of all of the analysis methods indicates that similar levels of accuracy can be achieved with both macro and micro modeling techniques.

One of the first hysteresis behavior models was developed by Bouc (1967) for general structures, which is called as Bouc-Wen-Baber-Noori (BWBN) model. Several researchers have contributed to the development of this model over the time by incorporating stiffness degradation, strength degradation and pinching capabilities. Foliente (1995) was one of them focusing on pinching behavior. He proposed a constitutive hysteresis model for wood joints and structural systems by modifying BWBN model and used it for nonlinear dynamic analysis of SDOF wood systems.

Stewart (1987) proposed a hysteresis model for wood framed plywood sheathed shear walls and presented the validation of this model with experimental data. The model had a single degree-of-freedom (SDOF) and was widely-used in early studies. Similarly, Dolan (1989) used an SDOF system including a hysteretic spring in order to obtain cyclic response of wood framed shear walls. Another hysteretic model for timber shear walls was presented by Folz and Filiatrault (2001) which includes rigid framing members, linear elastic sheathing material and nonlinear fasteners.

Fulop and Dubina (2002, 2004) and Dubina (2008) carried out experimental studies on full scale CFS framed wood sheathed shear walls and connections between steel framing members and sheathing. A trilinear hysteretic model was implemented in Drain-3DX for shear walls. Although their model can capture the overall shear wall response, it has a drawback that strength degradation is not taken into account.

As a part of a comprehensive research including both experimental and numerical studies on CFS shear walls, Della Corte et al. (2006) focused on seismic deformation demand by utilizing a mathematical model comprised of hysteresis response of shear

walls. This model does not consider strength and stiffness degradation. Figure 2.4 shows comparison of experimental and numerical results. It can be seen that shear strength was well predicted at the first loops. However, there is an overestimation in second and third loops due to lack of strength degradation capability of the model. In fact, overestimation in terms of dissipated energy increases as far as the shear panel approaches failure.

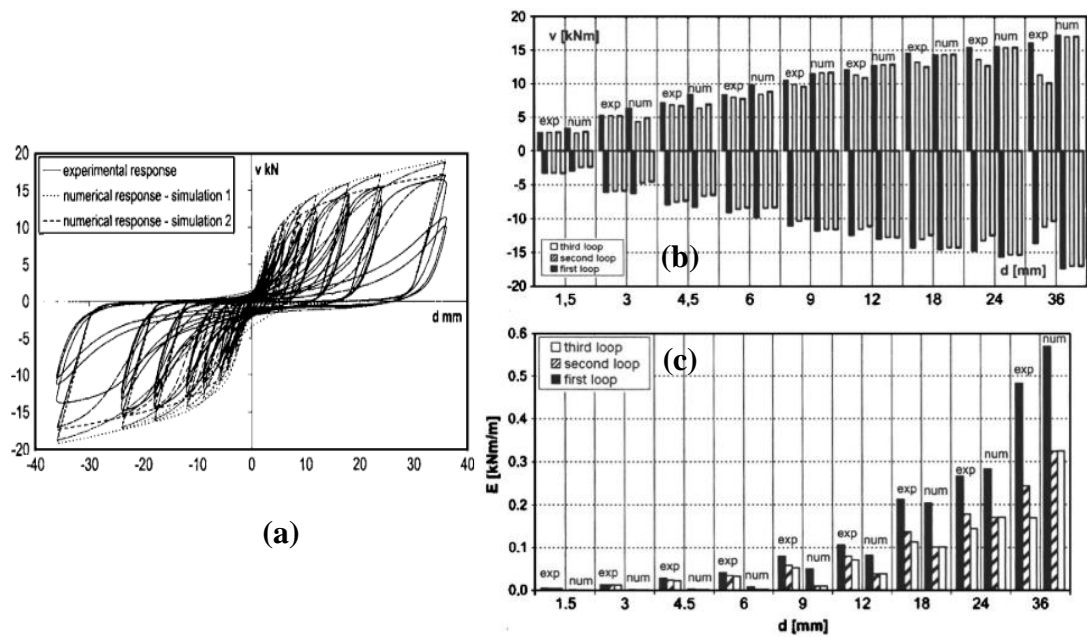


Figure 2.4 (a) Comparison of experimental and numerical results
 (b) comparison of experimental and numerical results in terms of shear strength
 (c) comparison of experimental and numerical results in terms of energy dissipation

Kim et al. (2007) conducted a shake table test on a one-bay two-story strap braced CFS structural system and developed a numerical model in Drain-2DX by using macro modeling techniques to predict the dynamic response accurately. Lee and Foutch (2010) introduced a similar model and studied two, four and six story prototype CFS buildings according to FEMA 355F assessment procedure.

Another extensive research study on seismic behavior of CFS framed shear walls was presented by Shamim (2012), Shamim and Rogers (2012) and Shamim et al. (2013)

at McGill University. Research includes dynamic shake table testing and numerical modeling of wood sheathed and steel sheathed CFS framed shear walls. Numerical models, shown in Figure 2.5, were developed in Opensees by using equivalent brace method and were calibrated with experimental data. Nonlinear hysteretic behavior of shear walls was incorporated in the numerical model by assigning Pinching4 material model to truss elements. The remaining components in the model, including CFS framing and floor framing between the first and second story walls were modeled as linear elements. Seismic performance of shear walls and the corresponding response modification factors (R) were evaluated based on FEMA P695 methodology.

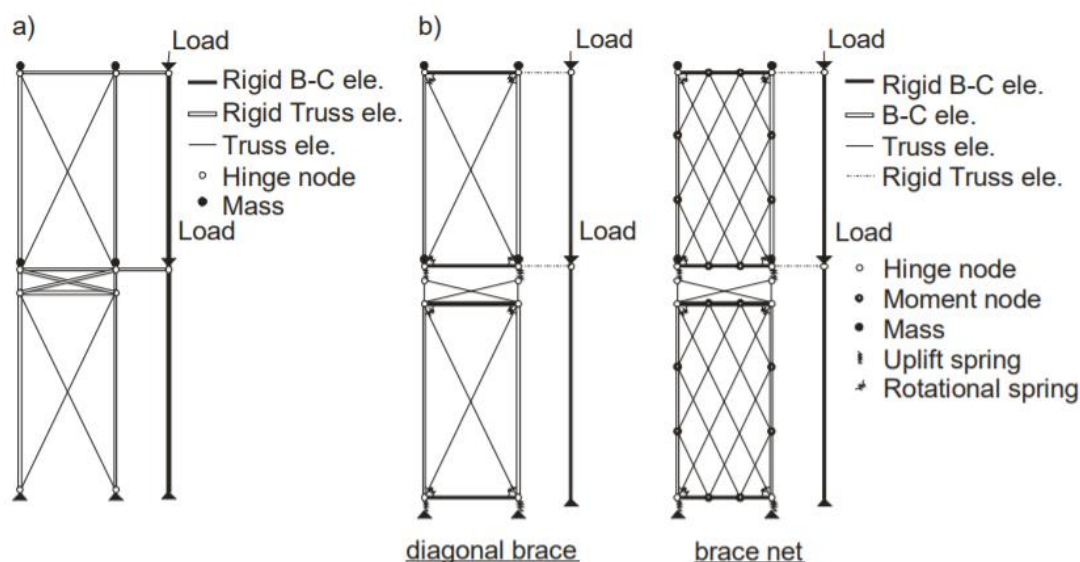


Figure 2.5 Numerical models developed in Opensees by (Shamim et al., 2013):
 (a) original model; (b) model modified based on experimental data

A two-story full-scale CFS building was tested on a shake table in 2013 as part of a National Science Foundation funded Cold-Formed Steel – Network for Earthquake Engineering Simulation (CFS-NEES) project. The lateral force resisting system of the test building consisted of OSB sheathed CFS framed shear walls. The CFS-NEES project was a comprehensive research including testing and numerical modeling of

individual members, shear walls and the full-scale building. Details of the investigations performed as part of this program are summarized by Schafer et al. (2016). Leng et al. (2012, 2013) provides an initial understanding of nonlinear lateral behavior of the CFS-NEES test building before shake table testing. Authors developed an Opensees model for the entire building. The Elastic Perfectly Plastic (EPP) idealization and Pinching4 approach for defining nonlinear shear wall response were compared and EPP was found inadequate. Displacement controlled pushover analysis and nonlinear time history analysis were performed based on FEMA P695 procedure and preliminary predictions were provided. The numerical model was later improved by Leng (2015) and Leng et al. (2017) in order to better simulate the experimentally determined response. The model was improved by utilizing fastener-based model as a surrogate modeling, which allows to predict shear wall response more accurately. Due to large size of the model, authors implemented fastener-based model response into nonlinear truss elements of equivalent brace model by using Pinching4, as illustrated in Figure 2.6.

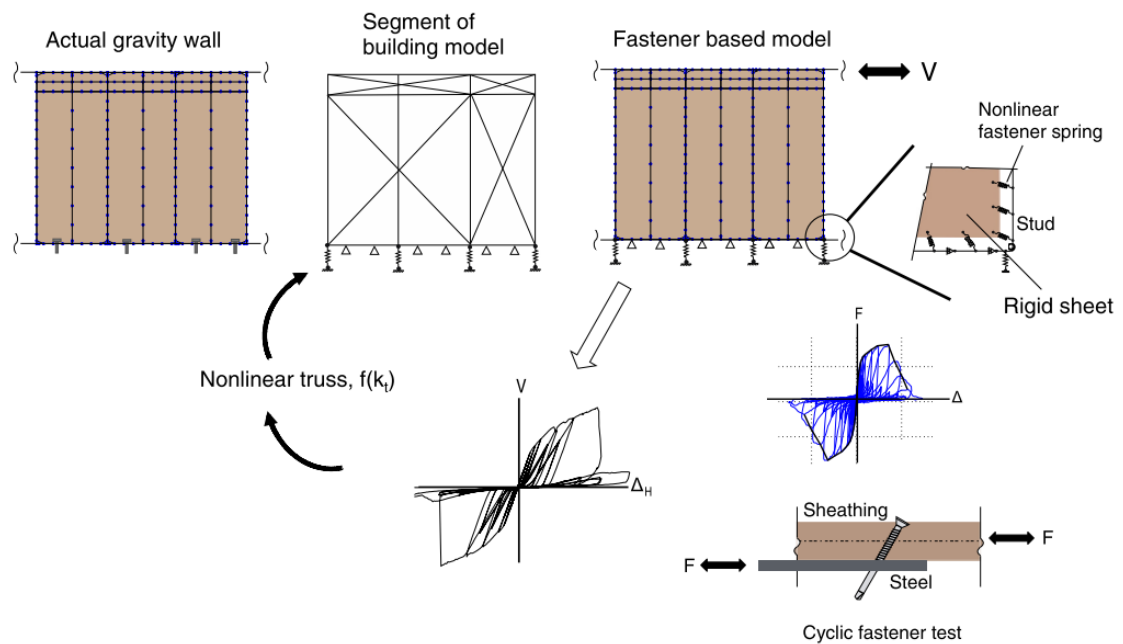


Figure 2.6 Implementation of fastener-based model response into equivalent brace model (Leng et al., 2017)

Fastener-based numerical modeling approach focuses on the screw connection between CFS framing and sheathing. To provide a hysteretic characterization of the stud-fastener-sheathing performance, the predefined Pinching4 hysteretic material model available in Opensees is frequently used. This material model accurately captures the hysteretic behavior of fasteners including stiffness and strength degradation. Behavior is defined with four positive and four negative points along the backbone curve, and additional parameters that define the pinched response during unloading/reloading phases (Peterman and Schafer 2013).

As companion to the CFS-NEES project, Tun (2014) and Buonopane et al. (2014) developed an Opensees shear wall model. The model comprised of rigid sheathing panels, beam-column elements for framing, semi-rigid rotational springs for stud-to-track connections, and vertical springs for hold-downs at wall base. Fastener spring elements connecting the sheathing to the CFS framing members were defined by using Pinching4 material model. Parameters required for the fastener material model were determined from fastener tests. The shear wall numerical model was validated with experimental data. Numerical model was analyzed under monotonic loading and comparison with cyclic experiments was done by using the measured backbone response. As an extension of these studies Buonopane et al. (2015) provided a more detailed investigation of framing members and individual fasteners. Axial force and bending moment diagrams of framing members were obtained. In order to visualize the magnitude and direction of the forces develop at fasteners, vector force diagrams were given for three different stages in the analysis which are elastic range, peak lateral force and peak lateral displacement.

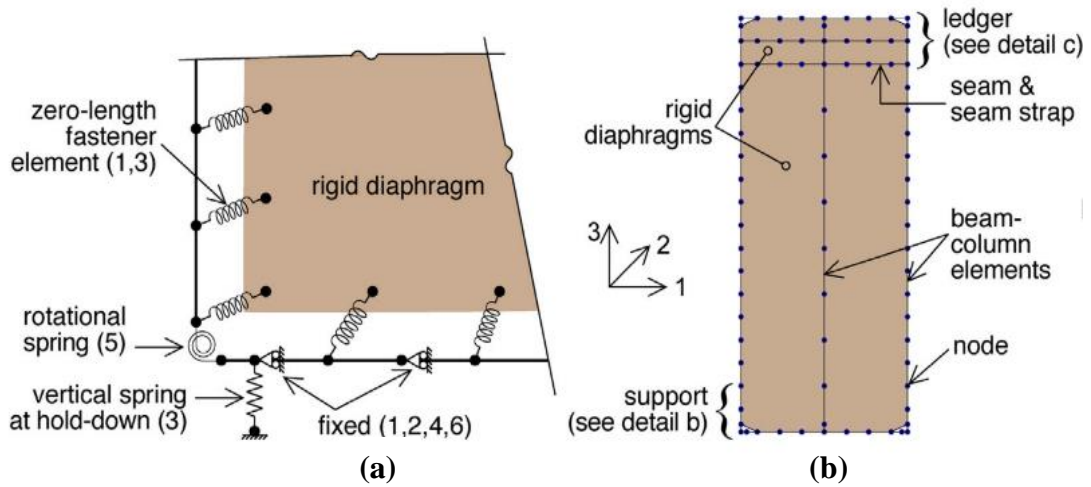


Figure 2.7 Details of shear wall numerical model by Buonopane et al. (2015):
 (a) details of fasteners and support; (b) general layout of shear wall

As part of the CFS-NEES project, fastener-based numerical models were developed by Bian et al. in Opensees (2014, 2015a, 2015b). The earlier model was capable of predicting lateral shear wall response as long as chord stud buckling or other limit states do not occur. Stud buckling limit state was later incorporated in the model so that the model can represent actual stud behavior. Pinching4 material model was used for stud behavior as well as fastener behavior. However, results showed that high level of gravity load is needed to switch the failure mode from fastener failure to stud buckling. Moreover, different shear wall and gravity wall combinations were also studied. It was demonstrated that gravity walls have a significant contribution to lateral performance of the building system.

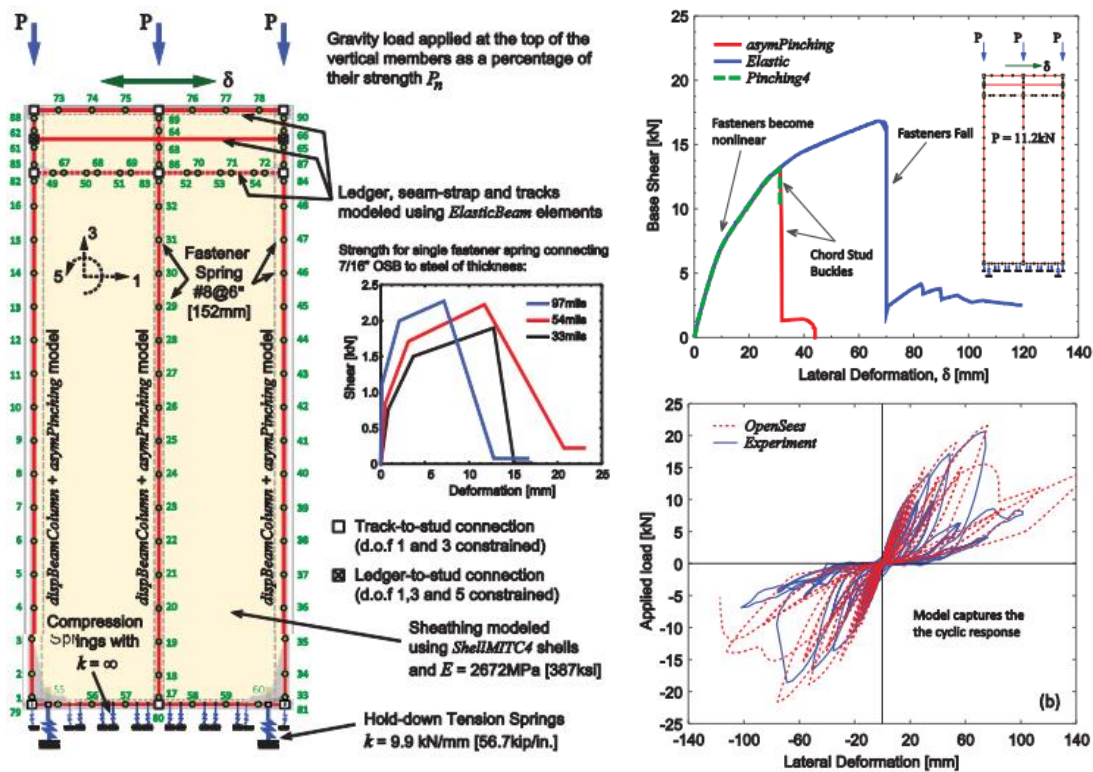


Figure 2.8 Details of shear wall modeling by Padillo (2015):

- (a) shear wall model layout and fastener material model;
- (b) comparison of shear wall model results with and without stud buckling;
- (c) comparison of predicted response and experimental data

Padillo (2015) carried out a series of tests on CFS C-section framing members to investigate their axial and flexural cyclic response. By using *asymPinching* feature available in *OpenSees*, axial and flexural behavior of CFS framing members were defined based on experimental data. This way, buckling failure of these members was included in the numerical model. Layout of the shear wall numerical model, the obtained results, as well as the effect of including the member buckling failure on the overall wall response are shown in Figure 2.8.

CHAPTER 3

SUMMARY OF CFS SHEAR WALL EXPERIMENTS

3.1. Introduction

An experimental testing program on lateral load behavior of CFS shear walls was conducted by another researcher in the same research group at Structural Mechanics Laboratory of the Middle East Technical University. Experimental data produced by this testing program was used for verification of the numerical models of wall panels. The purpose of this experimental study was to investigate seismic performance of CFS shear walls with wood-based sheathing. Preliminary studies on CFS structural systems indicated that the response of CFS wall panels is significantly influenced by the behavior of hold down devices while transferring tensile forces from CFS studs to the foundation system. Due to this nontrivial effect of hold down elements, the experimental program included testing of various hold down elements under tensile loading, in addition to lateral load testing of sheathed CFS wall panels. In the following sections important details of the testing program on wall panels and hold down elements are described and the test results are presented.

3.2. Wall Panel Tests

3.2.1. Test Specimens, Test Setup and Instrumentation

Each wall panel used in shear wall tests was 1220 x 2440 mm in dimension. CFS C-shaped profiles with 140 mm depth and 1.2 mm thickness (named as C140x1.2S350) were used for framing. Geometric details of the C-shaped section are given in Figure 3.1. The CFS profiles had a manufacturer specified yield strength of 350 MPa. End studs in wall panels were formed by placing two C140x1.2S350 profiles in back-to-back orientation, while tracks and intermediate studs were made of single profiles of the same size.

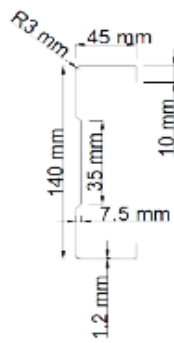


Figure 3.1 Cold-formed steel profile used in shear wall test specimens

The OSB sheathing panels used in shear wall specimens had 1220 x 2440 mm overall dimensions and 11 mm thickness. Self tapping screws having 4.2 mm diameter and 25 mm length were used to connect OSB panel to CFS framing members (Figure 3.2).

Wall panels were supported at their bases by a steel foundation plate, which itself was connected to two steel support beams fixed to the strong floor. Each wall panel was connected to the foundation plate with hold-downs and four shear anchors.

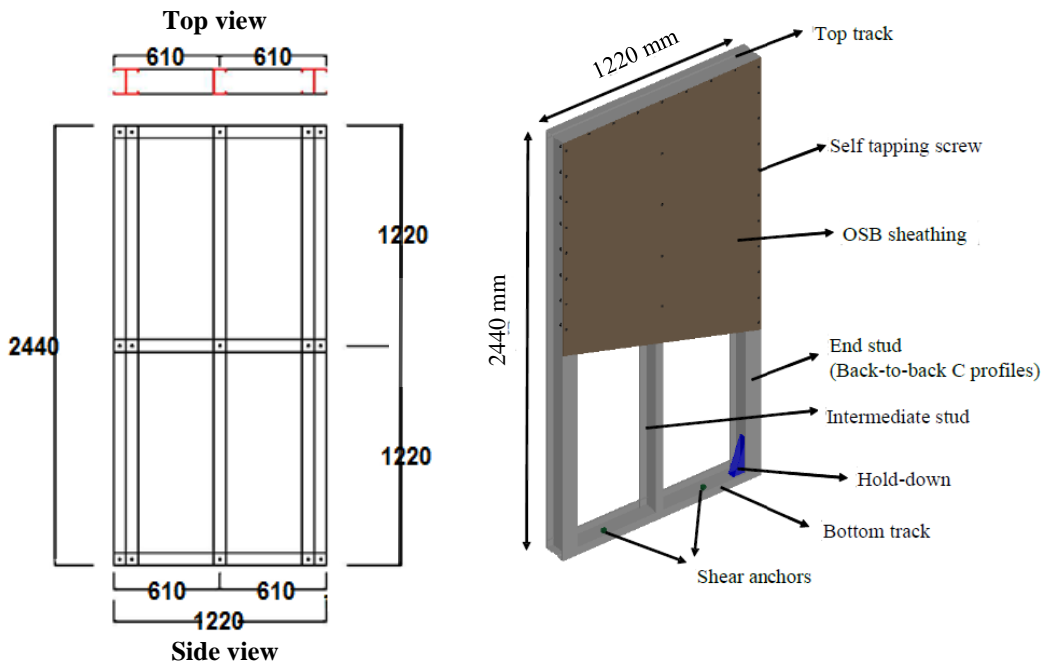


Figure 3.2 Details of a single panel shear wall specimen

Wall panel tests were conducted under displacement loading increased at a rate of 60 mm/min. Lateral displacement was applied at the top edge of wall panels by a hydraulic actuator with 300 kN load capacity and ± 250 mm stroke. For this purpose a steel channel was used as a load distribution beam. A loadcell was used between the hydraulic actuator and the load distribution beam to measure the load applied on wall panels (Figure 3.3). Wall panels were instrumented with four LVDTs in order to measure lateral displacement at the top of wall panel, lateral slip at wall base, and base uplift at hold down locations.

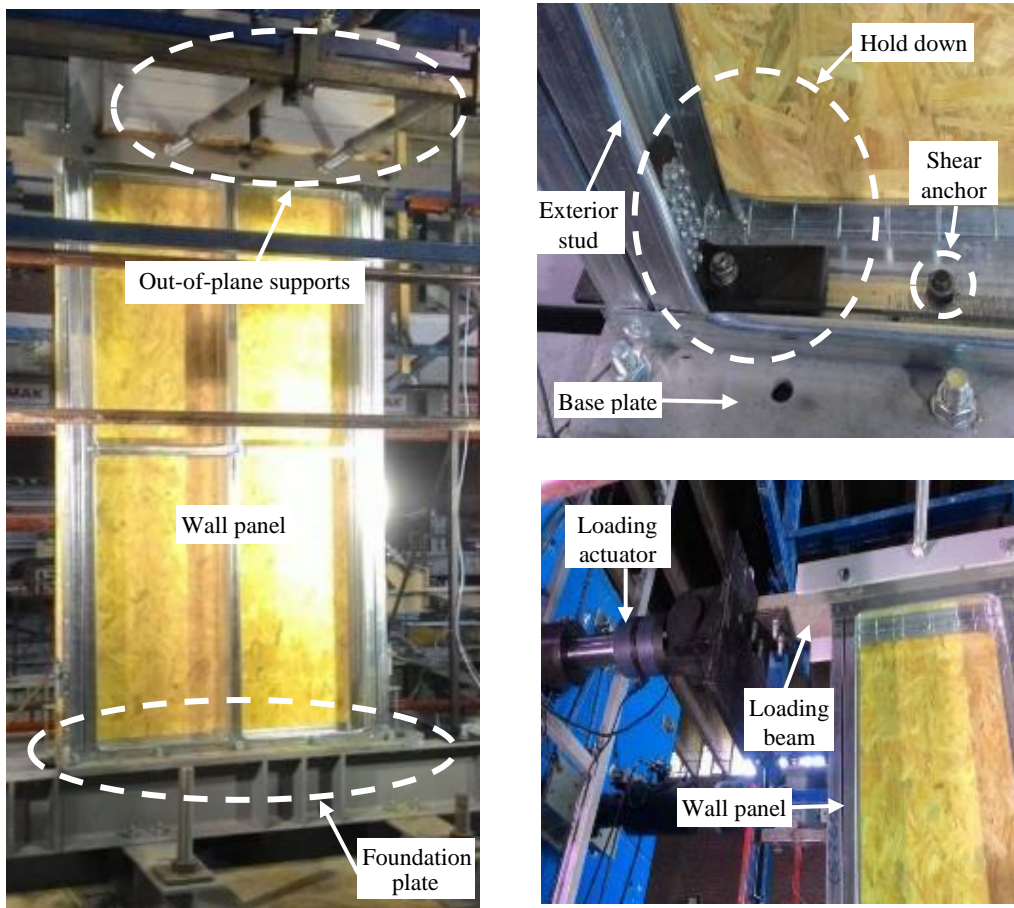


Figure 3.3 Details of wall panel setup (Pehlivan et al., 2018)

Within the test program, majority of the wall specimens were subjected to reversed cyclic loading and only a few specimens were tested under monotonic loading. For cyclic tests, CUREE loading protocol, shown in Figure 3.4 was used. Reference displacement which is necessary for CUREE was obtained from monotonic loading tests. After first six tests, this procedure was abandoned and the reference displacement was taken as 2% of wall height.

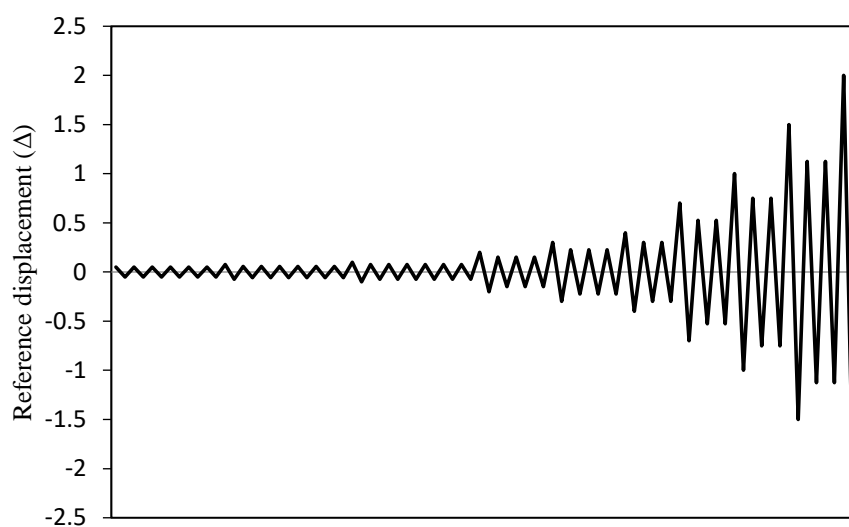


Figure 3.4 Displacement history of CUREE cyclic loading protocol

Shear wall specimens were formed by one, two, or four panels. With these arrangements, the overall specimen dimensions for the one-, two-, and four-panel specimens were 1220 x 2440 mm, 2440 x 2440 mm, and 4880 x 2440 mm, respectively. Photographs showing two- and four-panel specimens are given in Figure 3.5. Irrespective of the number of wall panels all specimens included two hold downs, one at each end of walls.

As part of the CFS shear wall tests, effects of fastener spacing, panel size, sheathing type, hold-down type and level of gravity load on the lateral capacity of wall panels were investigated. Two different fastener layouts were applied on wall panel specimens. The first fastener layout had 150 mm fastener spacing for end studs and tracks and 300 mm spacing for intermediate stud. The second fastener layout was more dense, including almost three times more screws with 50 mm spacing for end studs and tracks and 100 mm spacing for intermediate stud.

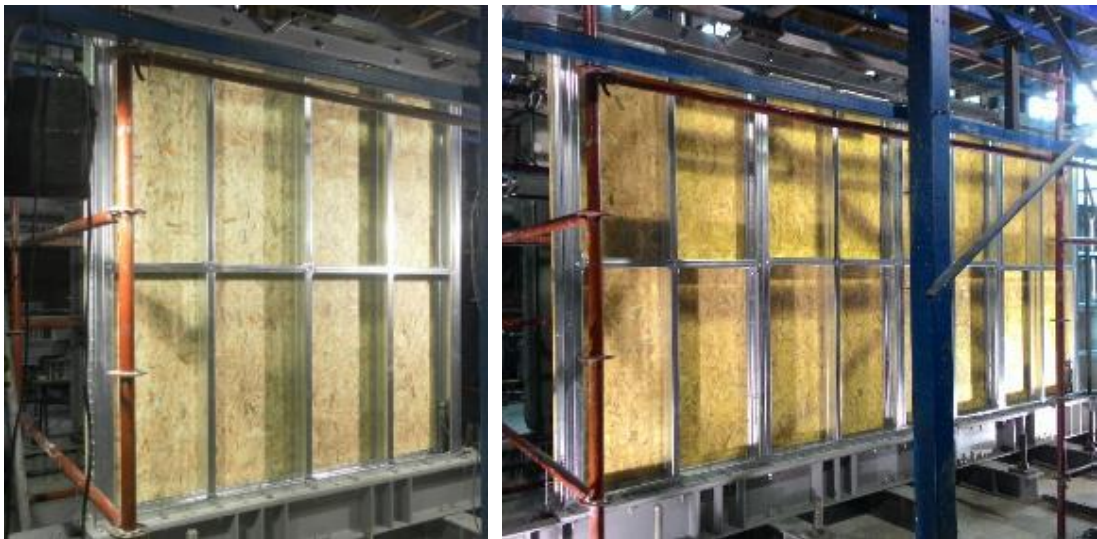


Figure 3.5 Two- and four-panel shear wall specimens

Due to the types of floor system used in CFS structures the load transfer from the floor system to wall panels is generally one-way. As a result of such one-way load transfer, no gravity loading acts on wall panels positioned parallel to the beams supporting the floor system, and the entire gravity loading is resisted by wall panels positioned perpendicular to the floor beams. In order to investigate the effect of gravity loading, lateral loading tests on wall panels were conducted both with and without vertical loading. Two levels of vertical loading, 20 kN and 32 kN, were used in the experimental program.

Another parameter used in CFS shear wall test program was the type of hold down device. Hold down device geometries shown in Figure 3.6 were utilized in wall specimens. Performance of these hold down devices had been investigated in a separate testing program conducted before the shear wall tests. Details of this hold down testing program is given in Section 3.3.

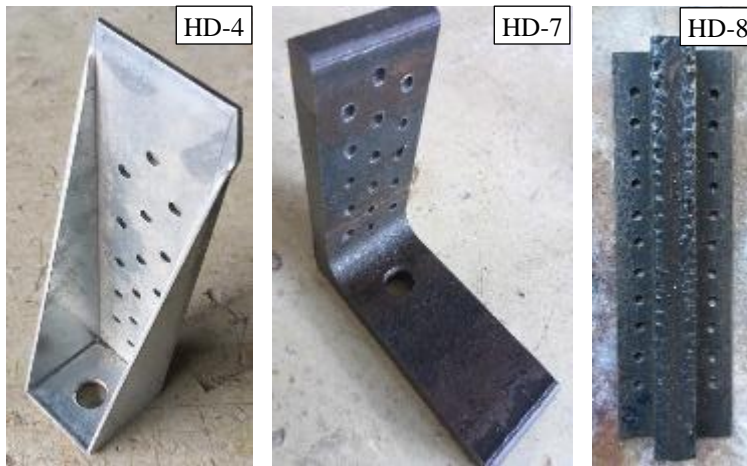


Figure 3.6 Hold down elements used in shear wall numerical models

Sheathing of wall panels can be single-sided or double-sided depending on the lateral force demand. In order to evaluate its effect on seismic performance, some of wall panel specimens were prepared as double-sided. In the case of double-sided, there are two OSB sheathing panels attached to the two flanges of stud.

3.2.2. Observed Deformation Modes

Deformation modes observed during the wall panel tests can be described as; tilting of screws connecting sheathing panel to CFS members, uplift of wall base, stud local buckling and rupture of anchor rods at hold down locations. Among these deformation modes, screw tilting and wall uplift at base were common to all of the tested wall specimens. Stud buckling was usually observed in specimens tested with high level of vertical loading and dense screw layout. Similarly, anchor rod rupture was usually

seen in the case of double-sided sheathing and dense screw layout because of increased force demand. Photographs provided in Figure 3.7 show deformation modes of screw tilting, wall uplift and stud local buckling.



Figure 3.7 Deformation modes observed in wall panel tests: (a) Tilting of screws and uplift of the base; (b) Stud buckling

3.2.3. Discussion of Test Results

Figure 3.8 shows a typical load-displacement response of CFS shear wall panels. The displacement values shown in the plot are the lateral displacements measured at the top of wall panel. As it can be seen, hysteresis response of CFS shear wall is severely pinched as a result of screw tilting and bearing of screws against OSB sheathing. This pinched response is a characteristic feature of this type of structural systems which was also observed in similar experimental studies such as Fülöp and Dubina (2004), Landolfo et al. (2006), Liu et al. (2014), Gao and Xiao (2017).

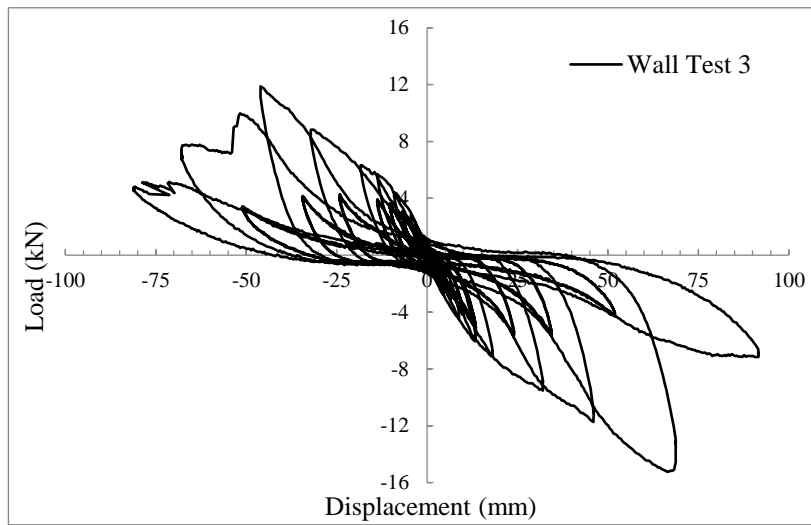


Figure 3.8 Load-displacement response of Wall Test 3

Another common feature observed in test results is the asymmetry between two loading directions. As it can be seen in the Figure 3.8, load capacity is 15.23 kN at positive displacement direction while it reaches only to 11.88 kN at negative displacement direction. This difference is because of the local bearing deformation of OSB sheathing around the connection screws during the first loading cycle (in positive displacement direction). When loading direction is reversed, deformation on OSB sheathing panel around screws prevents the load panel to reach the same load level.

Test results indicate that there is almost a linear relation between the load capacity of wall panel and the number of connection screws provided between sheathing panel and CFS framing members. Because more connection screws were utilized on wall panels with double-sided sheathing and closely spaced connection screws, these specimens exhibited higher load capacities compared to companion walls with single-sided sheathing or widely spaced screws.

As mentioned earlier, one of the common deformation mode observed during load testing of wall panels was uplift at wall base. As a result of this uplift deformation wall panels underwent rocking type motion under the effect of lateral loading. In this

case, behavior of hold down device transferring the force in tension chord member to the foundation system influences the overall wall response significantly. Use of different hold down devices having different stiffness and tension load capacity affected the lateral stiffness and strength of CFS shear wall. As hold-down device gets stiffer, a stiffer wall response is obtained. Similarly, hold down devices with relatively small tension load capacity limited the lateral load capacity of wall panels.

3.3. Hold Down Tests

A complementary test program on hold-down devices was conducted by Pehlivan et al. (2018). As part of the hold down testing program, several types of hold-downs, including devices frequently used in the industry and devices proposed by authors, were tested under monotonic and cyclic loading in order to investigate and compare their performance. The specimen details used in hold down tests, as well as the relation between the hold down test specimens and a typical wall panel are illustrated in Figure 3.9. The hold down devices were subjected to tensile forces by using the test setup shown in Figure 3.10.

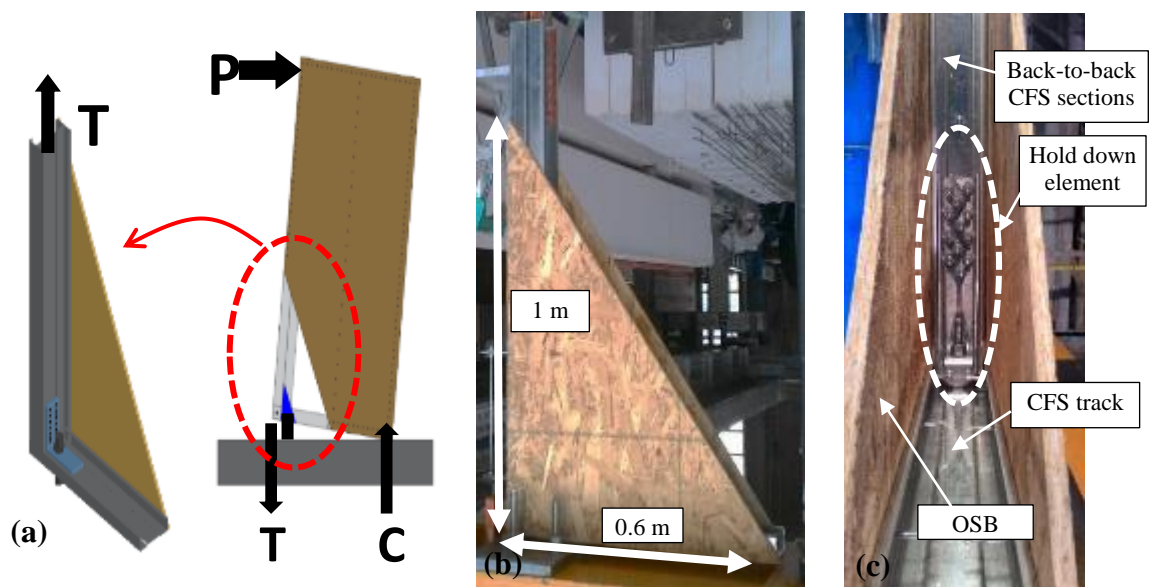


Figure 3.9 Details of hold down specimens: (a) relation between shear wall and hold down specimen; (b) hold down specimen dimensions; (c) position of hold down element in specimen (Pehlivan et al., 2018)

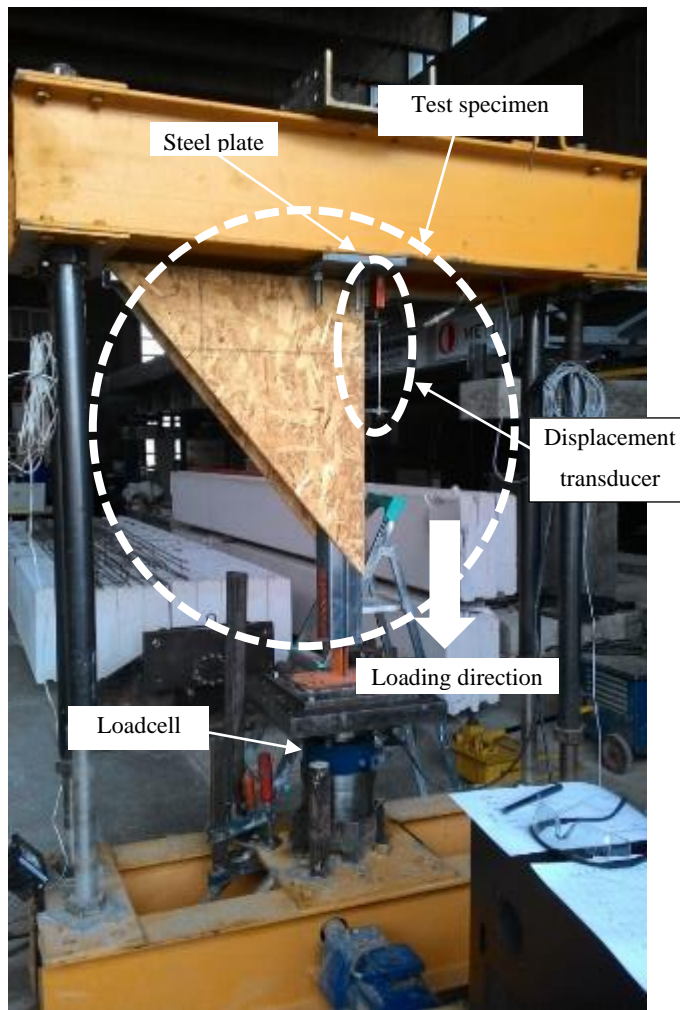


Figure 3.10 Setup used for testing of hold down specimens (Pehlivan et al., 2018)

Measured load-deformation responses of various hold down devices are shown in Figure 3.11. The differences among the hold down devices shown in this plot are the type of the device itself and the number of screws used to connect the device to CFS stud member. As evident, the behavior varies significantly in terms of strength and stiffness. Experimental results indicate that for hold down devices with sufficient strength and stiffness, the response was controlled by the behavior of the screws used to connect the device to the CFS stud member. In these cases increasing the number of connection screws resulted in improvement in the specimen response.

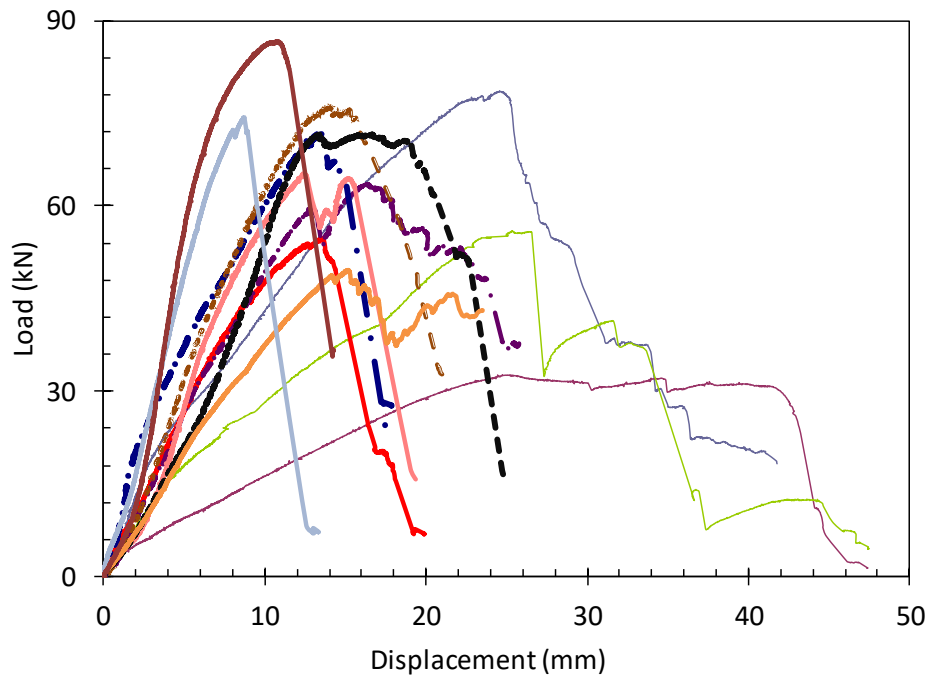


Figure 3.11 Load-deformation response of various hold down devices
(Pehlivan et al., 2018)

CHAPTER 4

FASTENER TEST PROGRAM

4.1. Introduction

As mentioned in the previous chapters, main energy dissipating mechanism in OSB sheathed cold formed steel wall panels when subjected to lateral loading is tilting deformation of the screws providing the connection between the sheathing panel and CFS framing members, as well as the local bearing deformation of OSB as a result of such screw tilting. When subjected to lateral loading a bare CFS frame deforms into a parallelogram while the OSB sheathing panel mostly undergoes a rigid body rotation with limited shear deformation due to its relatively high inplane stiffness (Figure 4.1). This difference in deformation modes of the two components resulted in a nonlinear behavior at screw locations. Such local nonlinear response of fasteners has a significant influence on the overall strength, stiffness and ductility response of shear wall panels. This complex local behavior, involving interaction among CFS member, screw and OSB sheathing, can be captured by fastener tests simulating the conditions in a wall panel.

A fastener testing program was conducted as part of the current study in order to obtain the local response of connection screws accurately. Local load-deformation response obtained from this testing program was then used for accurate numerical modeling of the local connection response between CFS framing members and OSB sheathing in shear wall numerical models. Details of the fastener testing program and the obtained results are presented in the following sections.

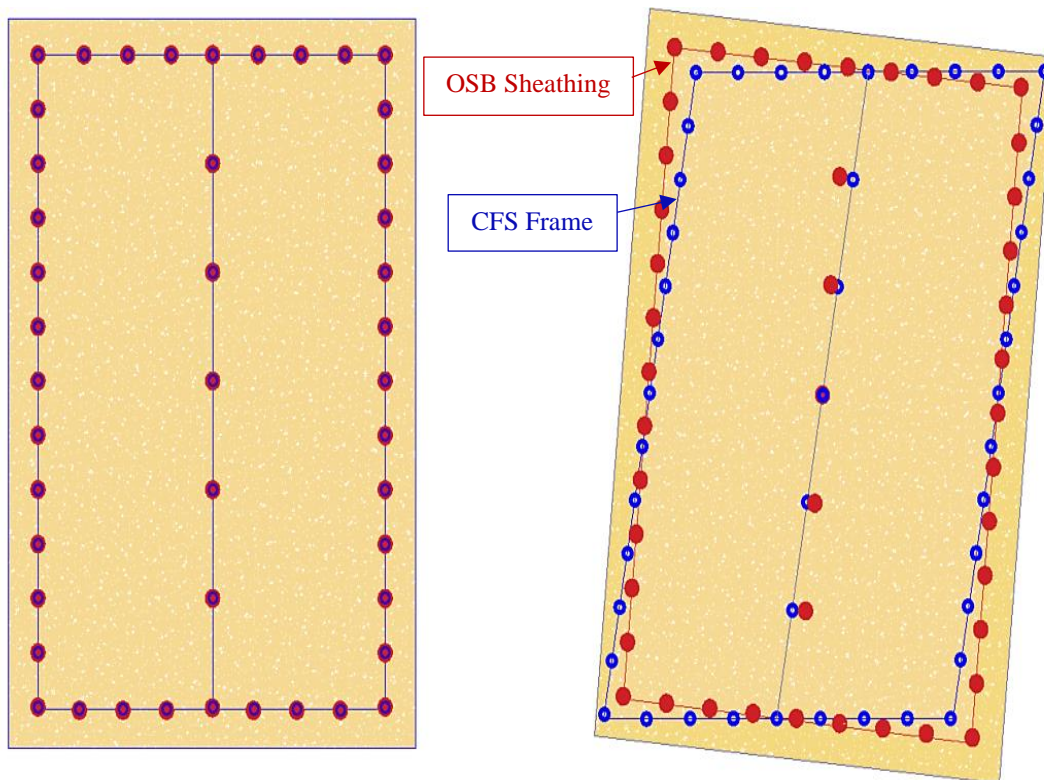


Figure 4.1 Difference in deformation modes of OSB sheathing and CFS frame

4.2. Test Specimens, Test Setup and Instrumentation

A total of ten tests under monotonic loading and six tests under cyclic loading were conducted on screw connection specimens at Structural Mechanics Laboratory of Middle East Technical University. Table 4.1 summarizes the major details of testing program. There are two different edge distances used in fastener test program. In wall panel experiments, screw edge distance was adjusted to 25 mm. In order to represent the real case, screw edge distance was determined as 25 mm for Test Group 1. Additionally, 15 mm edge distance was used for Test Group 2 in order to observe the effect of decrease in edge distance on the fastener behavior. Tests were repeated five times for monotonic loading and three times for cyclic loading. The reason behind this repetition was significant variation observed among the response of test specimens having identical test parameters.

Table 4.1 Basic fastener test matrix

Test	Edge Distance	Loading	
1	25 mm	Monotonic	Test Group 1
2	25 mm	Monotonic	
3	25 mm	Monotonic	
4	25 mm	Monotonic	
5	25 mm	Monotonic	
6	25 mm	Cyclic	
7	25 mm	Cyclic	
8	25 mm	Cyclic	
9	15 mm	Monotonic	Test Group 2
10	15 mm	Monotonic	
11	15 mm	Monotonic	
12	15 mm	Monotonic	
13	15 mm	Monotonic	
14	15 mm	Cyclic	
15	15 mm	Cyclic	
16	15 mm	Cyclic	

Details of test specimens and the setup used for tests are shown in Figure 4.2. Each specimen included two horizontally positioned 600 mm long CFS members and two vertically positioned 600 mm x 300 mm OSB pieces. OSB pieces were attached to these CFS members with self-tapping screws. In order to prevent any issue due to asymmetry, two OSB pieces were connected to CFS frames identically at each face. There were six self-tapping screws tested in total, which are connected to bottom CFS profile with 150 mm spacing. Similar setups have previously been used by other researchers for testing screw connections (Fiorino et al., 2007; Peterman and Schafer, 2013).

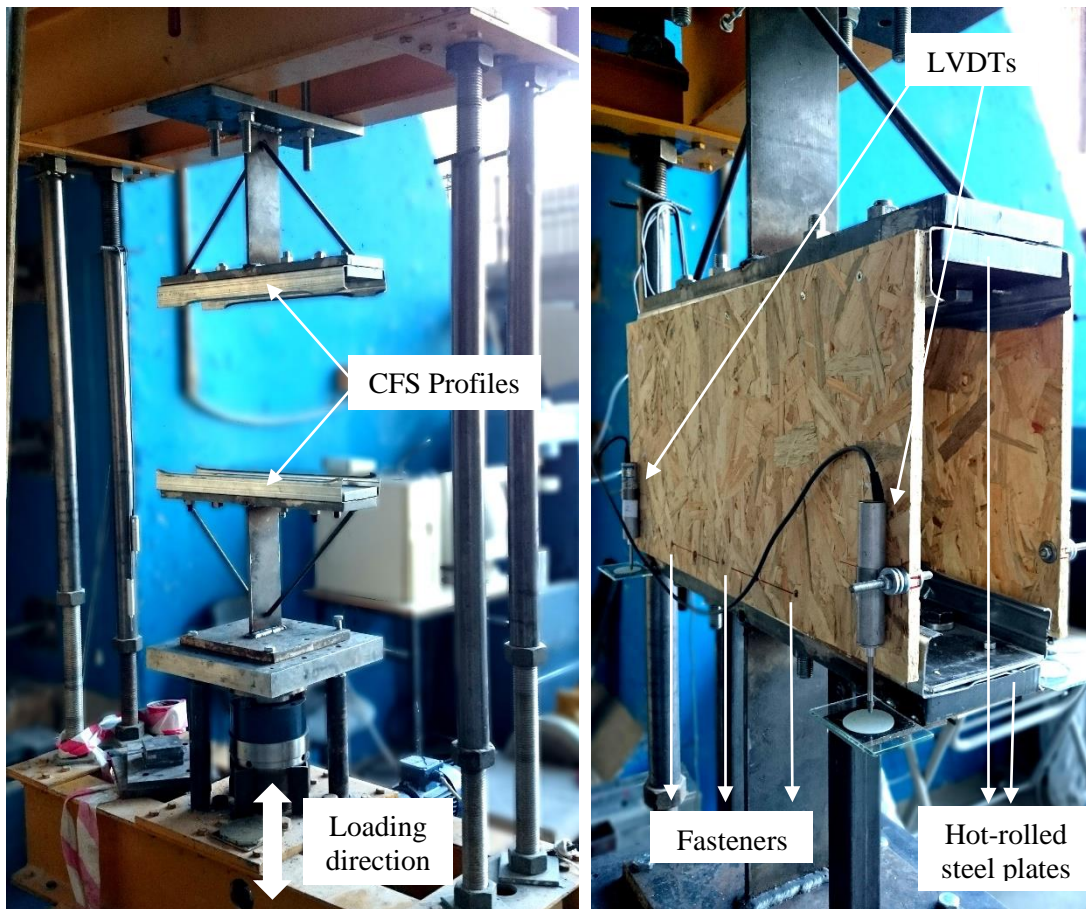


Figure 4.2 Details of fastener test specimens and test setup

CFS profiles used in specimens were of C140x1.2S350 with 1.2 mm sheet thickness and OSB pieces were of 11 mm thickness. The screws providing the connection between OSB pieces and CFS members were 25 mm in length and 4.2 mm in diameter. There were two hot-rolled thick steel plates bolted to web of CFS members to prevent any deformation or movement on the web part of CFS profile. However, one of the thick plates at the bottom CFS member was removed, instead, a thinner plate was bolted in order to allow free tilting of the fasteners providing the connection between the bottom CFS member and the OSB pieces. On the contrary, tilting of screws used to attach the OSB pieces to the top CFS member was limited intentionally by virtue of a thick steel plate. Loading was applied to the bottom CFS member in the form of

vertical displacement. Four displacement transducers (LVDTs) were used to measure the relative displacement at four corners between the bottom CFS member and OSB pieces.

All monotonic and cyclic fastener tests were carried out as displacement-controlled with a constant loading rate. For cyclic loading tests basic loading history developed by the CUREE-Caltech Woodframe Project (Krawinkler et al., 2000) was used. CUREE cyclic protocol is a reversed cyclic loading protocol developed based on the results of nonlinear dynamic analysis of similar structural systems subjected to ordinary ground motions. Figure 4.3 shows displacement history of the loading protocol, which comprised of initiation cycles, primary cycles and trailing cycles. Reference displacement (Δ_{ref}) which is necessary to calibrate the loading protocol was obtained from monotonic loading tests. The reference displacement was taken as 60% of the displacement that corresponds to 80% of the maximum load achieved during the monotonic loading test. Figure 4.4 indicates determination of reference displacement value from load-displacement curve of a fastener test under monotonic loading.

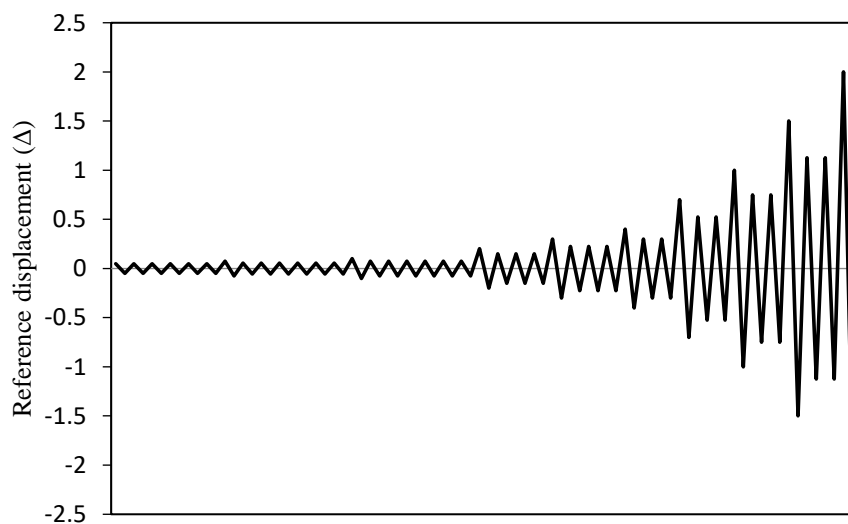


Figure 4.3 Displacement history of CUREE cyclic loading protocol

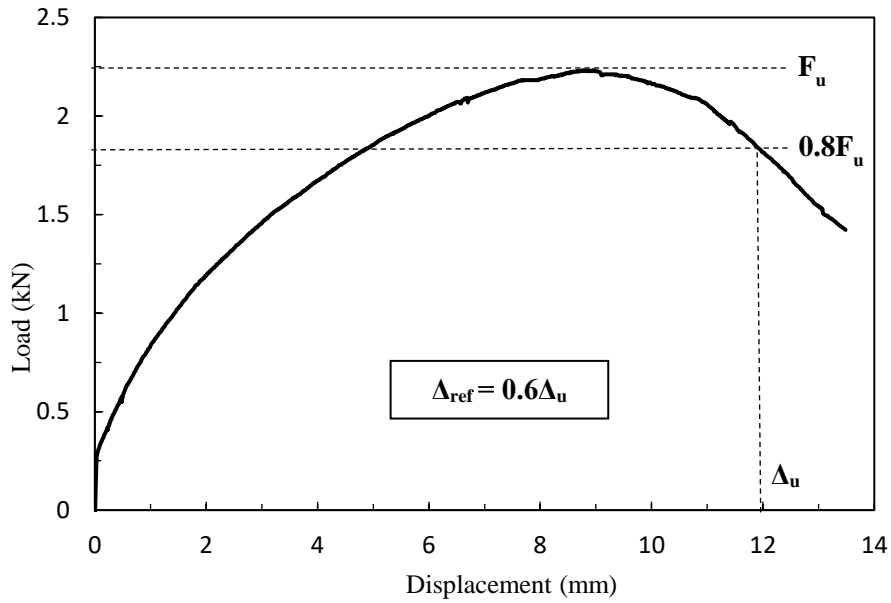


Figure 4.4 Calculation of reference displacement based on monotonic load-displacement response

4.3. Test Results

Main failure modes observed on Test Group 1 having 25 mm edge distance were tilting of screws and screw pull-through as shown in Figure 4.5b and Figure 4.5c. The level of these tilting and pull-through deformations were observed to increase as the loading was progressed. However, for Test Group 2 having 15 mm edge distance, failure mechanism turned into breaking of sheathing edge which is demonstrated in Figure 4.5d. No distinct difference was observed in terms of deformation mode between the monotonically and cyclically tested specimens for both test groups.

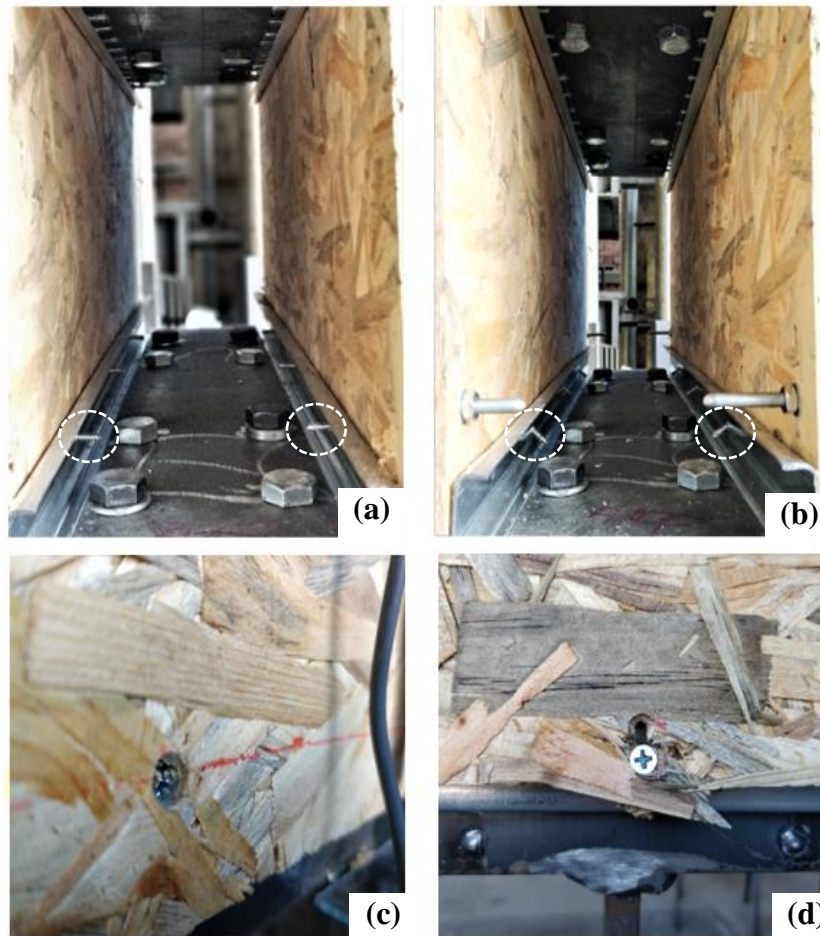


Figure 4.5 (a) Undeformed screws before load testing, (b) Tilting of screws, (c) Screw pull-through, (d) Breaking of sheathing edge

4.3.1. Test Group 1

Monotonic test results for Group-1 specimens are shown in Figure 4.6 and summarized in Table 4.2. The load values measured during loading tests were divided by six in order to obtain the force resisted by a single screw. Therefore, the provided tables and plots represent the behavior of a single screw connection. The stiffness values presented in Table 4.2 were determined as initial stiffness corresponding to $0.6P_{\max}$ for both monotonic and cyclic loading cases. The load capacities change between 1.71 and 2.23 kN, while the stiffness values change between 0.27 and

0.41 kN/mm. As evident, there is a marked variation in measured load capacity and stiffness of identical screw connection specimens. The variation may be attributed to the nonuniform structure of the OSB sheets. Because the strands forming OSB sheets are randomly oriented, the relative position of connection screws with respect to these strands has a major influence on local screw response.

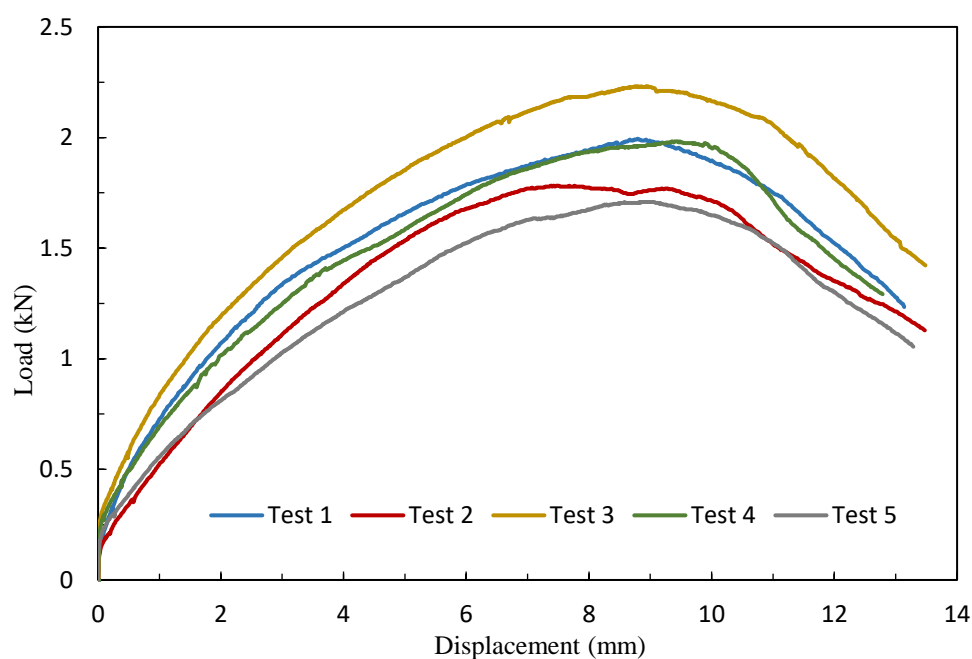


Figure 4.6 Load-displacement curves of Test 1-5.

Table 4.2 Monotonic test results of Test Group 1

Test	peak load (kN)	disp at peak (mm)	stiffness (kN/mm)
1	2.00	8.80	0.40
2	1.78	8.54	0.32
3	2.23	8.81	0.41
4	1.98	9.36	0.34
5	1.71	8.95	0.27

Results from cyclic testing of Group-1 specimens are provided in Figure 4.7 and Table 4.3. The level of variation in load-displacement curves is smaller in the case of cyclic loading when compared to the monotonic tests. All three specimens exhibited asymmetric load-displacement response with the load capacity being higher in the direction that was first loaded than the other direction. During testing when the loading was applied in the positive displacement direction screw tilting and a resulting local bearing deformation of OSB occurred. When the loading was reversed, the screws were able to resist only a smaller level of force as a result of already existing OSB damage. This mechanism showed itself in the form of reduced load capacity and stiffness in the positive displacement direction as compared to the negative displacement direction. Another observation that is valid in Figure 4.7 is the significantly pinched hysteresis curves. The reason for the pinched response is again related with the tilting of screws and the resulting local OSB damage in the vicinity of screws. As discussed in earlier chapters similar asymmetric response was also valid for wall panel specimens.

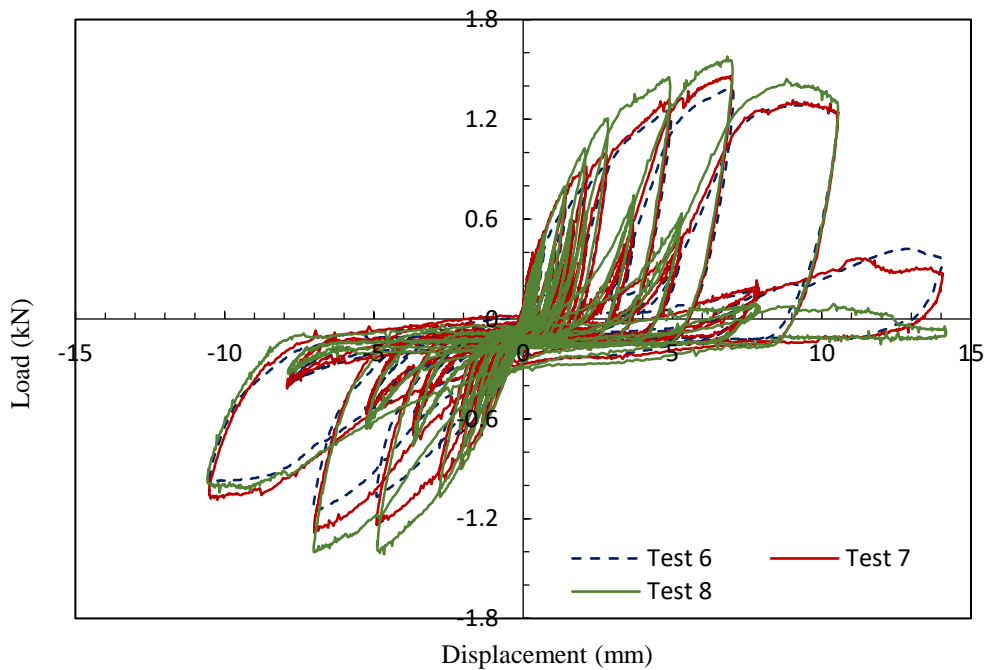


Figure 4.7 Load-displacement curves of Test 6-8.

Table 4.3 Cyclic test results of Test Group 1

Test	+ peak load (kN)	+ disp at peak (mm)	+stiffness (kN/mm)	- peak load (kN)	- disp at peak (mm)	-stiffness (kN/mm)
6	1.39	6.94	0.36	-1.16	-7.01	0.33
7	1.46	6.98	0.46	-1.27	-6.86	0.43
8	1.58	6.84	0.51	-1.41	-7.01	0.45

4.3.2. Test Group 2

Monotonic test results for Group-2 specimens are shown in Figure 4.8 and summarized in Table 4.4. Variation in measured load capacity and stiffness of identical screw connection specimens is more than Group-1 specimens. This relatively large variation can be attributed to the change in the failure mode observed in Group-2 specimens. Due to decrease in edge distance from 25 mm to 15 mm, failure mechanism turned into breaking of sheathing edge near screw locations. The limited edge distance resulted in an obvious decrease in strength values when compared with Group-1 specimens. The measured load capacities change between 0.99 and 1.72 kN, while the stiffness values change between 0.38 and 0.48 kN/mm.

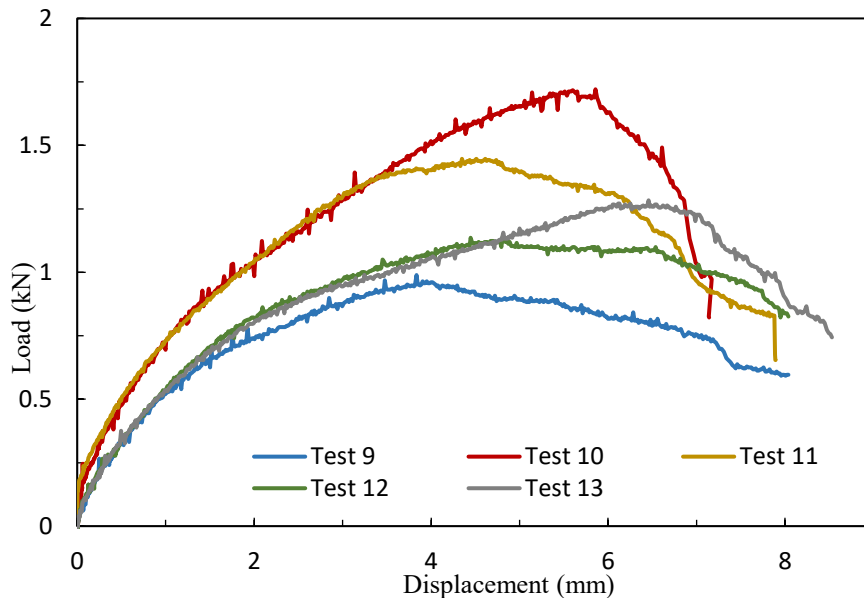


Figure 4.8 Load-displacement curves of Test 9-13

Table 4.4 Monotonic test results of Test Group 2

Test	peak load (kN)	disp at peak (mm)	stiffness (kN/mm)
9	0.99	3.84	0.42
10	1.72	5.51	0.44
11	1.45	6.60	0.48
12	1.14	7.76	0.42
13	1.28	7.61	0.38

Results from cyclic testing of Group-2 specimens are provided in Figure 4.9 and Table 4.5. Similar to the response observed in Group-1 specimens, these specimens also exhibited a slightly asymmetric load-displacement hysteresis curves with significant pinching.

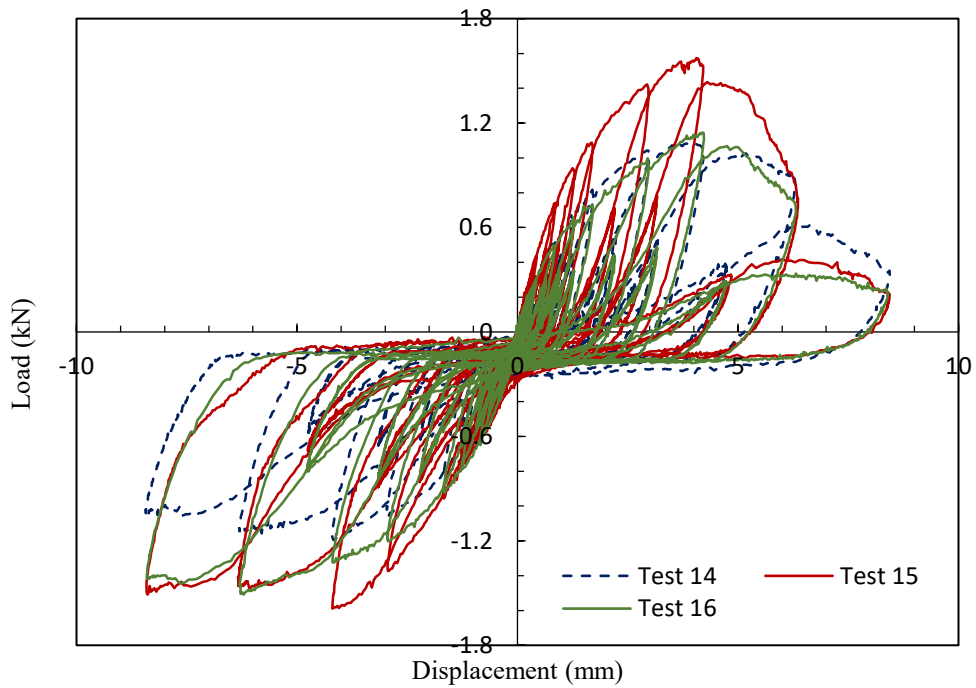


Figure 4.9 Load-displacement curves of Test 14-16

Table 4.5 Cyclic test results of Test Group 2

Test	+ peak load (kN)	+ disp at peak (mm)	+stiffness (kN/mm)	- peak load (kN)	- disp at peak (mm)	-stiffness (kN/mm)
14	1.08	4.03	0.56	-1.19	-4.14	0.60
15	1.57	4.06	0.75	-1.59	-4.05	0.59
16	1.14	4.21	0.46	-1.51	-6.21	0.58

4.3.3. Comparison with Previous Tests in Literature

As explained in Section 2.1, there were similar experimental studies on the connection between CFS and OSB. In order to compare current test results with previous tests in literature, experimental data was taken from Fiorino et al. (2007) and Peterman and Schafer (2013). It's known that load-displacement response of fasteners is highly dependent on edge distance, OSB thickness and CFS thickness. These parameters were taken differently in both studies. In order to make a fair comparison, tests with the closest parameters were taken from each study. Table 4.6 shows the parameters of a screw test from Fiorino et al. (2007) and two tests from Peterman and Schafer (2013).

Table 4.6 Parameters of screw tests from this study, Fiorino et al. (2007) and Peterman and Schafer (2013)

	CFS thickness (mm)	OSB thickness (mm)	Edge distance (mm)
Fiorino et al. (2006)	1.00	9	20
Peterman and Schafer (2013)-1	1.37	11	38
Peterman and Schafer (2013)-2	0.84	11	38
This study	1.2	11	25

Fiorino et al. (2007) conducted screw tests to examine the effect of sheathing orientation and edge distance. 100 x 50 x 10 x 1.0 mm CFS profiles and 9 mm thick OSB panels were used within the test program. There were three different edge distances (10 mm, 15 mm, 20 mm) adopted. Test results of the specimen having 20 mm edge distance was taken in order to compare them with Test Group 1 specimens, which were tested with 25 mm edge distance.

Peterman and Schafer (2013) used various CFS profiles having different member thicknesses. Test results of the specimens having 1.37 mm and 0.84 mm member thicknesses were taken and compared with Test Group 1 which has 1.2 mm CFS thickness.

Figure 4.9 shows load-displacement curves of these three tests from literature with Test Group 1 results. Stiffness values of Test Group 1 from current study are lower than previous tests. Although stiffness of test specimen with 0.84 mm thick CFS profile is very close to Test Group 1, theoretically a lower trend was expected due to the thinner CFS profile. It is also observed that all these three specimens can't achieve displacement values that Test Group reached. Possible differences in mechanical properties of OSB sheets were considered to be a reason for the discrepancy between the fastener response measured in the current study with the ones available literature. For this reason, an experimental investigation was conducted in order to study the in-plane shear behavior of the OSB sheets used in this study. Details of this investigation is explained in the following chapter.

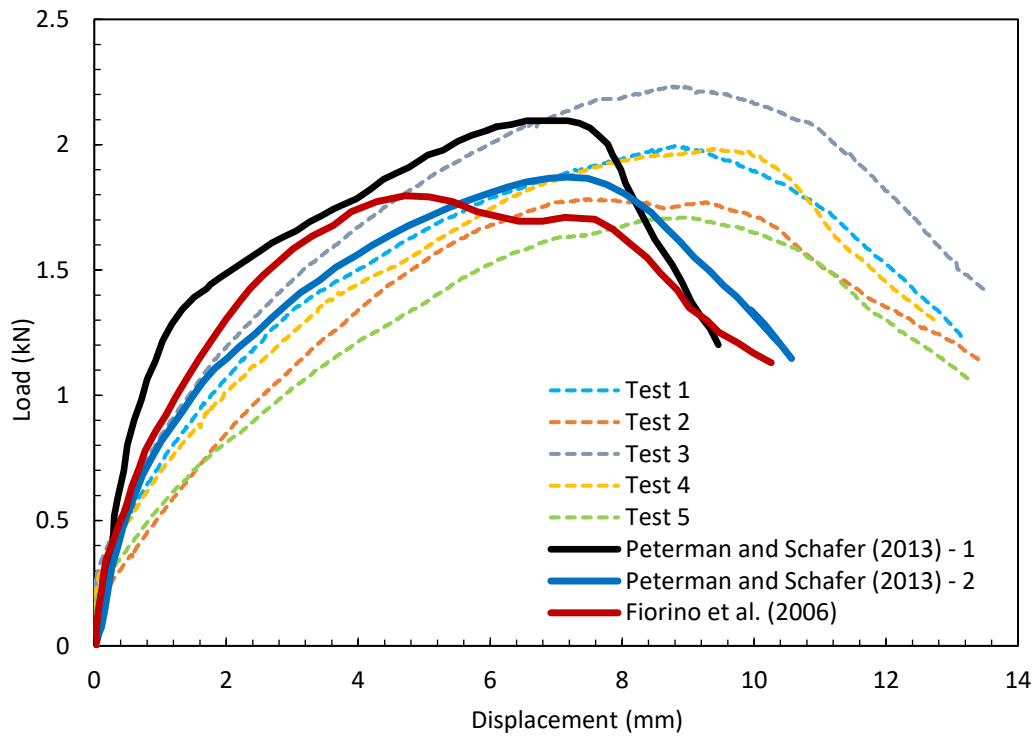


Figure 4.9 Load-displacement curves of Test Group 1 from this study and tests conducted by Fiorino et al. (2006) and Peterman and Schafer (2013)

CHAPTER 5

OSB TEST PROGRAM

5.1. Introduction

A testing program was conducted on OSB pieces in order to determine the available in-plane shear strength and shear modulus. Edgewise shear test presented in ASTM Standard D1037 was adopted as test procedure. Similar OSB in-plane shear tests were carried out previously by Boudreault (2005) and Iuorio et al. (2014). OSB sheets used in the wall panel testing program were obtained from a local supplier and the purpose of OSB testing program was to verify that these sheets have in-plane shear strength and stiffness comparable to those used in other studies available in the literature.

There were 22 specimens tested in total divided into four test groups. Parameters used in test specimens are given in Table 5.1. Although the wood strands forming the OSB sheets are usually assumed to be randomly oriented during production process, there might be a dominant direction affecting shear properties directly. In order to discover the presence and possible effects of a dominant direction, half of specimens were tested along their long side parallel to long side of the typical OSB panel (1220 x 2440 mm). On the contrary, the other half of the specimens were tested in an orientation such that their long side is parallel to short edge of the OSB panel. As a second parameter, OSB pieces used in specimens were taken from two different batches of product. Since OSB is not a widely used structural material, its mechanical properties may vary from time to time. In order to observe any possible difference in different batches, 10 specimens were taken from one batch and the remaining 12 specimens were cut from another batch.

Table 5.1 Parameters used in OSB test specimens

Test Group	Tests	Direction*	Order number
P1-PP	1-5	Perpendicular	1
P1-PL	6-10	Parallel	1
P2-PP	11-16	Perpendicular	2
P2-PL	17-22	Parallel	2

*Indicates whether long side of specimens is parallel or perpendicular to OSB panel

5.2. Test Setup and Instrumentation

Edgewise shear test setup as described in ASTM D1037 was used for load tests. Each specimen consisted an OSB piece with 240 x 90 mm dimensions and 11 mm thickness placed between two steel rails as illustrated in Figure 5.1. Care was taken to clamp the OSB piece in between the steel rails by tightening bolts in order to prevent any relative slip between the pieces. Width of steel rails was 30 mm, leaving a 30 mm OSB test region in the middle portion. Specimens were placed inside the testing machine and monotonically increasing displacement loading was applied on steel rails as seen in Figure 5.1. These steel rails transfer the applied load to the OSB pieces in the form of shear force. One LVDT's was used at each face to measure the relative displacement between the rails on either side of specimen along the longitudinal axis. The rate of displacement loading was adjusted to 0.5 mm/min as recommended by ASTM D1037.

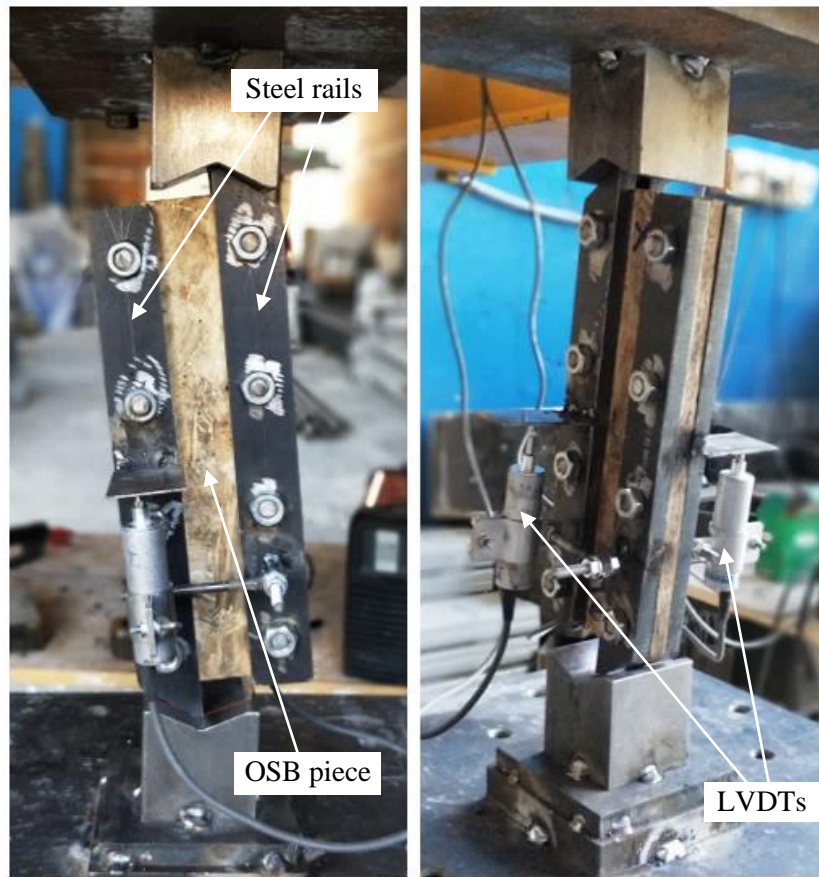


Figure 5.1 OSB test setup

5.3. Calculation of Shear Properties

Using the experimentally determined force and displacement values the in-plane shear strength (f_s) and shear modulus (G) were calculated with Equations 6.1 and 6.2 respectively.

$$f_s = \frac{P_{max} \times \cos 5^\circ}{L \times t} \quad [6.1]$$

$$G = \frac{P \times \cos 5^\circ \times b}{L \times t \times \Delta} \quad [6.2]$$

where P_{max} is the maximum compressive load recorded during load testing, L is length of specimen, t is thickness of specimen, b is width of the portion of the OSB piece subjected to shear forces and Δ is the displacement measured with LVDTs during load testing. There is a 5° rotation from the vertical axis which can be neglected in the calculations. (Figure 5.2)

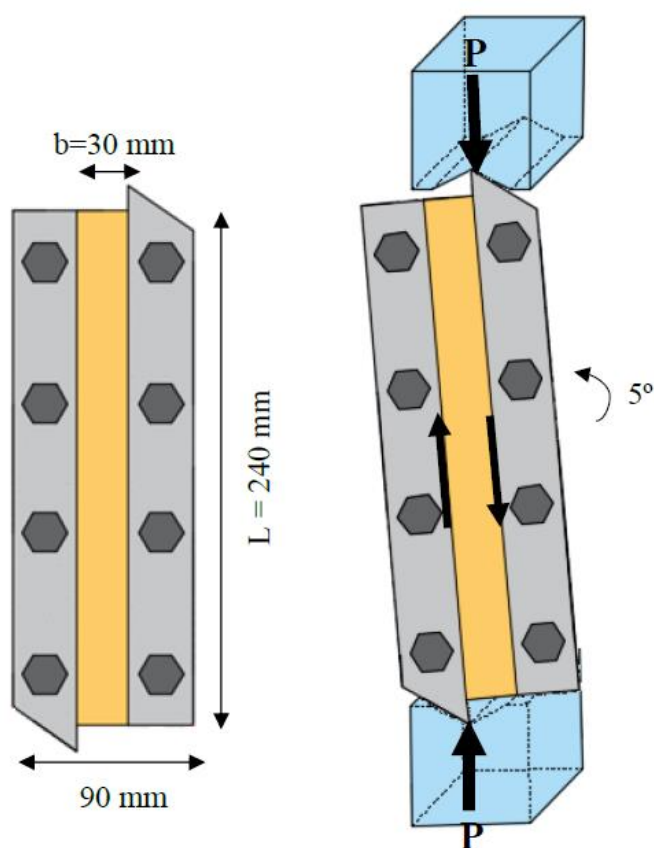


Figure 5.2 Dimensions of OSB panel test specimens

5.4. Test Results and Discussion

Figure 5.3 shows an OSB specimen after subjected to load testing. A shear crack is visible along its front face. There is no visible elongation or bearing damage in bolt holes, which is considered to be an evidence that no relative slip occurred between the OSB piece and steel rails during load testing.



Figure 5.3 Deformed OSB panel specimen

Load-displacement curves of 22 specimens are plotted together in Figure 5.4 and the same curves plotted based on the respective group of specimens are given in Figure 5.5. The load values in these plots represent the load applied by the testing machine at the top and bottom ends of the specimens, while the displacement values represent the relative displacement between the rails on either side of specimen along the specimen longitudinal axis. In-plane shear strength and shear modulus values calculated based on Equations 6.1 and 6.2 are presented respectively in Table 5.2 and Table 5.3. The calculated shear strength values are based on the maximum value of load attained during load tests, while the shear modulus values are based on the initial linear portion of the load-displacement curves.

As evident in the statistical values presented in Table 5.2 and Table 5.3, and also from the load-displacement plots there is a high level of variation in both shear strength and shear modulus values among specimens. The reason for such large variation can be attributed to the inherent nature of wood material and the randomly distributed orientation of grains forming OSB sheets.

Test results indicate no meaningful correlation between the in-plane shear strength and the investigated parameters. In other words, OSB pieces obtained from different batches exhibited similar shear strength values in two orthogonal directions. For in-plane shear modulus, it is seen that specimens obtained from the first batch of OSB panels had slightly favorable response than those taken from the second batch for both loading directions.

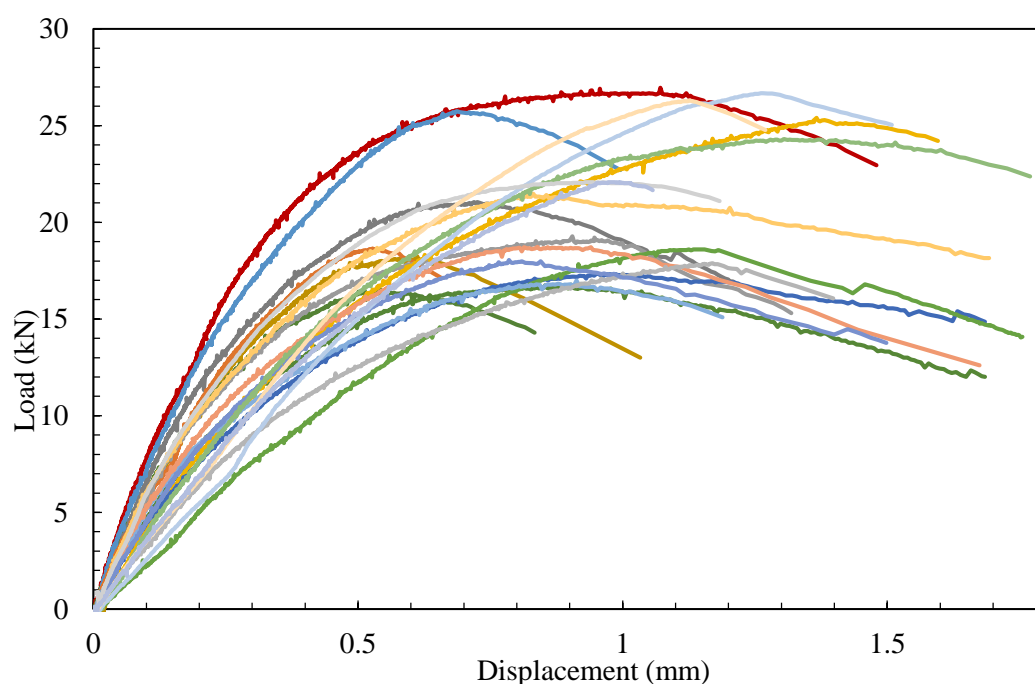


Figure 5.4 Load-displacement results of all 22 specimens

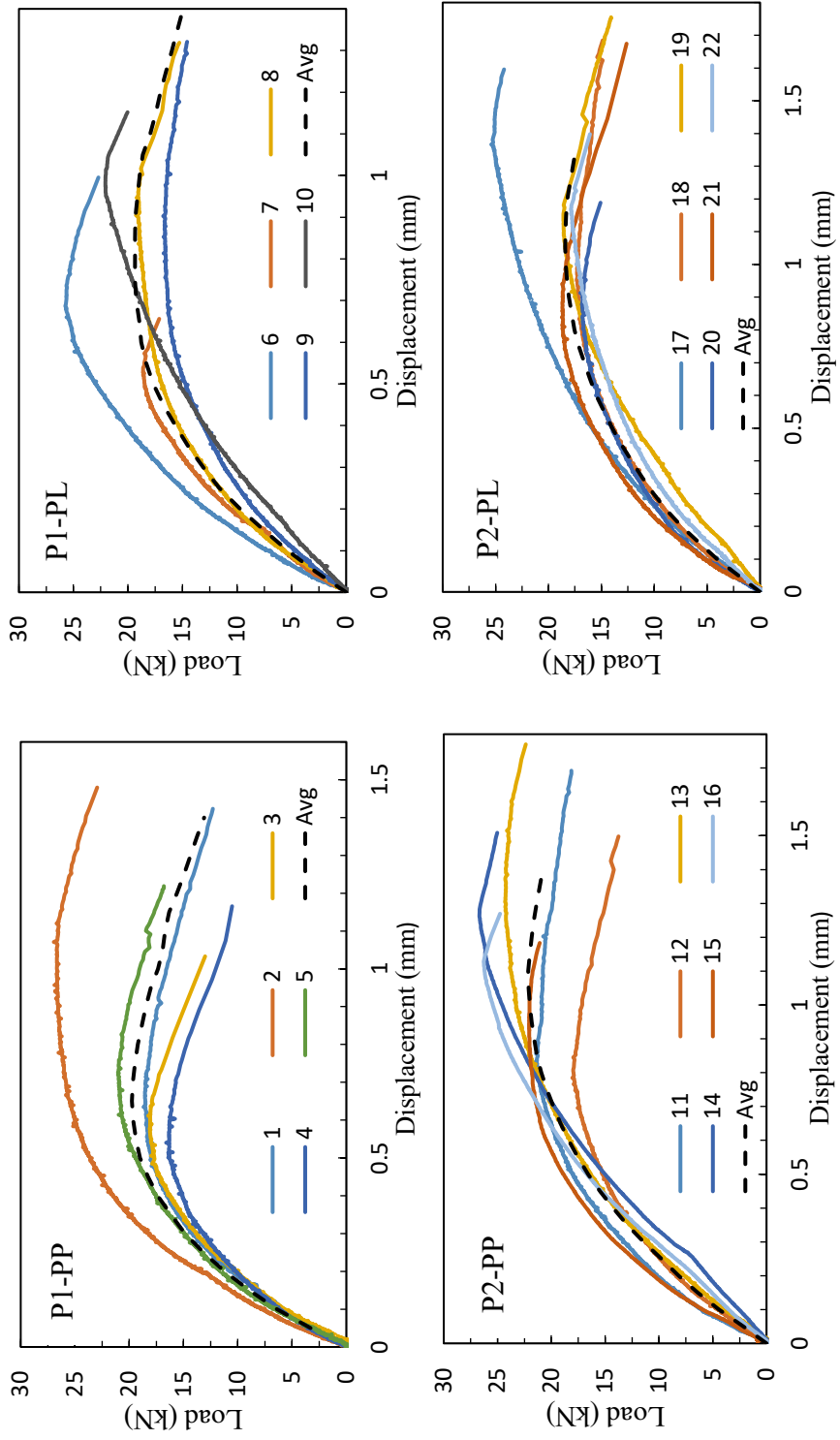


Figure 5.5 Load-displacement results of test groups

Table 5.2 Calculated in-plane shear strength values

Test Group	Number of Tests	Mean (MPa)	Standard Dev. (MPa)	Coefficient of Var. (%)
P1-PP	5	7.69	1.53	20
P1-PL	5	7.77	1.32	17
P2-PP	6	8.77	1.24	14
P2-PL	6	7.26	1.19	16
ALL	22	7.87	1.32	17

Table 5.3 Calculated in-plane shear modulus values

Test Group	Number of Tests	Mean (MPa)	Standard Dev. (MPa)	Coefficient of Var. (%)
P1-PP	5	654	69	11
P1-PL	5	561	144	26
P2-PP	6	477	127	27
P2-PL	6	423	100	24
ALL	22	529	110	22

In order to evaluate shear properties of the OSB panels used in CFS shear wall specimens, the in-plane shear strength and shear modulus values obtained in this study were compared with characteristic values provided by BS EN 12369-1:2001 and APA The Engineered Wood Association Technical Report (1999). Panel dry design rigidity and shear capacity through thickness is presented in APA Technical Report. Panel rigidity ($G_v t_v$) values vary between 4380 and 5430 kN/m and panel shear through thickness ($F_v t_v$) changes from 9 to 13 kN/m. Based on these values shear modulus (G_v) can be obtained to vary between 400 and 495 MPa for an OSB panel having 11 mm thickness. Similarly shear strength (F_v) varies between 0.84 and 1.19 MPa. These reported shear modulus values are approximately 15% lower than the values obtained from edgewise shear tests shown in Table 5.3. By considering the large variation within the experimental results, it can be considered that edgewise shear test results

obtained as part of the current study are in a good agreement with the values provided in APA Technical Report.

A comparison of the edgewise shear test results obtained in this study with the values provided by BS EN 12369-1:2001 indicate a significant difference between the two sets of values. In-plane shear strength (F_v) is presented as 6.8 MPa while in-plane shear modulus (G_v) is given as 1080 MPa in BS EN 12369-1:2001. These values indicate a great overestimation of the shear strength and approximately 100% difference in shear modulus. This also means that there is a significant discrepancy between the values presented in EN and APA standards.

Boudreault (2005) performed edgewise shear test with the same procedure as in the current study and obtained in-plane shear modulus and shear strength values consistent with the results of this study (Table 5.4). A more recent study conducted by Iuorio et al. (2014) yielded in-plane shear strength values in close agreement with the current study while the reported shear modulus values are almost two times of those obtained in the current study (Table 5.5).

Table 5.4 Test results for edgewise shear of wood sheathing panels (Boudreault, 2005)

Test Series	Thickness (mm)	Shear strength (v_p) (MPa)	Shear modulus (G) (MPa)	CoV (%)	G/ v_p
OSB-7/16-PL-A,B,C	11.26	9.05	473	10.4	52
OSB-7/16-PP-A,B,C	11.03	9.14	530	16.1	58

Table 5.5 OSB test results (Iuorio et al., 2014)

Typology	Number of tests	Shear strength (MPa)				Shear modulus (MPa)		
		Avg. value	Standard deviation	CoV (%)	Characteristic value	Characteristic design value	Avg. value	Avg. design value
P-O 09	15	7.62	0.87	0.11	6.17	3.00	1156	750
P-O 09⊥	15	7.06	0.56	0.07	6.19	3.00	953	750

In conclusion, several resources, including APA and EN standards, report significantly different in-plane shear modulus values for OSB sheets. Such large inconsistency might be related with different assumptions made in different codes to calculate the shear modulus using the in-plane shear load test data. As explained earlier, in this study the test width of OSB pieces subjected to shear forces was taken as the clear span between two rail plates (Figure 5.2). This was based on the condition that these plates were tightly bolted to the OSB piece and no relative slip between the plates and OSB piece was ensured. However, there is no clear instruction about calculation of shear modulus in ASTM D1037 and the width of test piece might be taken as bolt-to-bolt distance as well, as opposed to clear distance. These two different interpretations of specimen width values result in 100% difference in the resulting in-plane shear modulus values. Because the specimen width is not used in the calculation of in-plane shear strength, no such disagreement is observed in the shear strength values reported in different documents.

CHAPTER 6

NUMERICAL MODELING OF SHEAR WALLS

6.1. Introduction

OpenSees (Open System for Earthquake Engineering Simulation) platform was utilized to construct the numerical model of sheathed CFS shear walls. OpenSees platform has been developed to simulate seismic response of structural systems at Pacific Earthquake Engineering Research Center and provides a wide range of material models, elements and solution algorithms (McKenna et al., 2000). Since it is an open-source software having high computational speed at nonlinear static and dynamic analysis, it has been preferred widely in recent studies focusing on seismic response of structural systems.

As described in Chapter 3, an experimental study on CFS shear walls was conducted by another researcher as part of the same TUBITAK research project. Experimental data provided by this study was used to validate the numerical model in this chapter. Eight full-scale shear wall experiments were selected and simulated by the numerical model. Table 6.1 shows the modeling matrix and summarizes properties of CFS shear walls used in relevant experiments. All of these wall specimens were tested under reversed cyclic loading. Panel size, single- or double-sided sheathing, screw spacing, hold-down type and presence of an axial load were the main parameters considered.

Results from fastener tests presented in Chapter 4 were used to develop fastener material model used in shear wall model. Since the shear wall model is fastener-based, it is the key part of this modeling approach.

Table 6.1 CFS shear wall model matrix

Test& model	Wall size (cm)	Sheathing	Screw spacing (mm)	Hold-down type	Gravity load
3	122x244	Single-sided	150/300	HD-4	-
4	122x244	Single-sided	150/300	HD-4	20 kN
8	122x244	Single-sided	50/100	HD-7	-
18	122x244	Double-sided	50/100	HD-8	-
24	244x244	Single-sided	150/300	HD-8	-
37	488x244	Single-sided	150/300	HD-8	-

In both CFS shear wall experiments and fastener tests, basic loading history developed by the CUREE-Caltech Woodframe Project (Krawinkler et al., 2000) was used as cyclic loading protocol. In order to be consistent with experimental studies, CUREE loading protocol was adopted in numerical analysis as well. CUREE is a displacement-controlled, reversed cyclic loading protocol developed based on the results of nonlinear dynamic analysis of similar structural systems subjected to ordinary ground motions. Figure 6.1 shows displacement history of the loading protocol which is comprised of initiation cycles, primary cycles and trailing cycles. Reference displacement (Δ_{ref}) which is necessary to calibrate the loading protocol is usually obtained from monotonic loading tests. The reference displacement is then taken as 60% of the displacement that corresponds to 80% of the maximum load achieved during the monotonic loading test. However, in CFS shear wall experiments, after first six tests, this procedure was abandoned. Instead, 2% of wall height was taken as the reference displacement. In order to be consistent with experimental study and to be able to make a proper comparison, same reference displacements were adopted in numerical analysis.

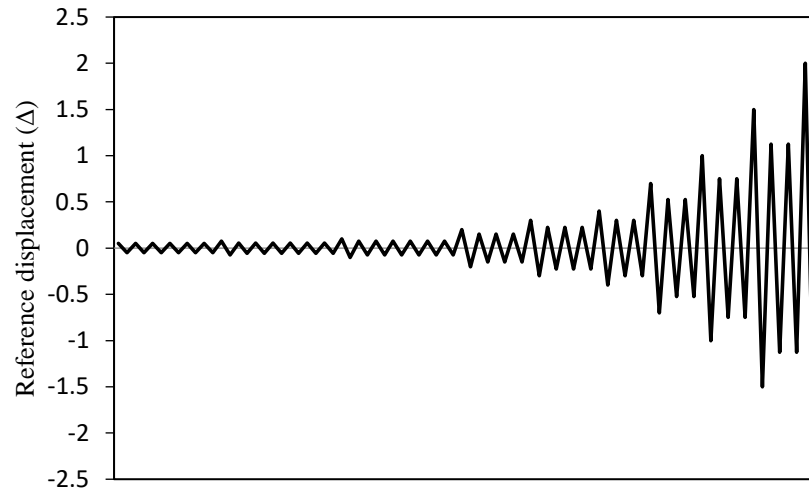


Figure 6.1 Displacement history of CUREE cyclic loading protocol

In the following sections, geometrical properties and elements of the shear wall numerical model are explained in detail. There are three material models implemented in numerical model representing hold-downs, fasteners and CFS framing. Hold-downs were modeled as linear elastic materials based on the measured stiffnesses. CFS framing members were also defined as linear elastic. In wall numerical models the only source of nonlinear behavior is the fastener elements provided between sheathing panel and CFS framing members. This type of modeling approach is known as fastener-based.

After description of numerical model, wall response obtained from the model is compared with shear wall experiments. Hysteresis and backbone curves as well as the stiffness degradation and energy absorption aspects are investigated in detail to validate the numerical model. It is important to understand local behavior of fasteners because they are the main energy dissipating elements in this structural system. In order to understand the local fastener behavior during analysis, additional effort was spent on investigating the status of individual fasteners at different time steps throughout loading.

6.2. Description of Shear Wall Numerical Model

Numerical model representing a single panel shear walls had overall dimensions of 1.22x2.44 m. General layout of the model is provided in Figure 6.2. Two sets of nodes were defined at the fastener locations: one set of node belongs to CFS member while the other set of nodes belongs to the sheathing panel. These two sets of nodes, sharing the same physical location, were then connected by zero-length spring elements simulating the screw connection. Loading was applied at the node located at top left corner of wall panel in the form of horizontal displacement.

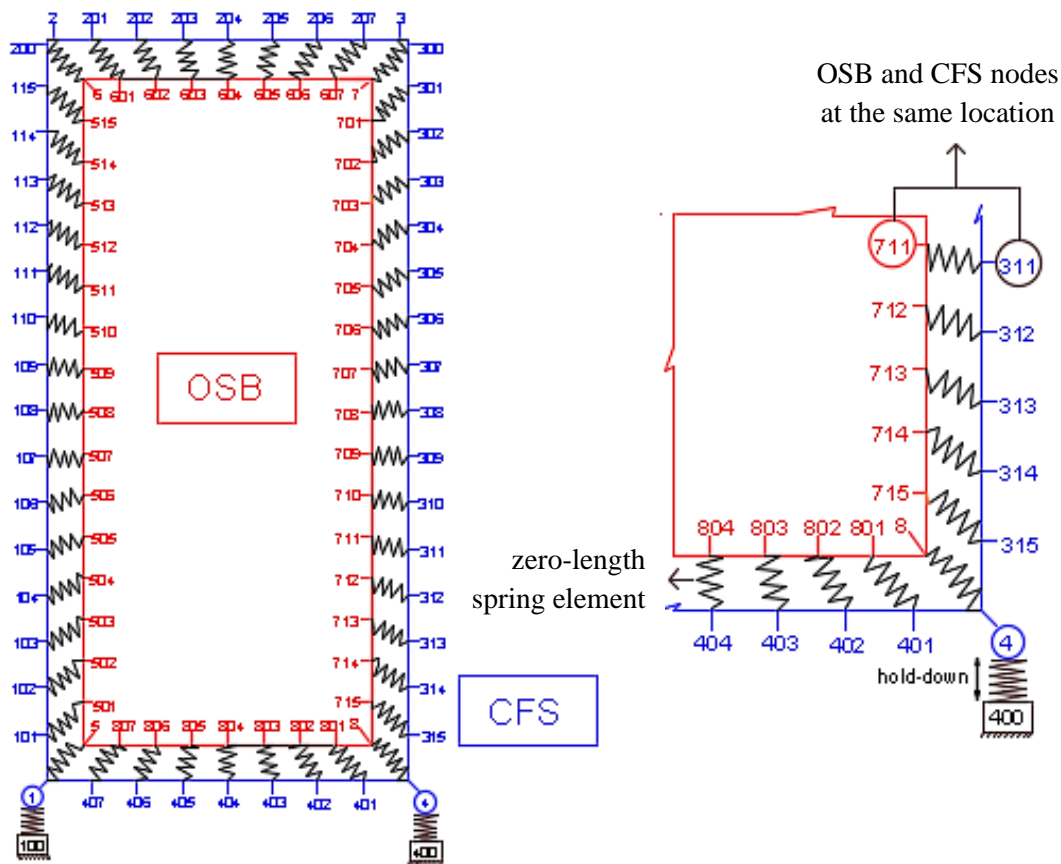


Figure 6.2 General layout of the OpenSees CFS shear wall model

Stud and track CFS members were divided into small-size frame elements. They were defined between adjacent fastener nodes as displacement-based beam-column elements. Table 6.2 shows geometric properties and elasticity modulus values used for CFS members. Since the studs are made of two CFS sections positioned back-to-back their geometric properties are different from those of the tracks. Intermediate stud available between two end studs in wall panel specimens was not incorporated in the numerical model since the effect of these members on overall wall response is negligibly small. Stud-to-track connections at the top corners of wall panels were modeled with rotational springs. These springs were assigned a linear moment-rotation behavior with a stiffness of 11.3 kN-m/rad based on a similar study of Bian et al. (2015).

In Chapter 5, shear modulus of OSB was calculated based on experimental data. However, these values couldn't be verified with previous test results in literature due to the lack of clear information. Also, there was a high level of variation in both shear strength and shear modulus values among current test specimens. For this reason, in majority of numerical models the OSB sheathing panel was modeled as a rigid diaphragm. This type of modeling approach provided a much higher computational speed during analyses. For this purpose, a master node was defined at the center of the panel and the nodes at panel edges were slaved to this master node. This type of modeling approach is consistent with the rigid in-plane behavior of sheathing panels observed during shear wall load tests. Such a rigid diaphragm assumption is a common method in numerical modeling of sheathed CFS shear walls and has previously been used by several researchers (Bian et al., 2014; Buonopane et al., 2015). As part of the parametric study validity of the rigid diaphragm assumption was evaluated by comparing the wall response with that obtained utilizing shell modeling of the OSB sheathing panel. Very slight difference was observed in wall response obtained from these two sets of analyses. Details of this study are provided in Section 7.7.

Table 6.2 Material and geometric properties assigned to framing members in shear wall numerical models

	E (GPa)	A (mm²)	I (mm⁴)
Stud	200	624.48	1748670
Track	200	312.24	874336

6.2.1. Hold-Down Material Model

Hold down devices at wall base were modeled by using zero-length elements. There are two fixed nodes, one at each bottom corner, representing the foundation and the zero-length elements were defined between the bottom corner CFS nodes and these fixed foundation nodes (Figure 6.2). These elements were assigned linear material behavior. Results from hold down tests that were conducted as part of another research study at Structural Mechanics Laboratory of the Middle East Technical University were used to model the hold down response in the current study (Pehlivan et al., 2018).

The measured load-displacement behaviors for the three types of hold down devices used in shear wall testing program (devices named as HD-4, HD-7 and HD-8) are shown in Figure 6.3. As it can be seen, hold down test results show almost linear response prior to the peak load. Based on this observation, the hold down devices in wall numerical models were represented as linear elastic spring elements with the tension stiffness values given in Table 6.3. Stiffness assigned to these spring elements in compression was 1000 times larger than the corresponding tension stiffnesses. With the boundary conditions used at wall base in numerical models, rocking motion of wall panels was allowed, while base slip was restrained.

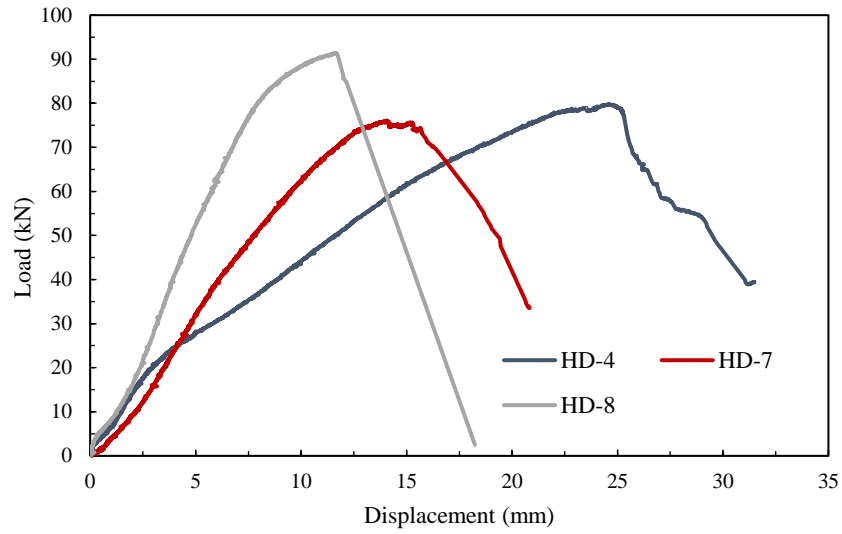


Figure 6.3 Load-displacement results of hold down devices HD-4, HD-7 and HD-8

Table 6.3 Hold-down tension stiffness values used in shear wall numerical models

	HD-4	HD-7	HD-8
Stiffness (kN/m)	3500	6000	10000

6.2.2. Fastener Material Model

Screws providing the connection between sheathing panel and CFS framing members were modeled using CoupledZeroLength element available in OpenSees. Different from simple zero-length element, CoupledZeroLength element is able to work with its vector resultant of two directional components. Material model for these elements was assigned by using Pinching4 model, which is a special hysteretic material model predefined in OpenSees. The Pinching4 material model is capable of capturing softening, strength degradation, and cyclic pinching responses and is defined with four positive and four negative backbone points shown in Figure 6.4.

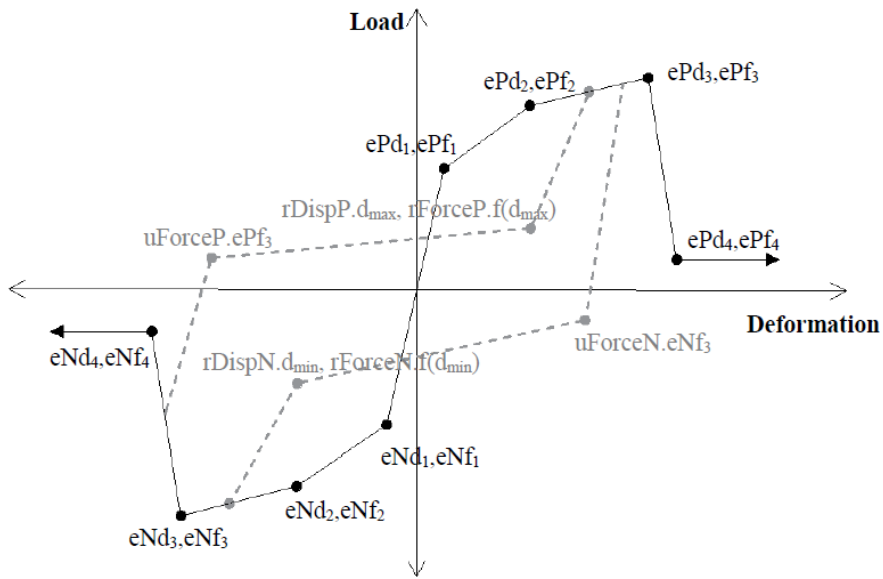


Figure 6.4 OpenSees Pinching4 model definition

Pinching4 parameters were determined according to the fastener test results obtained in Chapter 3. Since screw edge distance used in single panel wall specimens tested in shear wall program was 25 mm, results from Group-1 fastener tests were considered to define the fastener material model in wall numerical models. For monotonic loading case, three test results were selected from the group representing the upper bound behavior (Test 3), lower bound behavior (Test 5) and average behavior (Test 1). Figure 6.5 shows developed material models based on test results by defining four positive backbone points given in Table 6.4. As seen, each point on the curve is described by a force and a corresponding displacement value.

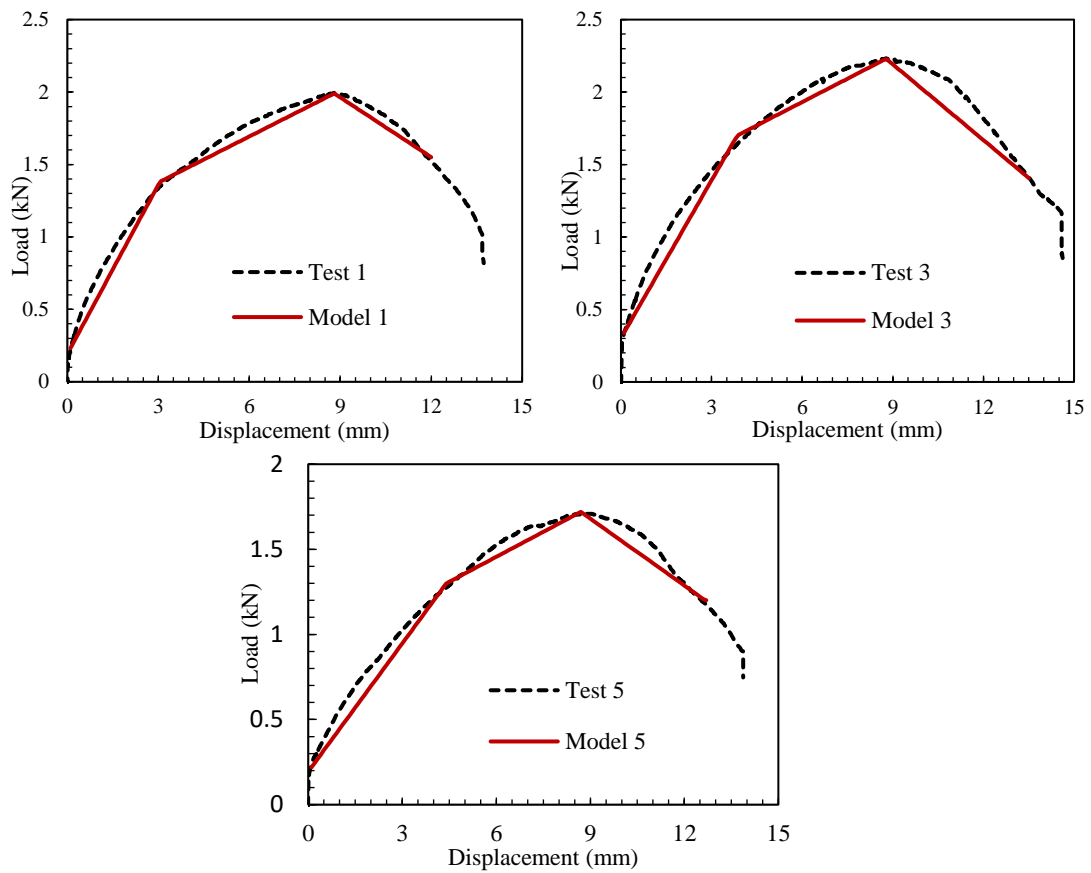


Figure 6.5 Fastener material models for monotonic loading

Table 6.4 Pinching4 backbone parameters for monotonic material model

Model number	ePf1 (kN)	ePf2 (kN)	ePf3 (kN)	ePf4 (kN)	ePd1 (mm)	ePd2 (mm)	ePd3 (mm)	ePd4 (mm)
1	0.20	1.38	1.99	1.55	0.02	3.05	8.80	12.00
3	0.31	1.70	2.23	1.40	0.02	3.85	8.78	13.54
5	0.21	1.30	1.72	1.20	0.06	4.41	8.70	12.66

For cyclic loading material model, 39 parameters are required in order to calibrate the response envelope ($ePfi$, $ePdi$, $eNfi$, $eNdi$), unloading stiffness degradation (gKi), reloading stiffness degradation (gDi), strength degradation (gFi), energy dissipation (gE), and damage type (Barandun, 2013).

In order to represent the actual fastener response accurately in wall numerical model a detailed calibration process was followed. In this process the goal was to obtain an acceptable match for all drift cycles between the material response defined in numerical model and the load-displacement response obtained during the fastener test program. A sample Pinching4 material model calibrated based on the measured response from one of the fastener specimens is shown in Figure 6.6 with the corresponding Pinching4 parameters given in Table 6.5. Match between the actual measured response and the adjusted behavior in various drift cycles is shown in Figure 6.7. Good agreement between the experimental data and the adjusted behavior in terms of stiffness, pinching and absorbed energy is evident in these plots.

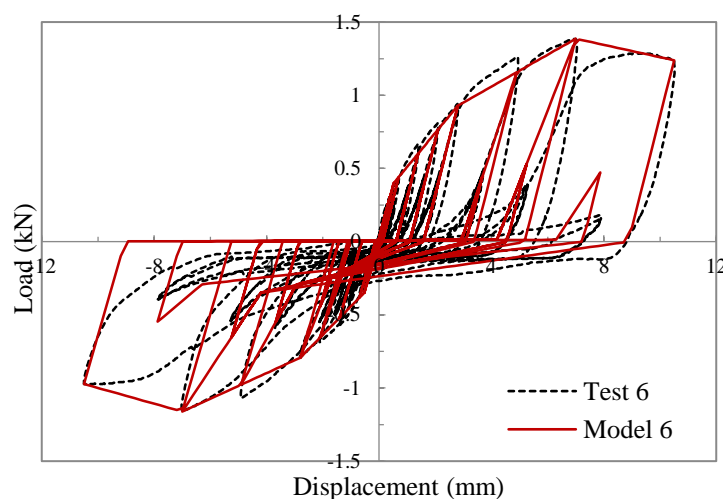


Figure 6.6 Cyclic fastener material model based on experimental data

Table 6.5 Pinching4 backbone parameters for cyclic material model

Point i	ePfi	ePdi	eNfi	eNdi
1	0.400	0.525	-0.350	-0.525
2	0.928	2.800	-0.793	-2.800
3	1.386	7.00	-1.161	-7.00
4	1.240	10.500	-0.973	-10.500

rDispP	rForceP	uForceP	rDispN	rForceN	uForceN
0.600	0.010	0.001	0.600	0.300	0.001

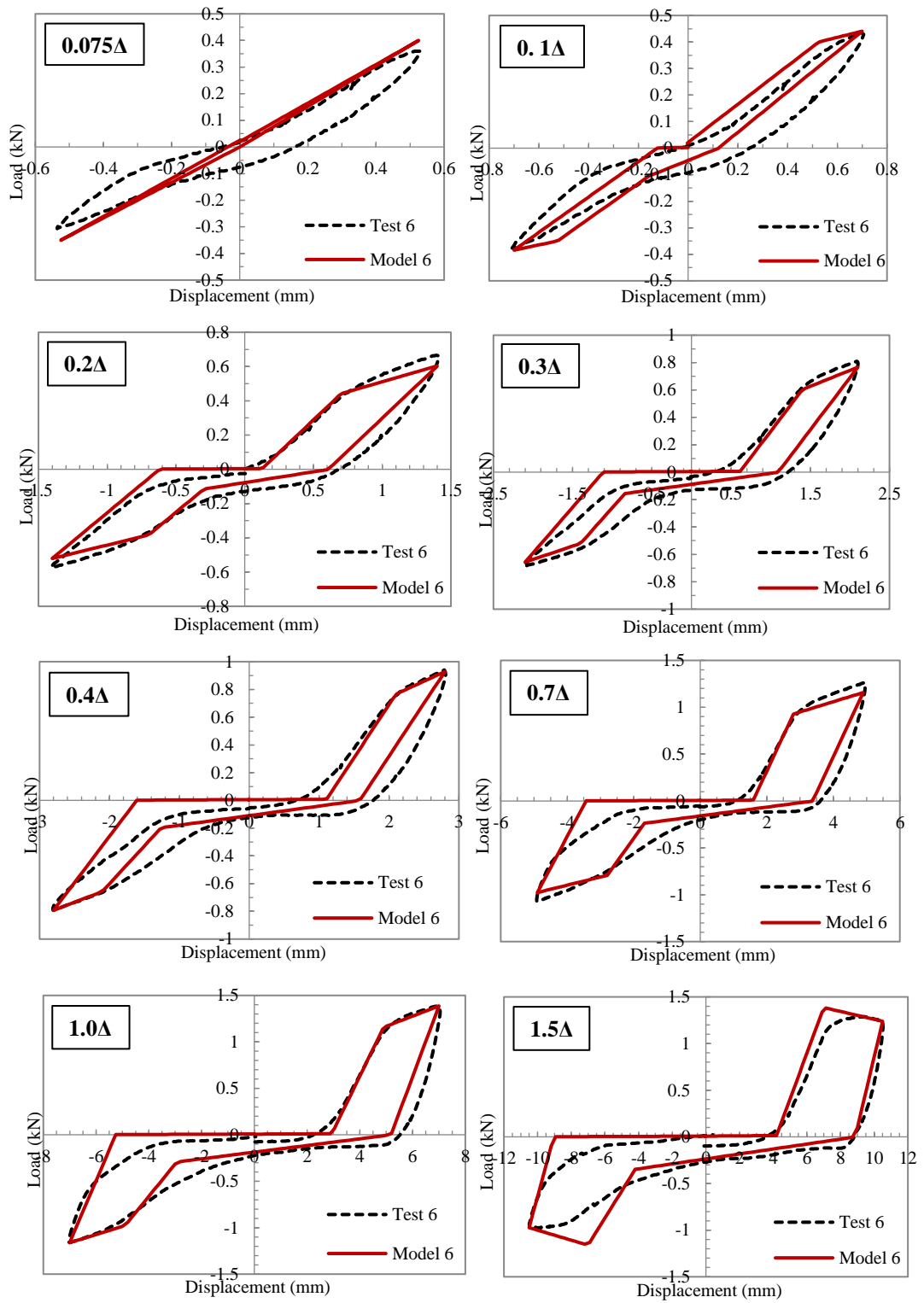


Figure 6.7 Cyclic fastener model calibration

6.2.3. Multi-Panel Wall Models

Numerical models of walls comprising two and four individual wall panels were also created and analyzed in order to investigate their behavior in relation to single panel walls. Details of these multi panel wall models, which had overall dimensions of 2.44x2.44 m and 4.88x2.44 m, are given in Figure 6.8. Each OSB sheathing panel in these models was represented by a separate rigid diaphragm. A single stud member was defined along the edge common to two neighboring diaphragms. Zero-length elements representing connection screws belonging to two neighboring diaphragms are connected to the same nodes located on these common stud members. Linear springs representing hold-down devices were defined only at the very ends of walls, in other words these spring elements were not used at the base of common stud members. Modeling technique used for the fasteners providing connection between sheathing panel and framing members was similar to that used for the single-panel wall model. Material models used for connection screws and hold down elements were also similar to those used for the single-panel wall model.

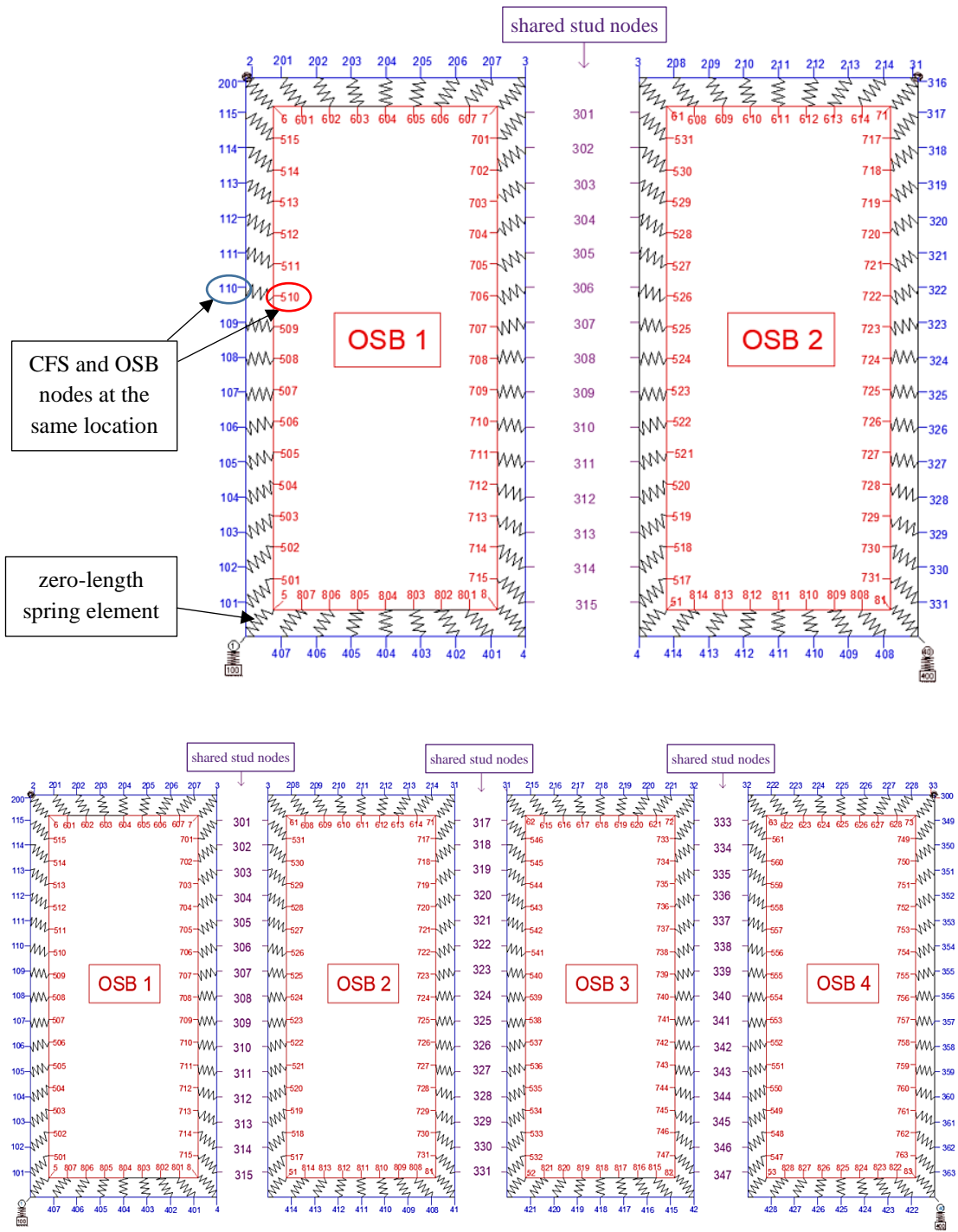


Figure 6.8 General layout of two- and four-panel shear walls

6.3. Wall Model Results

6.3.1. Investigation of Local Fastener Response

As mentioned earlier, behavior of sheathed CFS framed shear walls under lateral loading is mostly dictated by the local response around the connection screws. In order to study the relation between the local fastener response and the overall wall response results obtained from the shear wall numerical model are investigated in detail. In an attempt to study the response without the additional complication provided by reversed cyclic loading, results from the monotonic loading were used for this purpose.

The fastener material model used in one of the shear wall numerical models is given on the left hand side in Figure 6.9. Stiffness of the load-displacement response assigned to individual stiffeners changes at these four points. The plot on the right hand side in the same figure shows the overall load versus lateral displacement response of the shear wall as obtained from the numerical model. As evident, four points defining the local fastener response also appear on the global load-displacement response. This is a numerical evidence that the overall shape of the wall load-displacement response as well as the corresponding strength and stiffness levels are mostly dictated by the local fastener response.

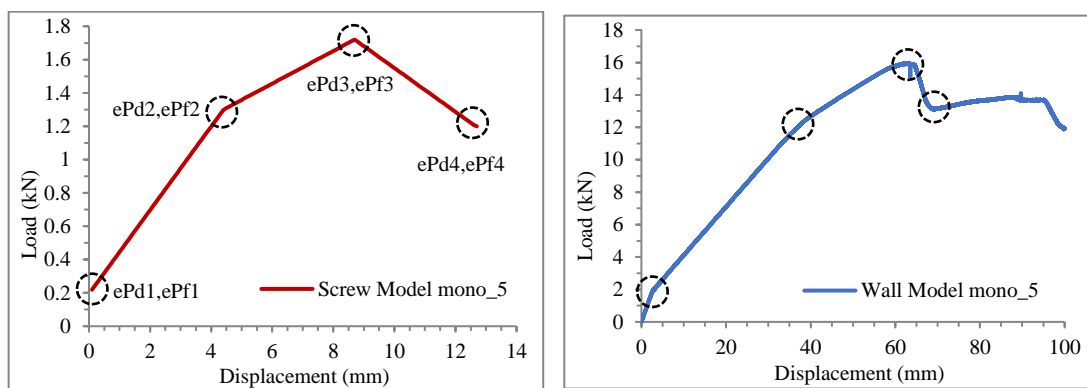


Figure 6.9 Similarity between fastener material model and overall shear wall response

In order to understand individual and group behavior of fasteners under different load levels, status of fasteners was investigated at different time steps during the analysis under monotonic loading. This investigation is summarized in Figure 6.10. Figure 6.10(a) shows four different stages in fastener material model having different stiffness values. This fastener model is based on the measured response from Fastener Test 5. Different colors were selected to represent each of these four stages in local fastener response. Stage-1 (blue zone) starting with first defined point has a certain stiffness value. After passing second defined point, stage-2 (green zone) begins which still has a positive slope with a lower stiffness value. At the end of stage-2, fasteners reach maximum capacity. In stage-3 (red zone), softening occurs and as a result capacity decreases as displacement increases. After passing the last defined point, stage-4 (purple zone) starts in which load remains constant and stiffness is set to zero. This last stage having constant capacity is an implemented feature into the Pinching4 material model to represent the failure of the fastener. Even though this approach for simulating the fastener failure might seem unrealistic, it was deemed suitable in the current study because the post-failure behavior of walls was not of interest.

Figure 6.10(b) presents load-displacement response of the CFS shear wall model with the fasteners represented by the material model shown in Figure 6.10(a). This wall model is the simulation of Wall Test 3 including HD-4 type hold-down. Analysis was continued up to a total wall lateral displacement of 100 mm. In Figure 6.10(b) the load-displacement response was divided into 20 equal segments with each segment corresponding to a wall lateral displacement of 5 mm.

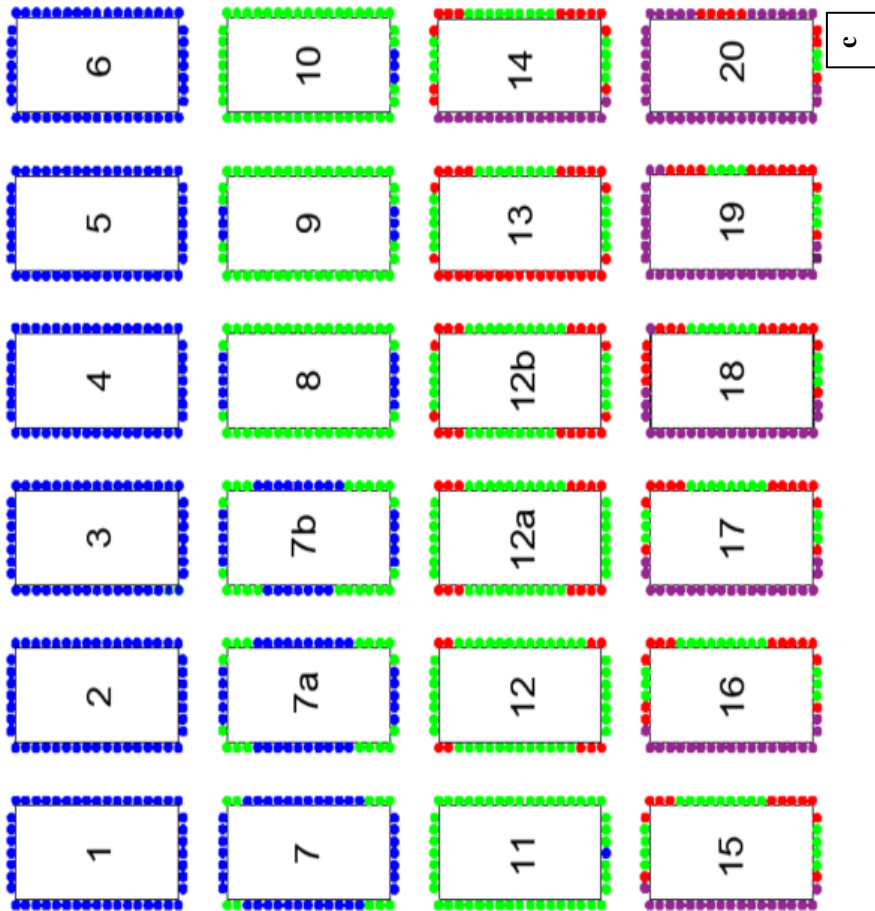
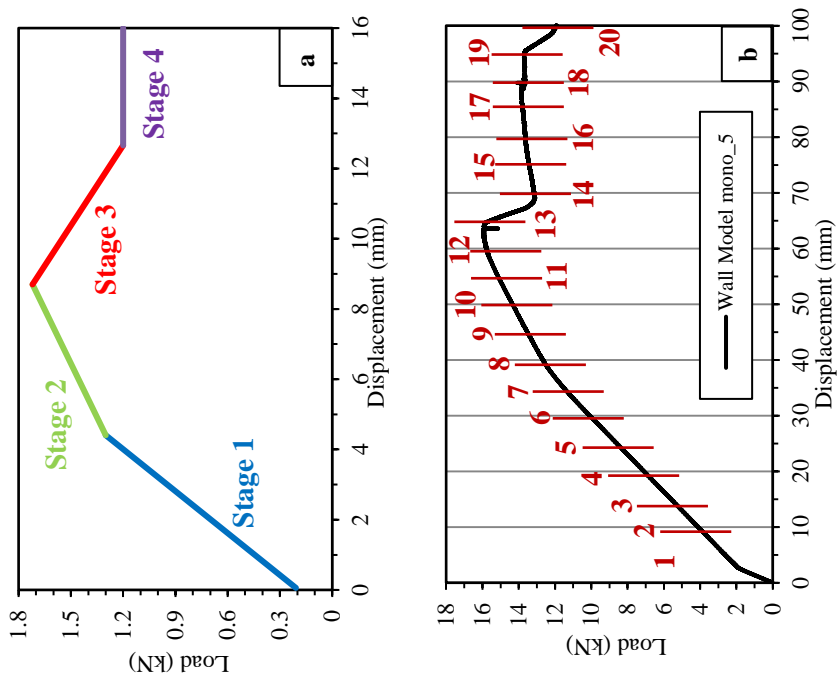


Figure 6.10 (a) Screw material model (mono-5) showing Stages 1-4 (b) Wall model response divided into 20 time steps (c) Stage of fasteners at each time step

For each of these 20 stations, stage that each individual fastener element falls in was determined. The stage that each individual fastener element falls in at each of the 20 stations marked on the overall load-deflection response is indicated with four different colors in Figure 6.10(c). Colors of fasteners indicate the four different stages shown in Figure 6.10(a). Distinctively, time steps 7-8 and time steps 12-13 were subdivided into smaller time steps in order to capture the change in status of fasteners more clearly.

As it can be seen from Figure 6.10(c) until station-7 all fasteners are in stage-1 (blue zone) and this reveals on Figure 6.10(b) as an increasing capacity with a constant stiffness. First major reduction in wall stiffness occurs at approximately 35 mm displacement (station-7). This reduction in wall lateral stiffness corresponds to transition of the fasteners at wall corners from stage-1 to stage-2. By the time wall top displacement reaches 40 mm (station-8) all of the fasteners located in tension and compression studs entered into stage-2. Because stage-2 (green zone) in local fastener response still has a positive slope, the lateral force resisting capability of the wall continues to increase even all fasteners have entered into stage-2.

In wall response, a major stiffness change occurs at approximately 60 mm displacement (station-12). As evident in Figure 6.10(c), this point corresponds to entering of the fasteners located in wall corners into stage-3. Immediately after the fasteners started to enter into stage-3, lateral force resisting ability of the wall has deteriorated rapidly. The reason for this behavior is the fact that in stage-3 fasteners exhibit softening response with negative slope in local load-displacement response.

After station-13, it is observed that stud fasteners enter into stage-4 rapidly. Starting from station-14, there are fasteners on boundary framing members that have entered into stage-2, stage-3 and stage-4. Because of the positive stiffness that the fasteners possess in stage-2, force resisting ability of the wall increases slightly between station-14 and station-19. As explained before, even though stage-4 provides a constant fastener capacity with an increasing displacement, this stage actually corresponds to

failure of fasteners. Therefore, part of the overall wall response for displacement values higher than 70 mm (i.e., after station-14) does not represent the actual behavior, as failure of the wall has already initiated at this level.

By considering 20 stations, changes in fastener stages are involved in numerical model and represented very well with load displacement response of shear wall. Fasteners located at corner locations of wall panel were observed to lead the fasteners at other locations in terms of following the local force-displacement response. Corner fasteners are followed by stud fasteners, which themselves lead track fasteners.

Figure 6.11 shows vector plot of the forces on individual fasteners. This plot enables an examination of magnitude and direction of forces develop in fasteners located at different parts of the shear wall. Magnitudes of fastener force were calculated for three different time steps: (1) elastic range (station-4), (2) maximum lateral load (station-13) and (3) maximum displacement (station-20). This plot also indicates higher fastener forces at wall corners consistently for all three stations shown. Fastener forces at studs are also higher in magnitude relative to those at chord members.

Figure 6.12 shows the variation of axial force in stud members when maximum lateral load was reached (station-13). Because this particular model was analyzed with no vertical gravity load, axial force in both the tension and compression studs are equal in magnitude. Axial force in studs increases from top of wall to the base. As evident in Figure 6.11, vertical component of fastener forces are all in the same direction for the tension and compression stud members. Axial force develops in studs as a result of force transfer from fasteners to these members when going down from top of wall to the base. Stud force changes along wall height almost linearly, indicating that the vertical component of forces in individual fasteners are almost the same for the stud members.

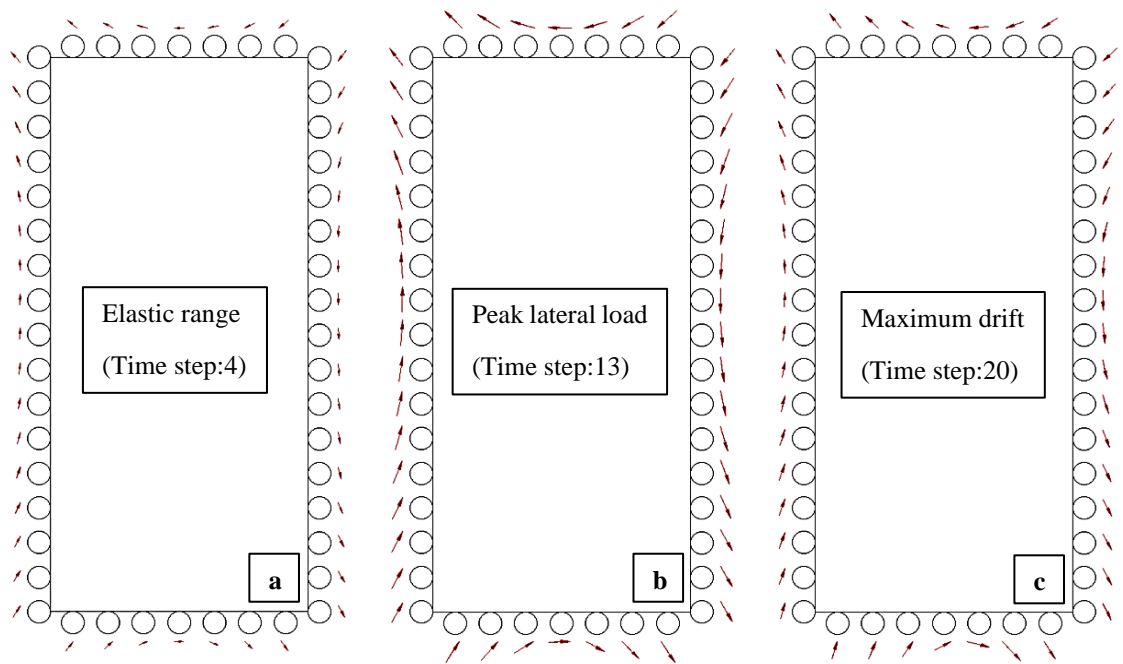


Figure 6.11 Vector plot of forces on fasteners at three different levels: (a) elastic range; (b) peak lateral load; (c) maximum drift

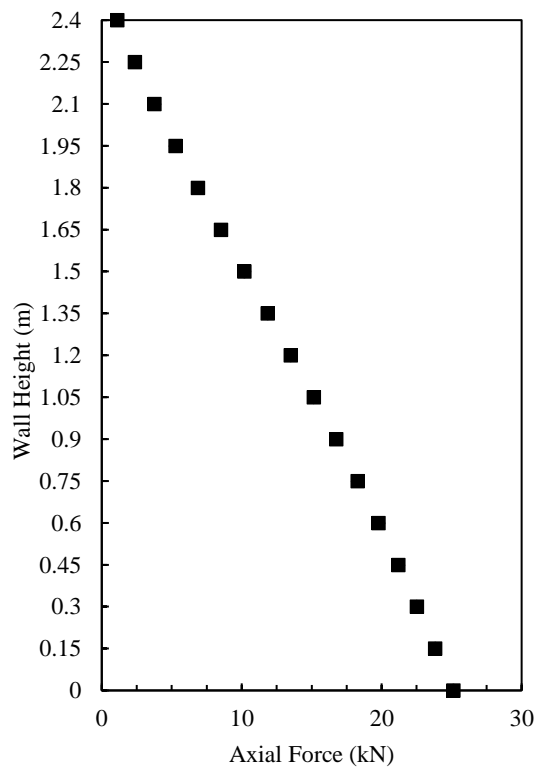


Figure 6.12 Axial forces in studs at peak lateral load

6.3.2. Comparison of Numerically Predicted and Measured Wall Response

Wall Model 3

Wall specimen-3 comprised of single-sided sheathing with 150 mm screw spacing and HD-4 hold down. The experimentally determined load-displacement response for this specimen was compared to the numerically determined response in Figure 6.13 - Figure 6.16. Comparison of load-displacement hysteresis curves obtained during the course of load testing (Figure 6.13) indicates the general agreement between the measured and predicted behaviors. Measured and predicted load-displacement hysteresis curves for several drift ratio cycles are presented in Figure 6.14. The numerical model performed satisfactorily in terms of accurately predicting not only the strength and stiffness of wall panel, but the significant pinching observed in the measured response was also accurately predicted.

In experimental data, there is an asymmetry in load-displacement hysteresis curves between positive and negative directions. As explained in Chapter 3, the reason behind this asymmetric response is the local deformation in OSB panel and CFS members around the connections as a result of tilting and bearing of screws. When the loading direction was reversed, connection screws were able to develop a smaller level of force due to already existing local bearing deformation in OSB panel and CFS members. As a result, the wall panel exhibited smaller load capacity and stiffness in one loading direction compared to the other direction. However, numerical model produced symmetric load-displacement behavior for wall panel with similar load capacity and stiffness in positive and negative loading directions.

Change in the stiffness and energy absorption capability of wall panel are presented in Figure 6.15 and Figure 6.16. The plots include both the measured and numerically predicted responses for both loading directions. Wall panel suffered from significant stiffness degradation as loading progressed. As evident in the plots, the numerical wall model was able to accurately predict the measured stiffness degradation response. On the other hand, the numerical model consistently underpredicted the energy absorbed by wall panel at each drift cycle.

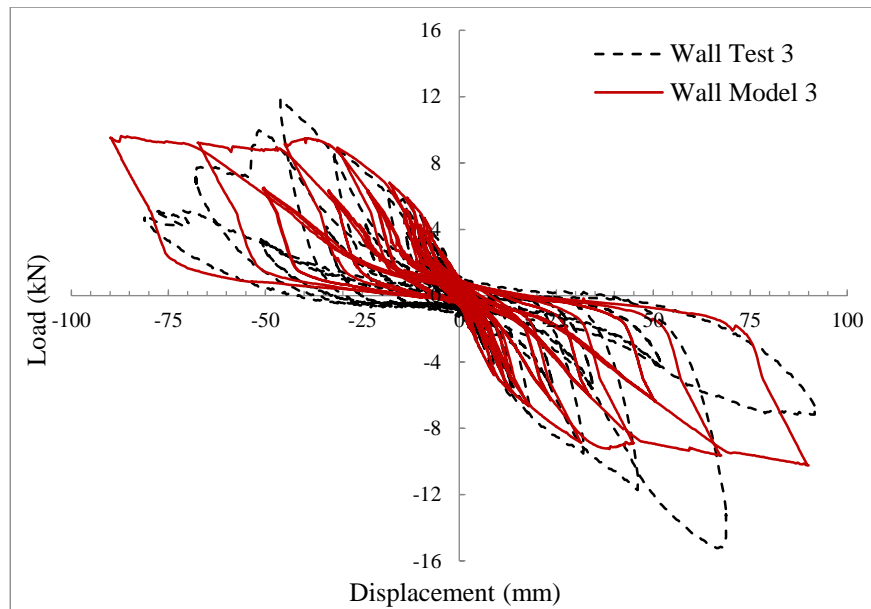


Figure 6.13 Load-displacement responses of shear wall test 3 and model 3

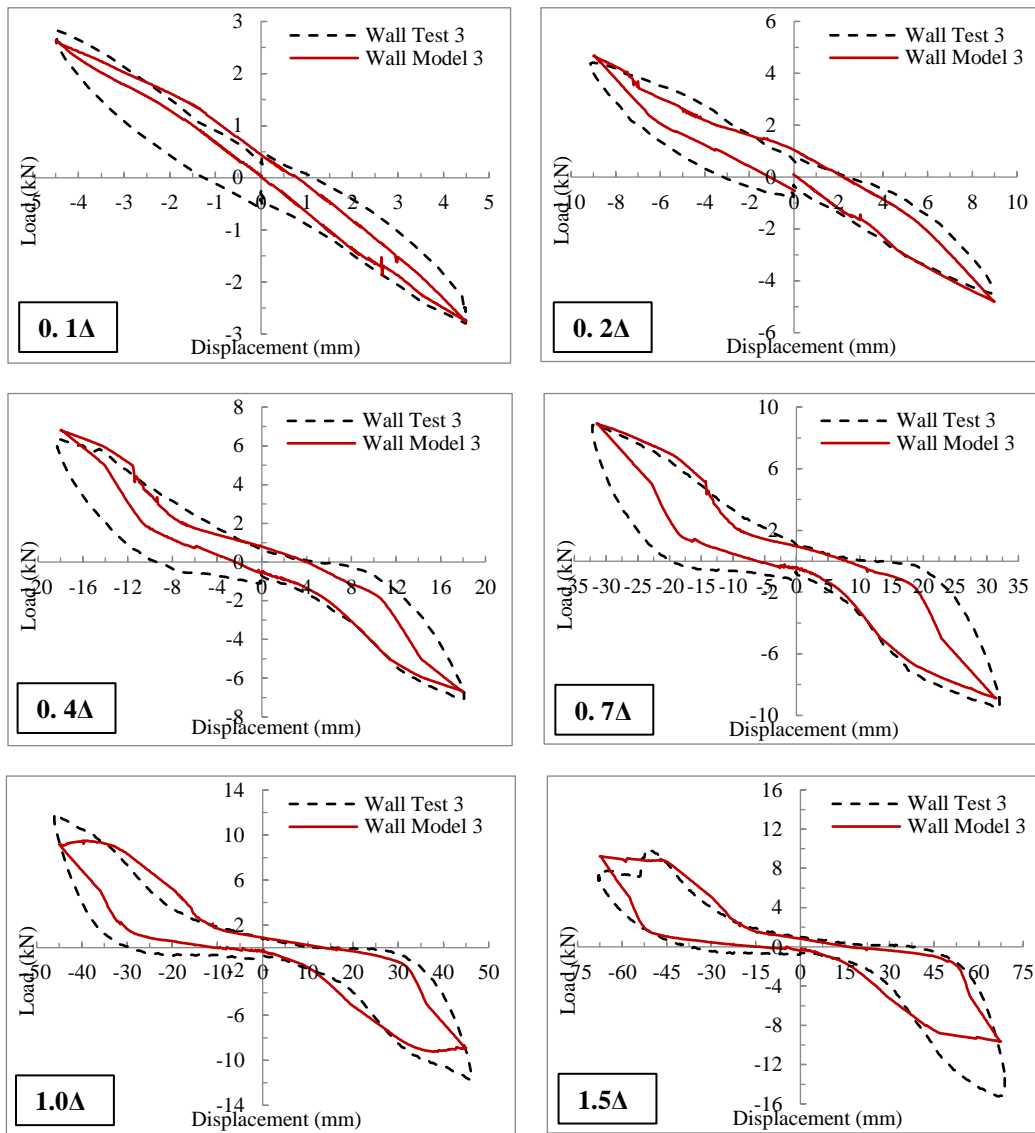


Figure 6.14 Comparison of test 3 and model 3 results through main cycles

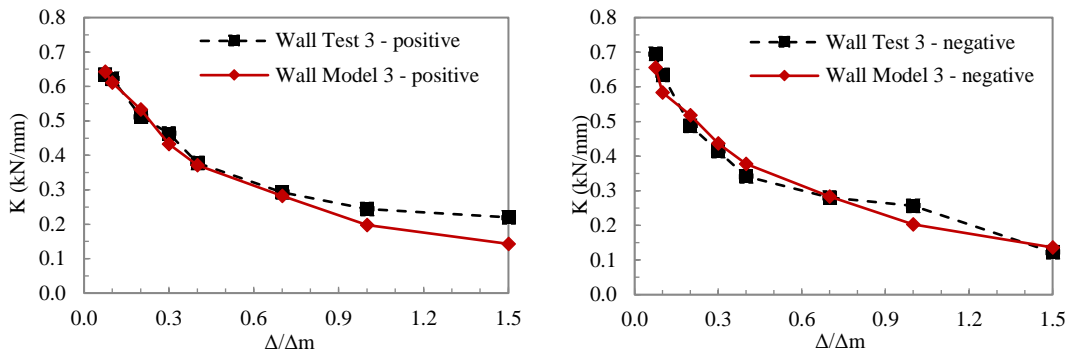


Figure 6.15 Comparison of test 3 and model 3 results through stiffness curves

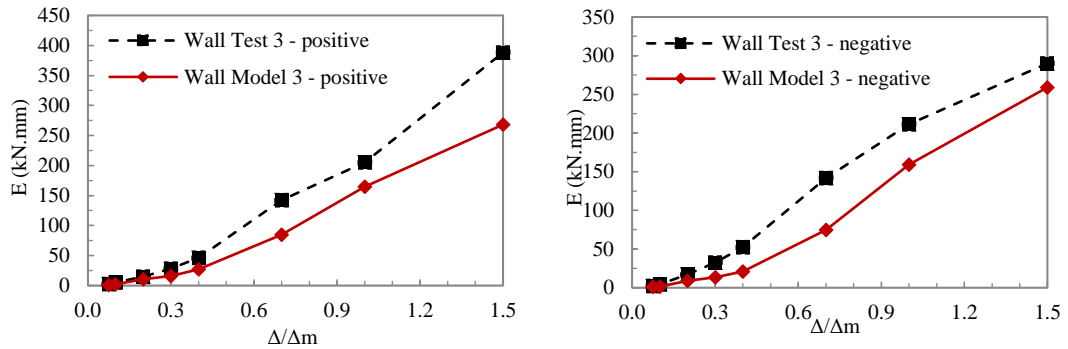


Figure 6.16 Comparison of test 3 and model 3 results through energy curves

Wall Model 4

Wall specimen-4 had the same sheathing and screw layout as well as the hold down device as the previously investigated specimen-3. Unlike the previous specimen, wall specimen-4 was subjected to 20 kN vertical gravity load during lateral load testing. The response obtained from the numerical model for this wall is presented in Figure 6.17-Figure 6.20. During load testing of the specimen screws located near the top corners of wall panel were observed to pull out of the OSB panel. This damage resulted in sudden decreases in load resisting ability of the wall specimen as shown in Figure 6.17. On the other hand, because this type of local damage was not reflected in the material model used for the fasteners in the wall numerical model no such load

drops are observed in the numerically determined load-displacement curves. As evident in Figure 6.18, the numerically predicted load-displacement hysteresis behavior agrees well with the experimental measurements prior to the occurrence of failure in the specimen, indicating the ability of the wall numerical model to accurately predicting the wall response even with the presence of gravity loading. Similar accuracy is also valid in the stiffness degradation and energy absorption behaviors predicted by the wall numerical model (Figure 6.19 and Figure 6.20).

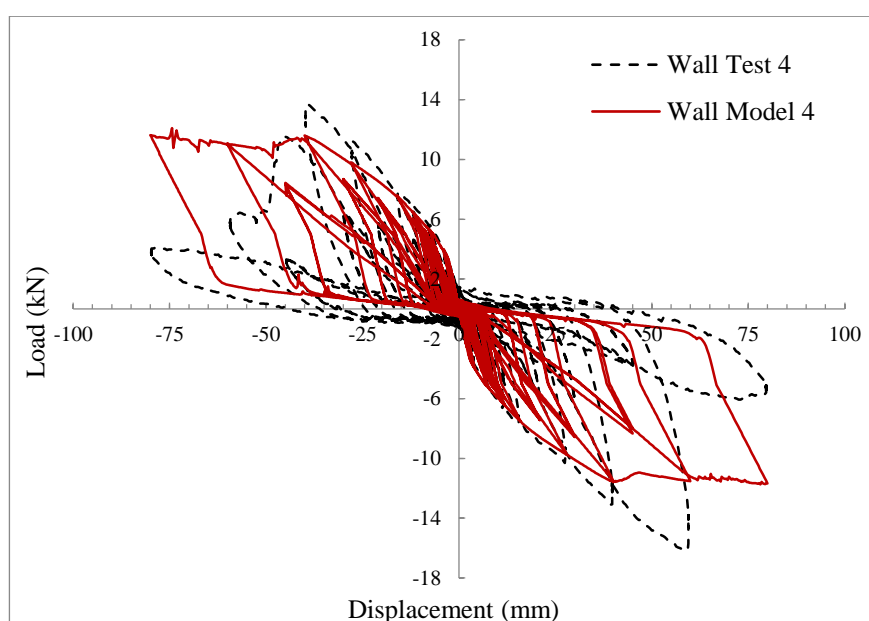


Figure 6.17 Load-displacement responses of shear wall test 4 and model 4

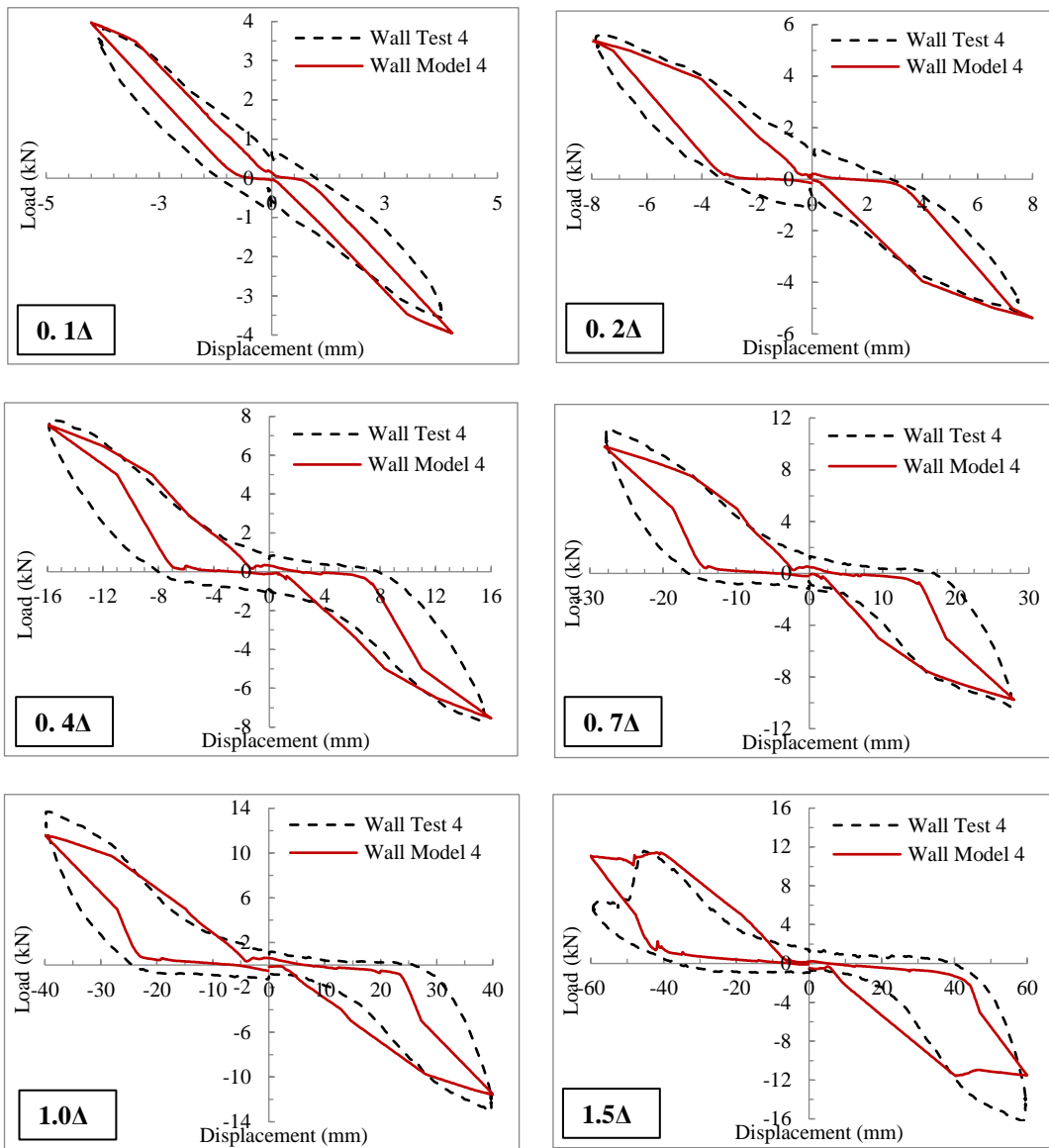


Figure 6.18 Comparison of test 4 and model 4 results through main cycles

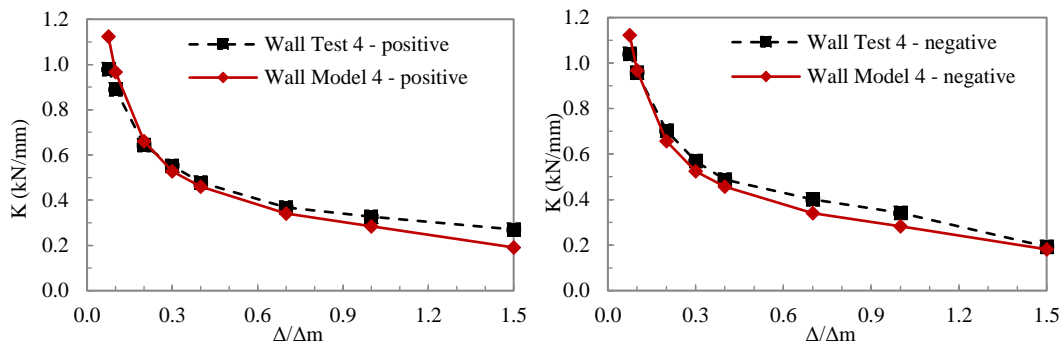


Figure 6.19 Comparison of test 4 and model 4 results through stiffness curves

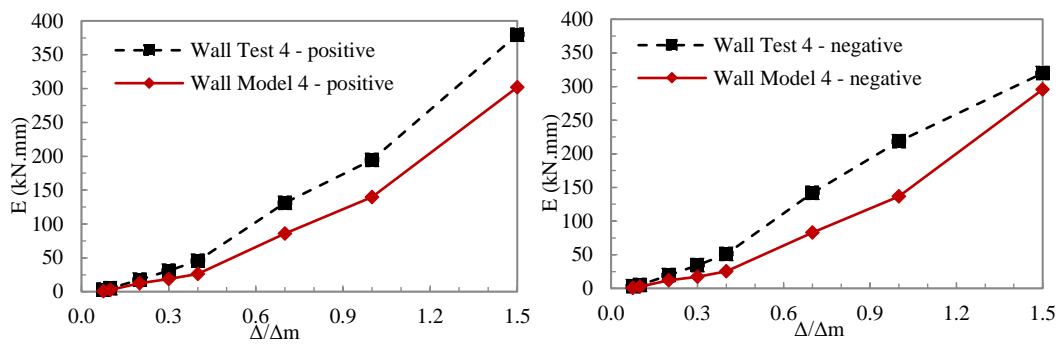


Figure 6.20 Comparison of test 4 and model 4 results through energy curves

Wall Model 8

Different than the previously investigated wall specimens, specimen-8 was tested with a dense screw layout. In this specimen screws providing the connection between OSB sheathing panel and CFS profiles were placed at 50 mm spacing, as opposed to the 150 mm spacing used in the previously investigated specimen-3 and specimen-4. This dense screw layout resulted in relatively high stiffness and load capacity in wall response. This wall specimen included HD-7 type hold down devices and was subjected to lateral loading with no gravity load. The experimentally determined load-displacement response for this specimen was compared to the numerically determined response in Figure 6.21-Figure 6.24. Numerically determined response for this wall panel tested with a dense screw layout agrees well with the experimentally determined response for all drift cycles.

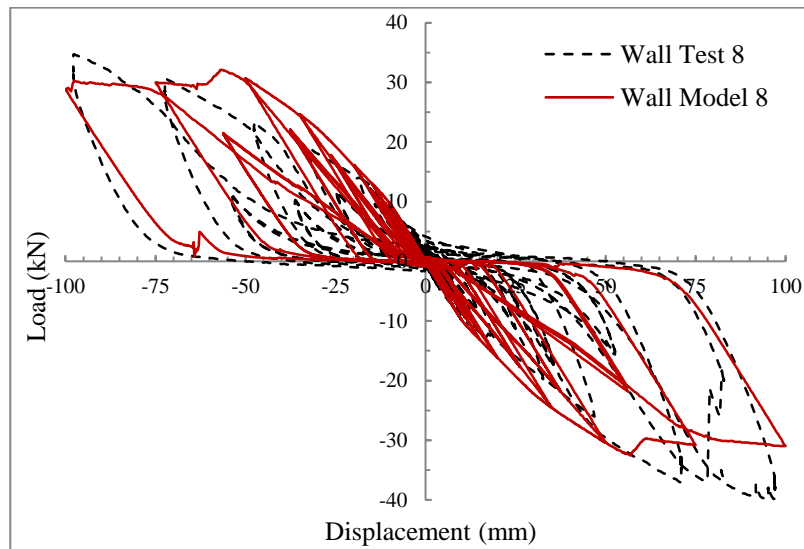


Figure 6.21 Load-displacement responses of shear wall test 8 and model 8

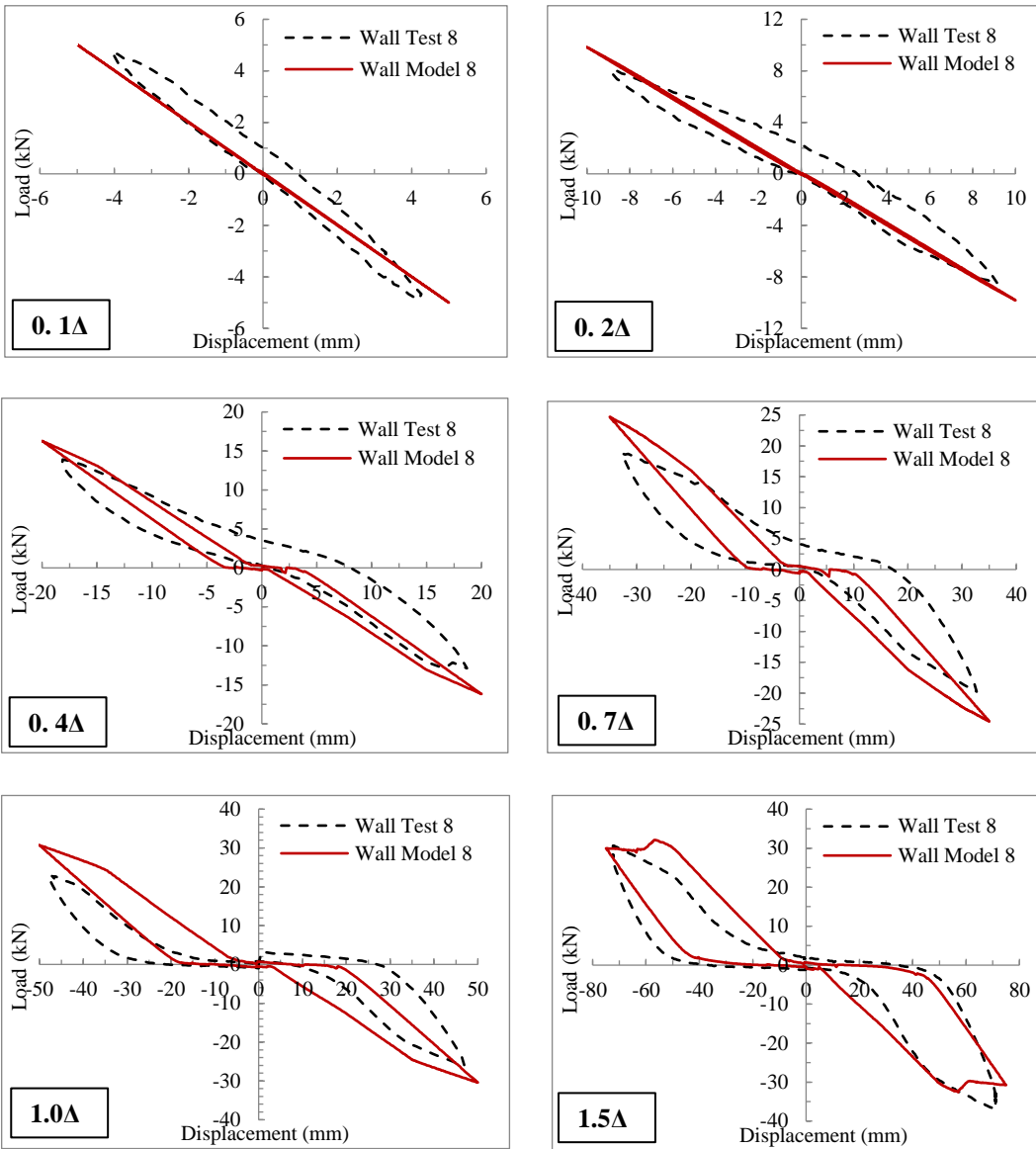


Figure 6.22 Comparison of test 8 and model 8 results through main cycles

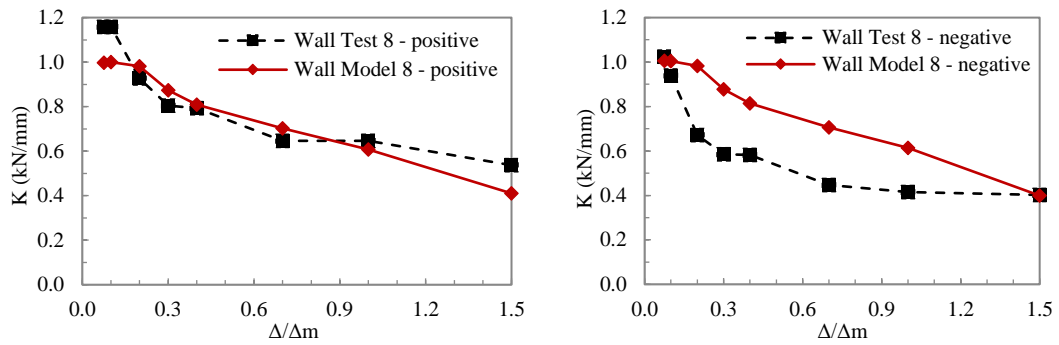


Figure 6.23 Comparison of test 8 and model 8 results through stiffness curves.

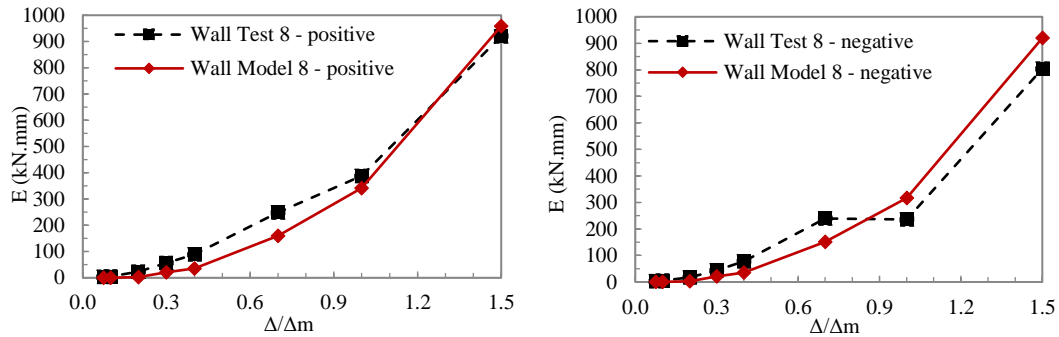


Figure 6.24 Comparison of test 8 and model 8 results through energy curves

Wall Model 18

In order to improve the wall stiffness and load capacity two-sided sheathing was used together with a dense screw layout (i.e., 50 mm screw spacing) in wall specimen-18. HD-8 type hold down devices were used and the wall was subjected to lateral loading with no gravity load. As a shortcoming of the 2D numerical modelling approach adopted in this study, double-sided sheathing condition could not be modeled. Instead, the number of screws was doubled with a single-sided sheathing by reducing the screw spacing to 25 mm in wall numerical model. The experimentally determined load-displacement response for this specimen was compared to the numerically determined response in Figure 6.25 - Figure 6.28. Numerically determined response for this wall panel tested with a double-sided dense screw layout agrees well with the

experimentally determined response for all drift cycles. Both the experimentally obtained and numerically predicted load capacities and stiffnesses are higher than the previously investigated walls. The numerical model overestimated the wall stiffness for both loading directions, with the degree of overestimation being higher between drift values of 0.4% and 1.5%. Other than the discrepancy between the predicted and measured stiffness values, the wall numerical model provides an accurate estimation of hysteresis curves and energy absorption characteristics.

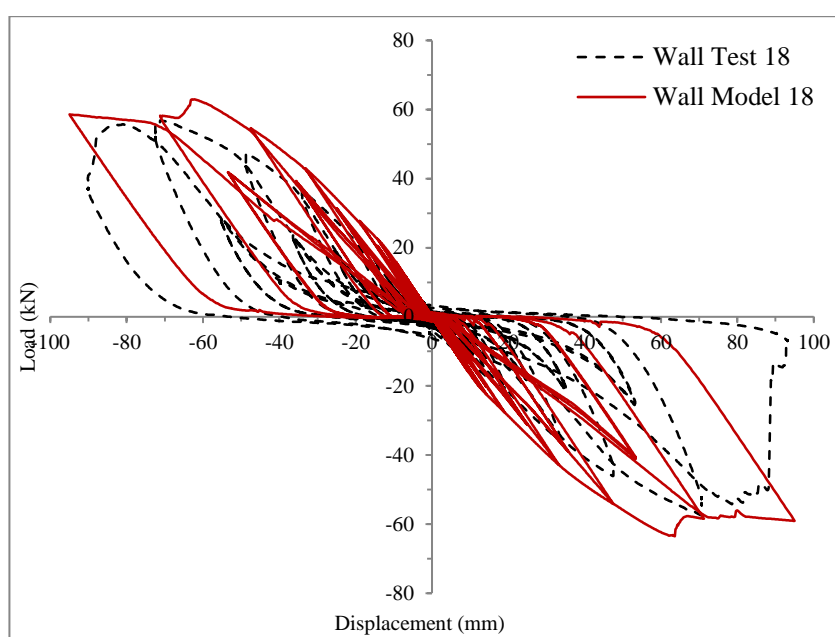


Figure 6.25 Load-displacement responses of shear wall test 18 and model 18

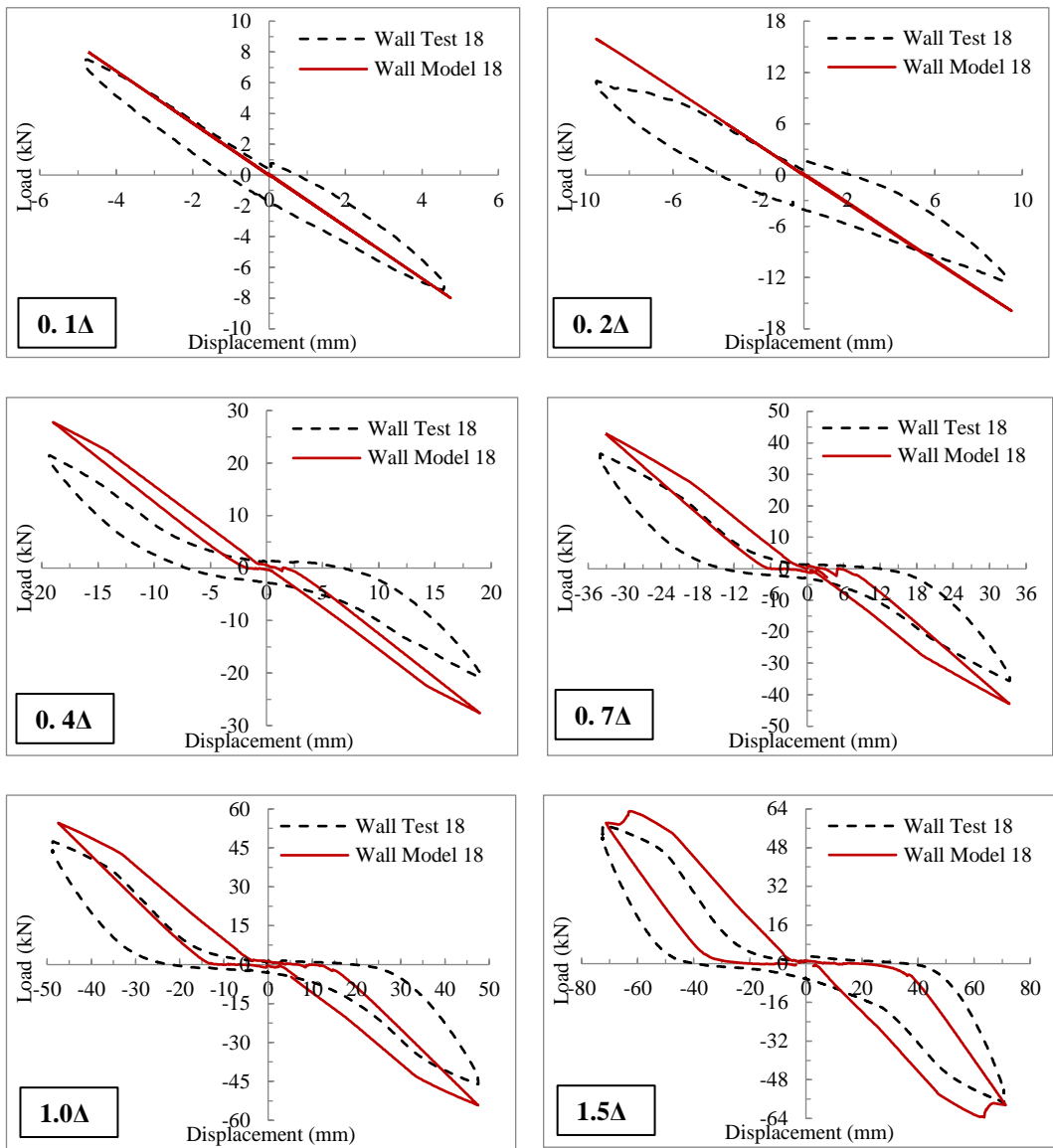


Figure 6.26 Comparison of test 18 and model 18 results through main cycles

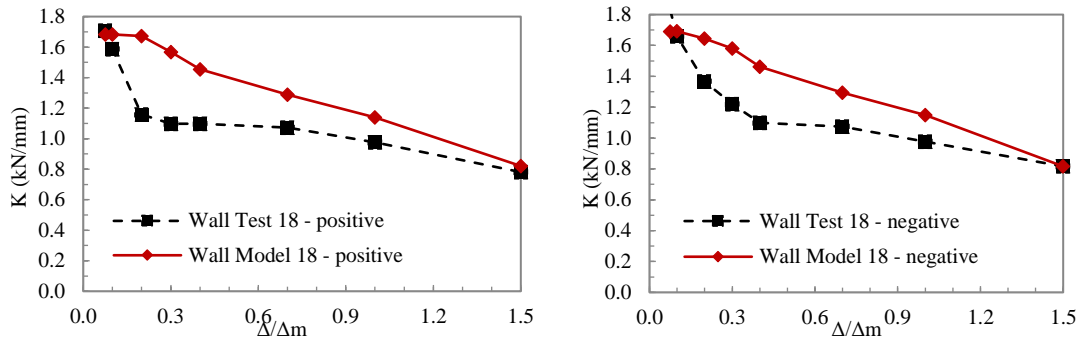


Figure 6.27 Comparison of test 18 and model 18 results through stiffness curves

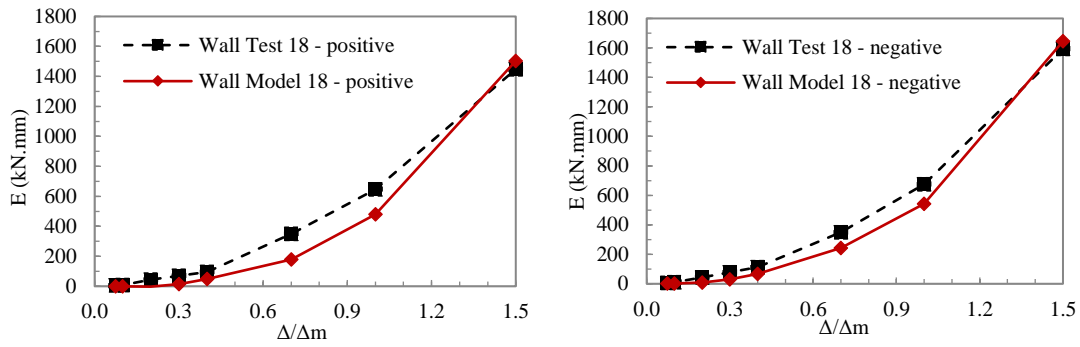


Figure 6.28 Comparison of test 18 and model 18 results through energy curves

Wall Model 24

Specimen-24 comprised of two wall panels and had overall dimensions of 244 cm x 244 cm. The wall had single-sided sheathing with 150 mm spaced screws and was tested with no gravity loading. Screws located at top track member were observed to pull out of the OSB panel during load testing of this specimen. Sudden drop in load resisting ability present in load-deflection plot at approximately 3% drift ratio resulted from this pull out failure. As explained earlier, this type of damage was not reflected in the material model used for the fasteners in the wall numerical model. Therefore, the numerically obtained response does not exhibit the effect of experimentally observed failure. As evident in Figure 6.29 and Figure 6.30, the numerically predicted load-displacement hysteresis behavior agrees with the experimental measurements for all drift ratios up to 2% (i.e., 1.0Δ). Similar observations are valid between the predicted and measured stiffness degradation and energy absorption characteristics. These observations indicate that the numerical model developed in this study is capable of predicting the response of two-panel walls with similar accuracies as single-panel walls.

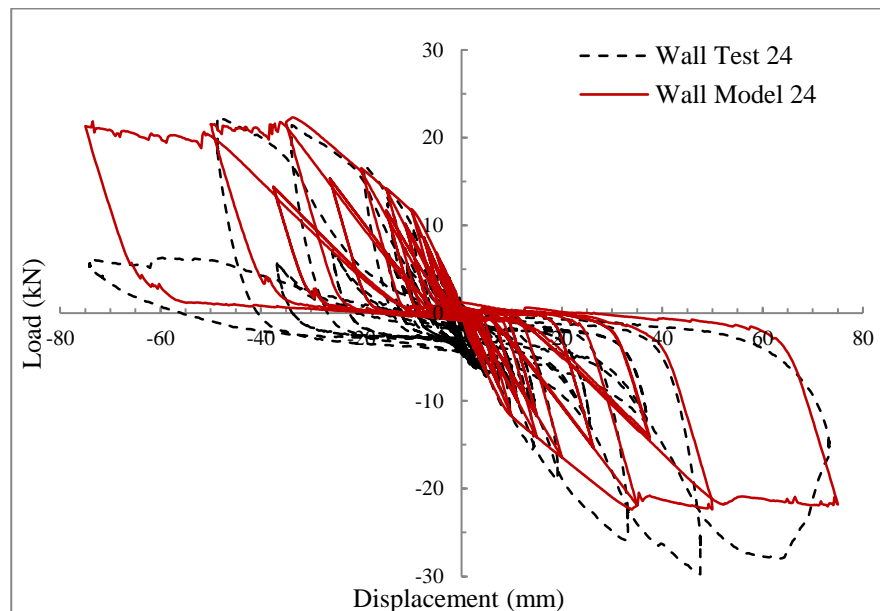


Figure 6.29 Load-displacement responses of shear wall test 24 and model 24

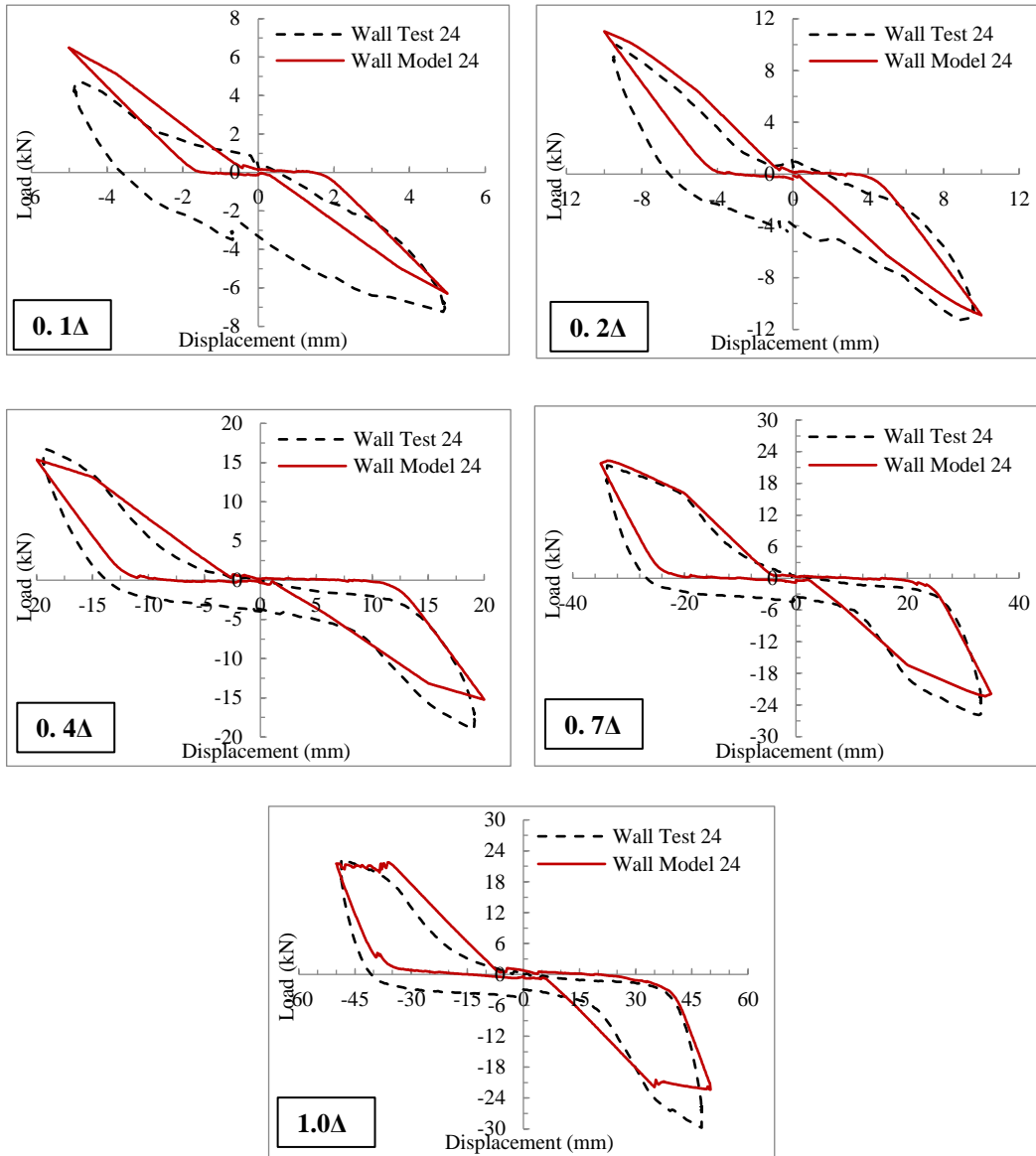


Figure 6.30 Comparison of test 24 and model 24 results through main cycles

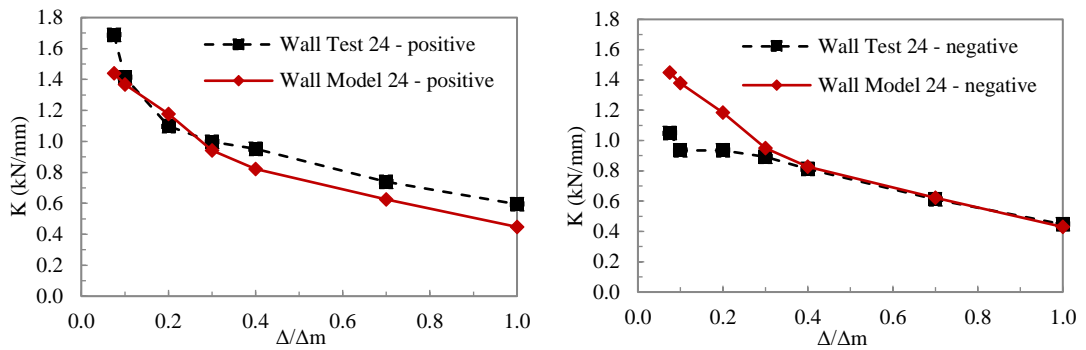


Figure 6.31 Comparison of test 24 and model 24 results through stiffness curves

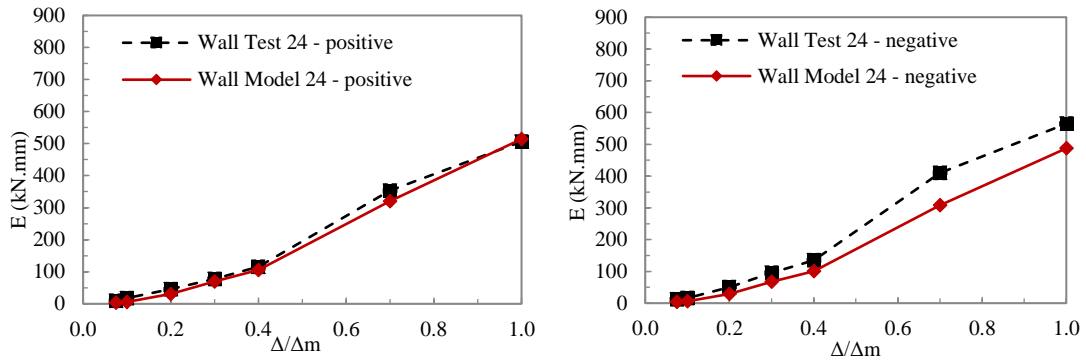


Figure 6.32 Comparison of test 24 and model 24 results through energy curves

Wall Model 37

Specimen-37 comprised of four wall panels with single-sided sheathing and had overall dimensions of 488 cm x 244 cm. A screw spacing of 150 mm was used in all four wall panels, and the specimen was tested with no gravity loading. Failure was observed during testing of specimen as a result of pull out of the screws located at one of the stud members from the OSB panel during the 3% drift cycle. As evident in Figure 6.33-Figure 6.36, the level of agreement between the numerically determined and measured response of this four-panel wall specimen is not as high as the predictions for the previously investigated wall specimens. The numerical model

consistently underpredicts the load capacity, stiffness and energy absorption of wall specimen. The reason for this underprediction can be attributed to the difference in boundary condition at the wall base between the model and the load tested specimen. Although the bottom tracks of wall panels in the specimen were restrained against downward displacement, this type of restraint did not exist in the wall numerical model due to numerical difficulties experienced during analyses. This additional deformation present in the numerical model resulted in underprediction of wall stiffness and load capacity. This issue was valid for the two-panel wall model as well, but its effect remained minimal. Discrepancy between the predicted and measured wall response due to improperly restrained wall base tends to increase as the number of wall panels forming the entire wall increases.

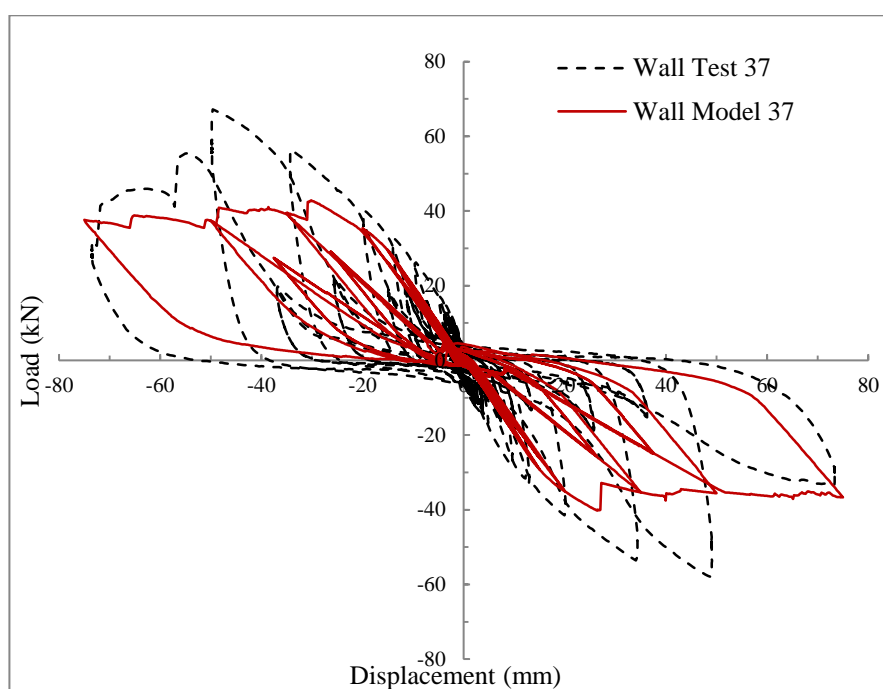


Figure 6.33 Load-displacement responses of shear wall test 37 and model 37

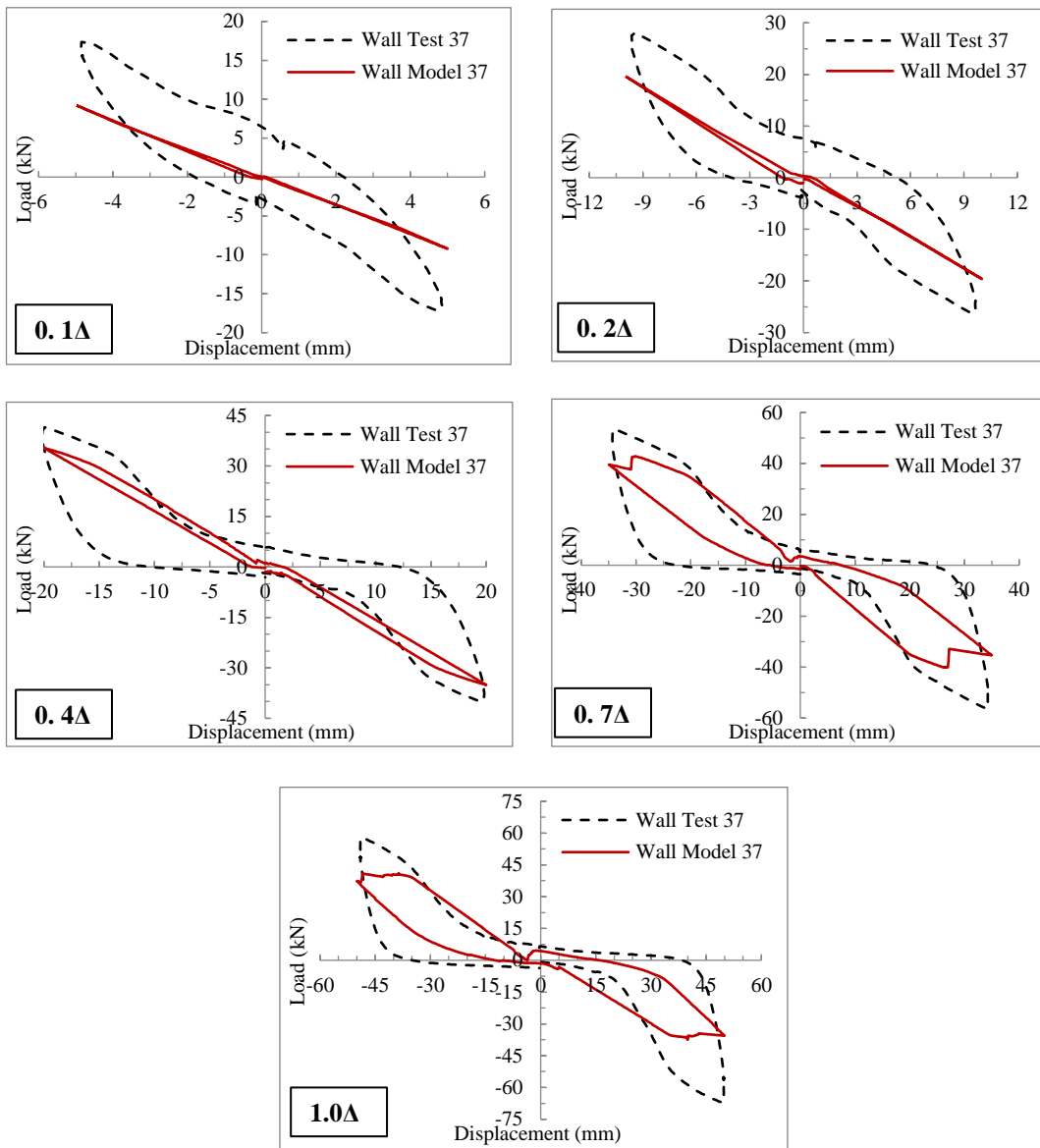


Figure 6.34 Comparison of test 37 and model 37 results through main cycles

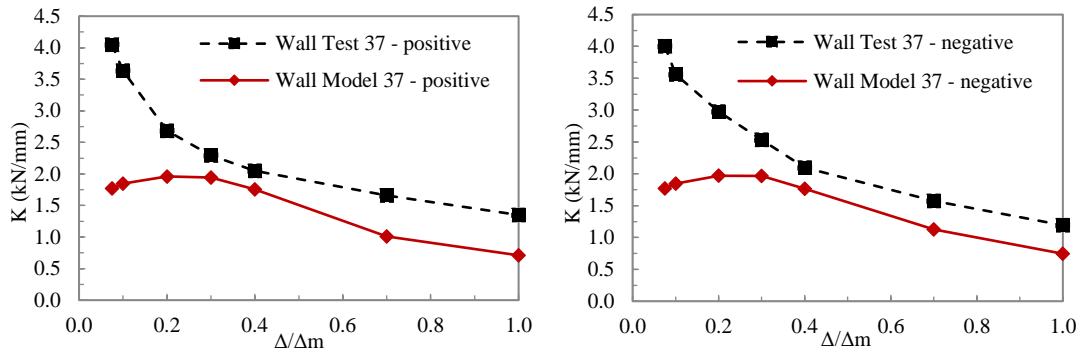


Figure 6.35 Comparison of test 37 and model 37 results through stiffness curves

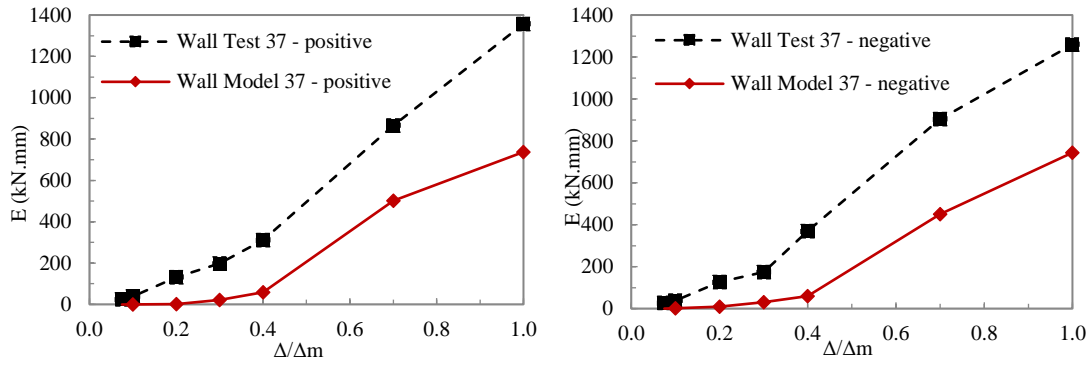


Figure 6.36 Comparison of test 37 and model 37 results through energy curves

CHAPTER 7

PARAMETRIC STUDY

In this chapter, effects of various parameters such as the local fastener behavior, fastener spacing, rigidity of stud-track connection, stiffness of CFS framing members, stiffness of hold-down members and the level of gravity loading on overall wall response are studied in detail. The analyses were conducted under monotonic loading in order to avoid the additional complexity due to reversed cyclic loading.

7.1. Effect of Local Fastener Behavior

As explained in Section 6.2.2, three different fastener material models were developed for monotonic loading based on measured data from fastener test program. These three models represent the upper bound (Test 3), lower bound (Test 5) and average (Test 1) response. In the wall numerical model these three material models (Figure 7.1) were assigned to the zero length elements simulating the fasteners between the sheathing panel and framing members. Overall wall responses as predicted by the numerical model for these three different fastener models are compared in Figure 7.2. Variation in the measured fastener response resulted in 28% difference in load capacity and 12% difference in stiffness of wall panels.

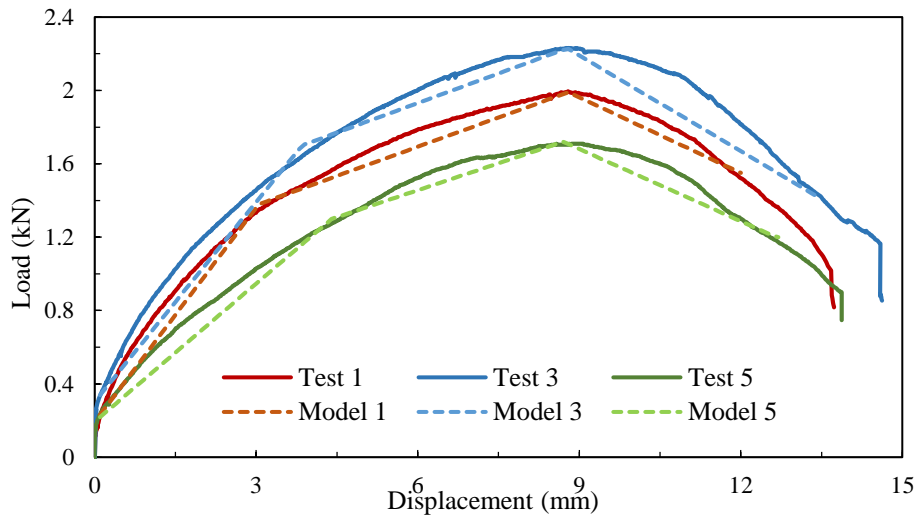


Figure 7.1 Selected fastener tests and their material models

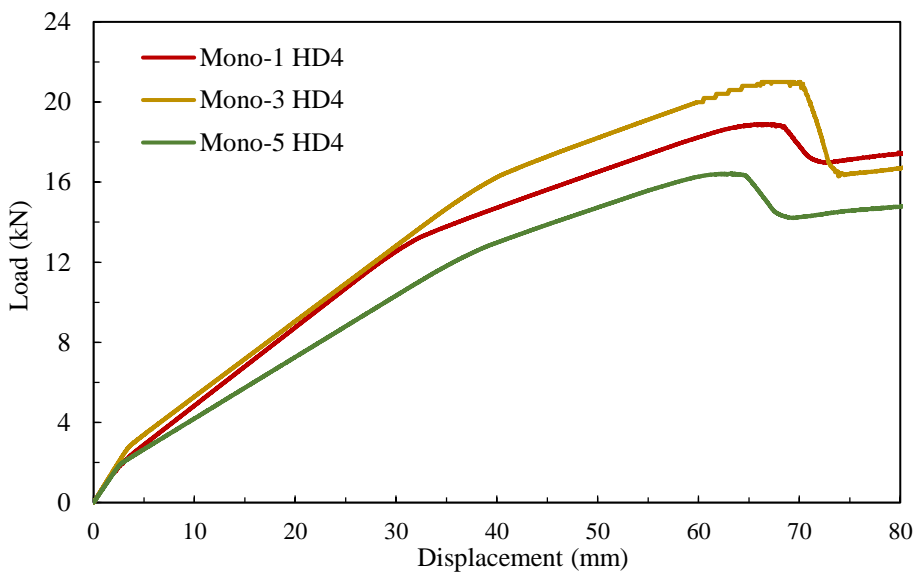


Figure 7.2 Comparison of wall model responses including different material models

7.2. Effect of Fastener Spacing

Since fastener spacing is directly related with number of fasteners providing force transfer between sheathing panel and framing members, it is an important parameter for a fastener-based numerical model. There were two different fastener spacing values used in wall tests; 150 mm and 50 mm. The same wall model was analyzed additionally with 300 mm and 25 mm fastener spacings. These spacing values can be considered as the practical upper and lower limits for fastener spacing to be used in sheathed CFS wall panels. The aim was to obtain the overall wall responses with these limiting fastener spacing values. Figure 7.3 shows load-displacement response of four wall models with fastener spacing values varying between 25 mm and 300 mm. As a result of the fastener-based approach used in wall numerical models, load capacity of wall panel is expected to be directly proportional to the total number of fasteners provided between sheathing panel and framing members. There are 48 fasteners in the case of 150 mm fastener spacing. When fastener spacing is reduced to 50 mm, number of fasteners becomes 144. Therefore, capacity for the model with 50 mm fastener spacing is expected to be three times of the one with 150 mm spacing. This expected trend in wall load capacity exists in numerical results as seen in Figure 7.3. In order to build a better understanding, direct effect of number of fasteners on the load capacity is shown in Figure 7.4. As evident in this plot, decreasing the fastener spacing resulted in a proportional increase in load capacity. Another observation that is valid in Figure 7.3 is that wall lateral stiffness also increases with decreasing screw spacing.

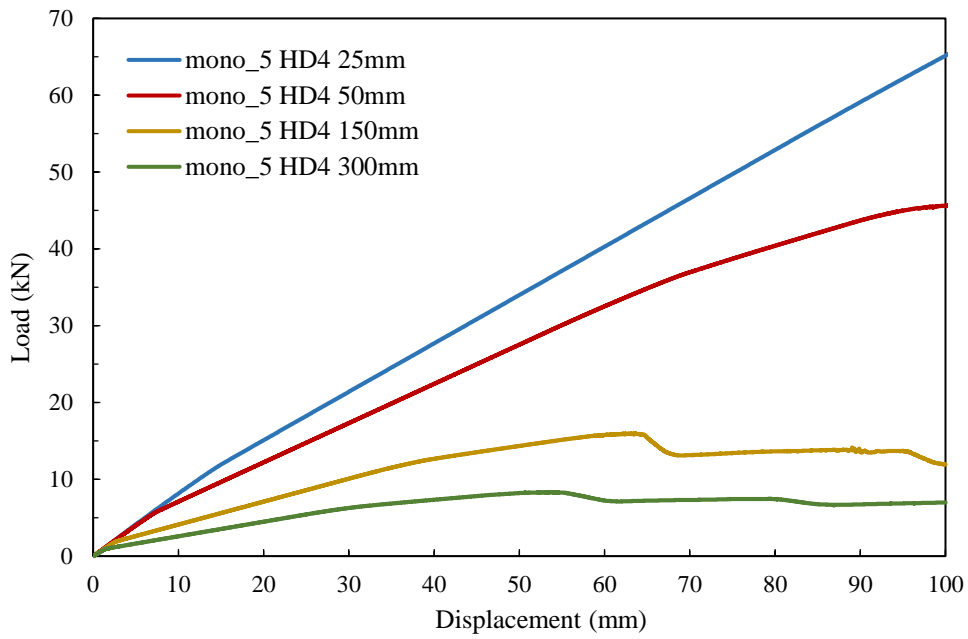


Figure 7.3 Load-displacement response of wall models having various fastener spacing

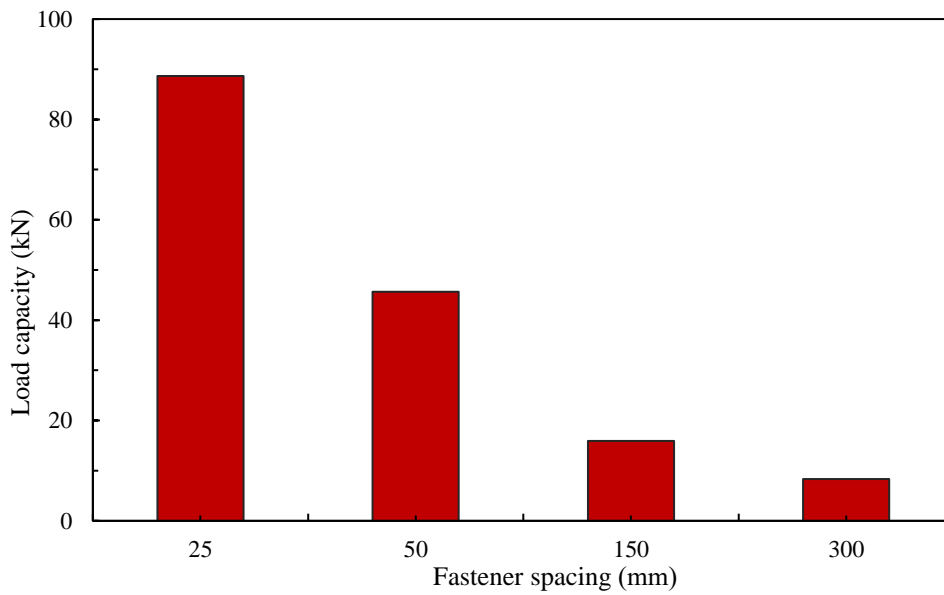


Figure 7.4 Relationship between number of fasteners and load capacity of wall panel

Effect of fastener spacing on wall response is studied in detail in Figure 7.5. This figure shows the result of a similar study with Section 6.3.1. It was aimed to see the differences in local behavior of fasteners due to fastener spacing. For this reason, two wall models were selected with 150 mm and 300 mm fastener spacing. Figure 7.5(a) shows four different stages in fastener material model. These stages are characterized by different stiffnesses. This fastener model is named as mono_5 which is the simulation of Fastener Test 5. Wall model responses for the cases of 150 mm and 300 mm fastener spacing were plotted together in Figure 7.5(b). Wall models were subjected to a total lateral displacement of 100 mm applied at the top level of wall, and this total displacement was divided into 20 segments. Therefore, each segment shown in Figure 7.5(b) corresponds to 5 mm lateral displacement. For each of the 20 stations, which are 5 mm lateral displacement apart from each other, stages of all fasteners were specified and schematized in Figure 7.5(c) with two rows. First row indicates the wall model with 150 mm fastener spacing while the second one shows the wall with 300 mm spacing.

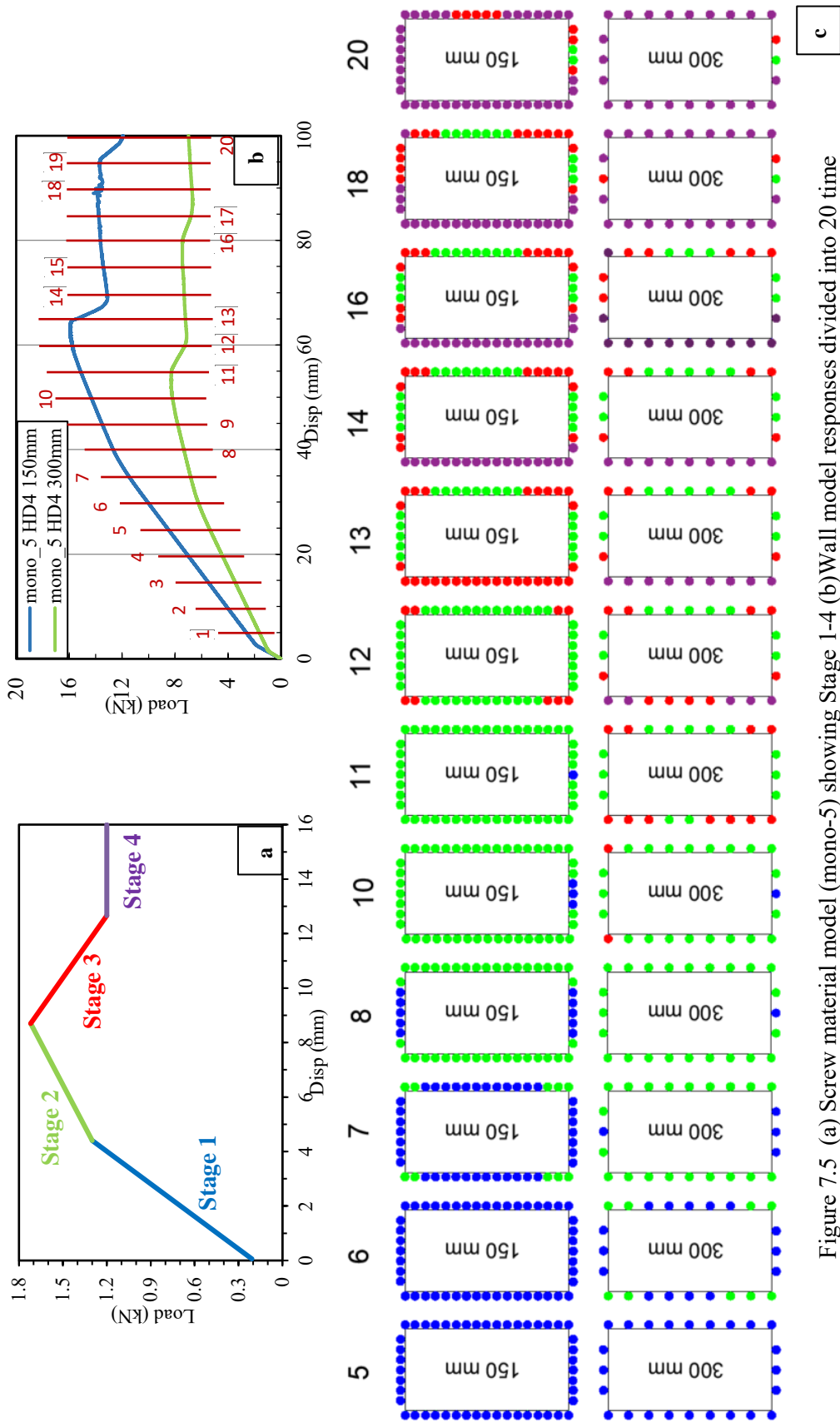


Figure 7.5 (a) Screw material model (mono-5) showing Stage 1-4 (b) Wall model responses divided into 20 time steps (c) Stages of fasteners at each step

Analysis results indicate that transition of screws from one stage to the next one occurs earlier in the wall model containing fewer screws (i.e., the model with 300 mm screw spacing) than the other model. This behavior is valid for all four stages of local fastener response. In other words, the wall model with 150 mm screw spacing lags behind the model with 300 mm screw spacing in terms of local fastener damage. For example, in the wall model containing fewer screws all screws entered into stage-2 at station-8 (i.e., at a lateral displacement of 40 mm), whereas in the other wall model this condition did not occur until station-11 (i.e., lateral displacement of 55 mm).

7.3. Effect of Hold-Down Stiffness

As explained in Section 6.2.1, three hold-down models, named as HD-4, HD-7 and HD-8, were used in wall panel model. Stiffness values calculated from load testing of these three hold-down devices were 3500 kN/m, 6000 kN/m and 10000 kN/m, respectively. In order to study the effect of hold-down stiffness on the overall wall panel response wall numerical model was analyzed with various hold-down stiffnesses. In addition to the existing HD-4, HD-7 and HD-8 devices, hypothetical hold-downs with 2000 kN/m and 1000 kN/m stiffnesses were also analyzed. These stiffness values represent very flexible hold down devices that deform significantly under tensile forces. In order simulate an idealized condition of a rigid hold down device the same wall numerical model was also analyzed with a pin support defined at bottom corners of wall panel instead of link elements simulating the hold down devices. Wall model responses obtained from these analyses are plotted together in Figure 7.6.

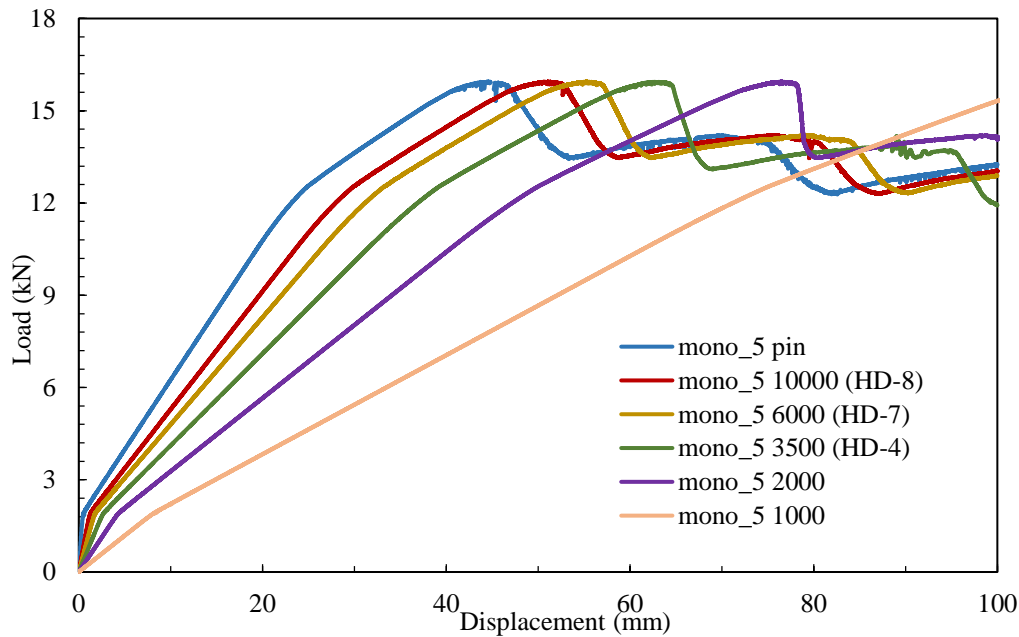


Figure 7.6 Load-displacement response of wall models having various hold-downs

As seen in Figure 7.6, wall model response is highly affected from the stiffness of hold-downs. Using higher hold down stiffness resulted in stiff wall response without changing the wall load capacity. Therefore, it can be concluded that assignment of a realistic value for hold-down stiffness is very important for the accurate representation of overall wall response. Another observation that is valid in Figure 7.6 is that the HD-8 hold down device used in wall panel test program is close to a rigid device in terms of wall panel response.

7.4. Effect of CFS Framing Member Stiffness

As mentioned earlier, CFS C-shaped profiles with 140 mm depth and 1.2 mm thickness (named as C140x1.2S350) were used for framing members in wall panel testing program. These members were defined as linear elastic elements in wall panel model. In order to study the effect of CFS member stiffness on wall response, CFS C-shaped profiles with 2.4 mm and 3.6 mm thickness were also considered in

addition to the already existing case of 1.2 mm thickness. The change in profile thickness was reflected in wall numerical model by changing the cross-sectional area and moment of inertia of framing members.

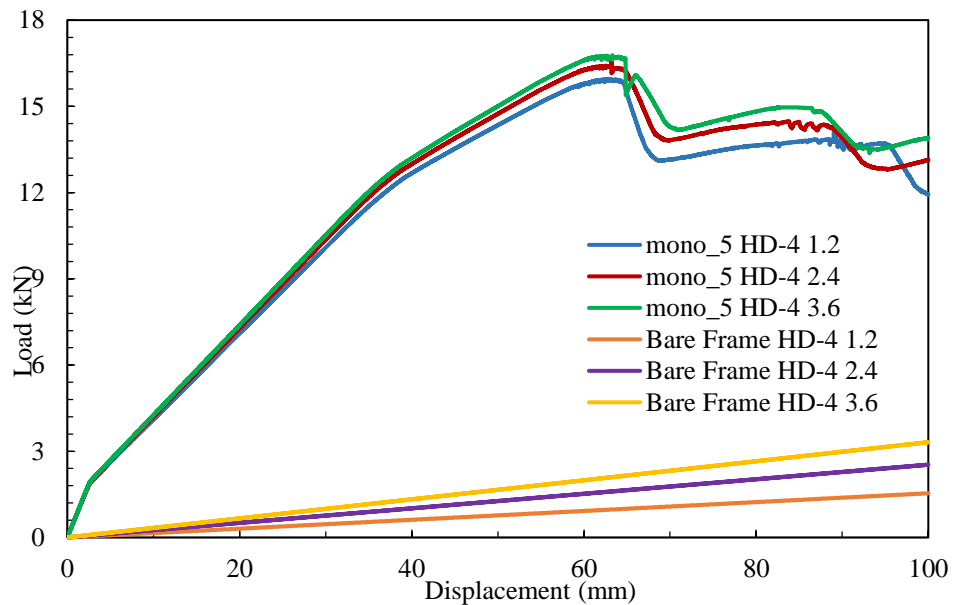


Figure 7.7 Load-displacement response of wall models having CFS with various thicknesses

Load-displacements curves for wall panels representing three different profile thicknesses are plotted in Figure 7.7. There is no significant difference between the wall model responses having different CFS thicknesses. This is because the wall response is mostly dictated by the local response at fastener locations and CFS frame itself has a small contribution. However, without OBS sheathing, it is expected that CFS frame thickness should have a direct effect on wall model response. Figure 7.7 also shows bare frame load-displacement responses with three different CFS profile thickness values. Lateral stiffness of the bare frame increases significantly with increased CFS profile thickness, as expected.

Plots provided in Figure 7.7 clearly indicate that the CFS framing itself possess very limited stiffness compared to the sheathed wall. From this observation it can be concluded that major part of the stiffness of a on OSB sheathed wall is provided by the sheathing panel itself with negligible contribution by the CFS framing.

It should be noted that the plots in Figure 7.7 do not represent the actual behavior of wall panels having 2.4 mm and 3.6 mm thick CFS framing members. Because an increase in the thickness of CFS profile would also result in an improvement in local fastener response. Peterman and Schafer (2013) conducted a series of connection experiments. One of their testing parameters was thickness of CFS profile. They studied CFS profiles with 0.8 mm, 1.4 mm and 2.5 mm thicknesses and found that profile thickness has a significant effect on the local fastener response. As it can be seen in Figure 7.8, CFS thickness has an effect on both the initial stiffness and load capacity of screws. Besides, studs having 2.5 mm thickness resulted in a less ductile response. However, in the current study, the only data for local fastener response is based on 1.2 mm CFS profile thickness. So, this same local fastener response was used in all numerical models, and only the cross sectional properties of the framing members was updated to reflect the increase in profile thickness. Therefore, the results explained above consider the effect of increasing the axial and flexural stiffness of framing members without any consideration on the beneficial effect of increased profile thickness on local fastener response.

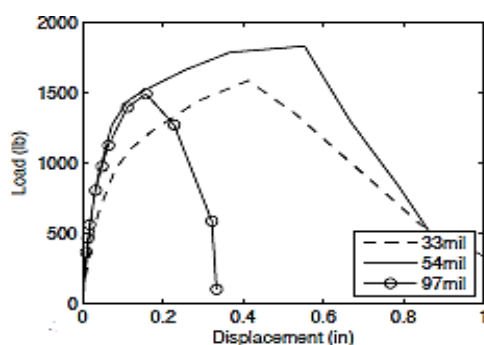


Figure 7.8 Effect of CFS thickness on fastener response (Peterman and Schafer, 2013)

7.5. Effect of Stud-Track Connection Rigidity

As explained in Section 6.2, rotational springs were defined at top corners in wall numerical model to represent the moment restraint at stud-track connections. These spring elements were assigned a relatively small stiffness value of 11.3 kN-m/rad based on the values reported by Bian et al. (2015). In order to reveal the influence of the stiffness present at stud-track connections, the wall numerical model was analyzed with idealized rigid and pinned stud-track connections. In order to simulate a rigid connection rotational stiffness of the spring was defined as 1000 kN-m/rad, while a stiffness value of 0.1 kN-m/rad was used for simulating the pinned condition. Analysis results are plotted in Figure 7.9 together with the results of wall model having 11.3 kN-m/rad rotational spring. As seen the spring stiffness value of 11.3 kN-m/rad used in the analyses presented in the previous sections is closer to the case of a pinned connection rather than a rigid connection. The effect of stud-track connection stiffness on overall response of the bare CFS frame is also presented in the same figure. The connection stiffness has a more profound effect on bare CFS frame response than the response of sheathed wall.

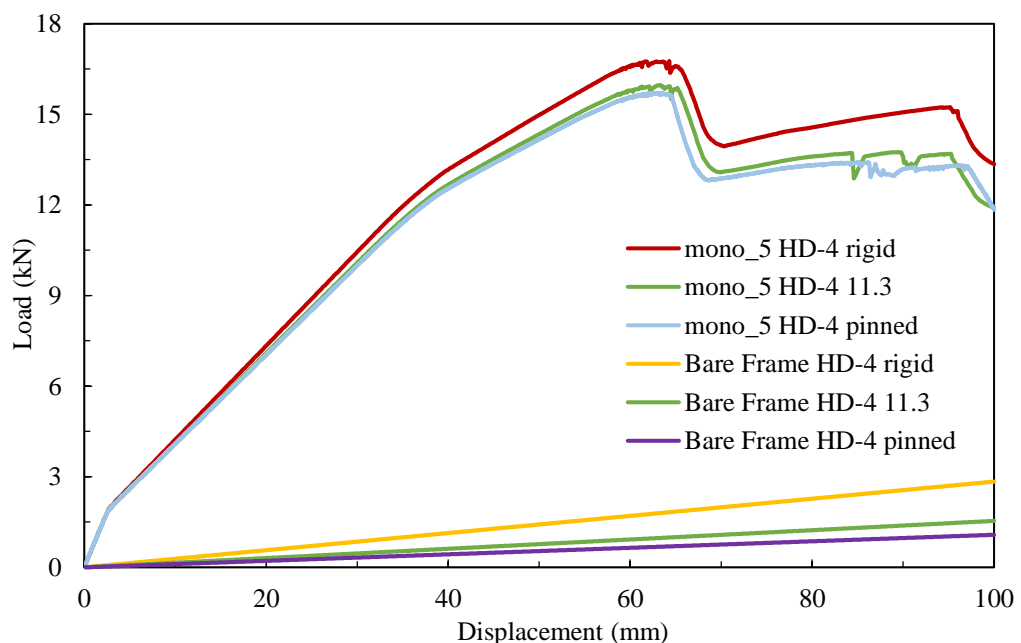


Figure 7.9 Load-displacement responses of wall models with various stud-track connections

7.6. Effect of Gravity Load Level

As mentioned earlier, 20 kN of vertical gravity loading was applied on some of the wall specimens tested as part of the wall testing program. In order to study the influence of the level of gravity loading on overall lateral response of wall panels, wall numerical models were analyzed with three different vertical load values of 20 kN, 40 kN and 100 kN. In these analyses the total gravity load was divided into two and applied on the two top corners of wall model.

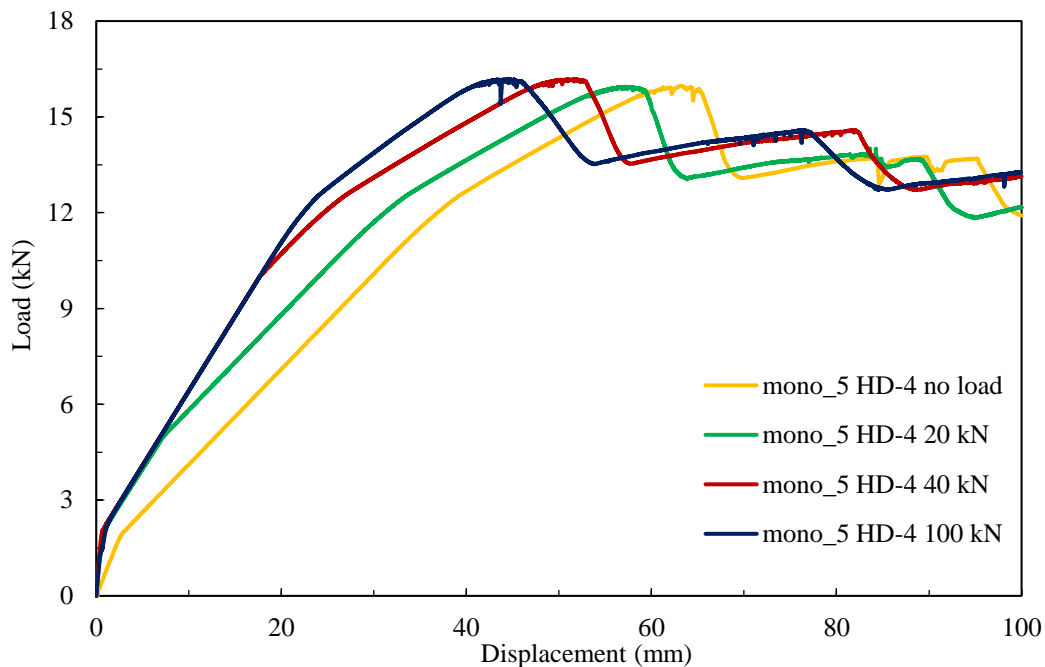


Figure 7.10 Load-displacement response of wall models applied various gravity load

Figure 7.10 shows load-displacement curves of wall models analyzed with vertical loads of 20 kN, 40 kN and 100 kN, as well as the base case of no vertical loading. Lateral stiffness of wall panels is observed to increase with increasing level of vertical gravity loading with no appreciable change in load capacity. The reason for the stiffness increase is because of the fact that the moment caused by gravity loading counteracts

the overturning effect of lateral loading when the wall undergoes rocking type of deformation. Minor increase in stiffness with the presence of gravity load was also observed in CFS shear wall experiments (Pehlivan et al., 2018).

It should be noted that CFS stud members in wall numerical models were defined as linear elastic elements. Therefore, the model is not able to consider deformation modes such as material yielding and buckling in stud members. When the level of gravity loading acting on wall panel gets high, the stud members are expected to suffer from local buckling failures. Therefore, the wall responses presented in Figure 7.10 are valid only for the range where no inelastic action occurs on stud elements in wall panels.

7.7. Effect of Modeling Approach of OSB Panels

For the numerical modeling, OSB sheathing panel was assumed as rigid diaphragm as explained in Section 6.1. In this section, applicability of rigid diaphragm assumption was evaluated. For this purpose, OSB sheathing was modeled by using ShellMITC4 element available in Opensees. Sheathing panel was divided into shell elements of 150 mm x 150 mm size (Figure 7.11). Since there is no out of plane deformation, Elastic Membrane Plate Section was defined to these shell elements. Shear modulus (G) was taken as 529 MPa which was the mean value of measurements from in-plane shear tests as presented in Section 5.4. Elasticity modulus value was calculated as 1270 MPa by using Equation 7.1 with a poisson's ratio of 0.2. The calculated elasticity modulus value was assigned to the shell elements.

$$E = 2G(1 + \nu) \quad [7.1]$$

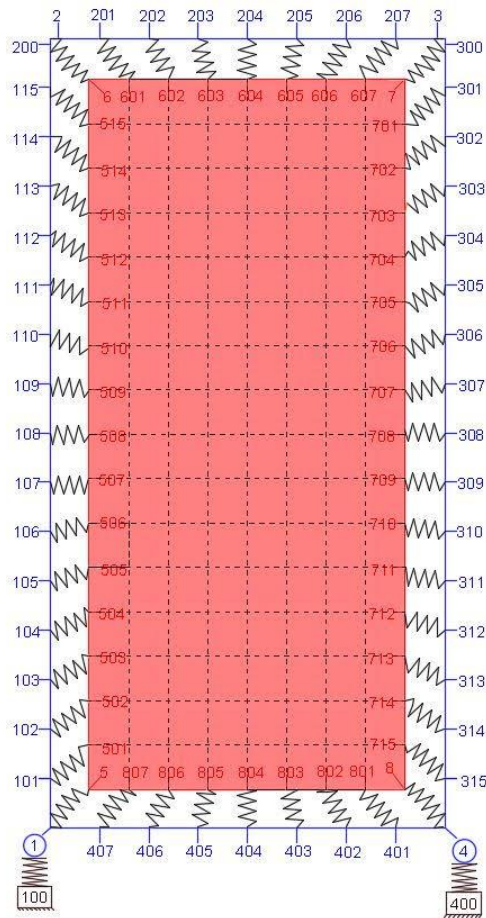


Figure 7.11 CFS shear wall model layout with shell elements for OSB sheathing

The same wall model was analyzed additionally by changing elasticity modulus to 130 MPa and 13,000 MPa in order to further analyze the influence of the in-plane stiffness of sheathing panels. These additional elasticity modulus values are ten times smaller and ten times larger than the value that belongs to the OSB sheathing panels used in wall panel test specimens.

Load-displacement results with three different OSB sheathing stiffness values are presented in Figure 7.12 together with the results obtained from a rigid diaphragm assumption. As it can be seen, wall model having OSB sheathing with 13,000 MPa elasticity modulus exhibited almost same response as the wall model with rigid

diaphragm approach. When elasticity modulus was reduced to 1300 MPa, which represents the in-plane stiffness possessed by the OSB sheathing panels used in wall panel test specimens, stiffness of wall panel was decreased slightly with no change in load capacity. Therefore, it can be said that rigid diaphragm assumption is applicable by neglecting this slight decrease in stiffness of wall panel. Wall model was also analyzed with a very flexible OSB sheathing having 130 MPa elasticity modulus. Although there is no change in capacity, stiffness of wall panel decreased dramatically for this case.

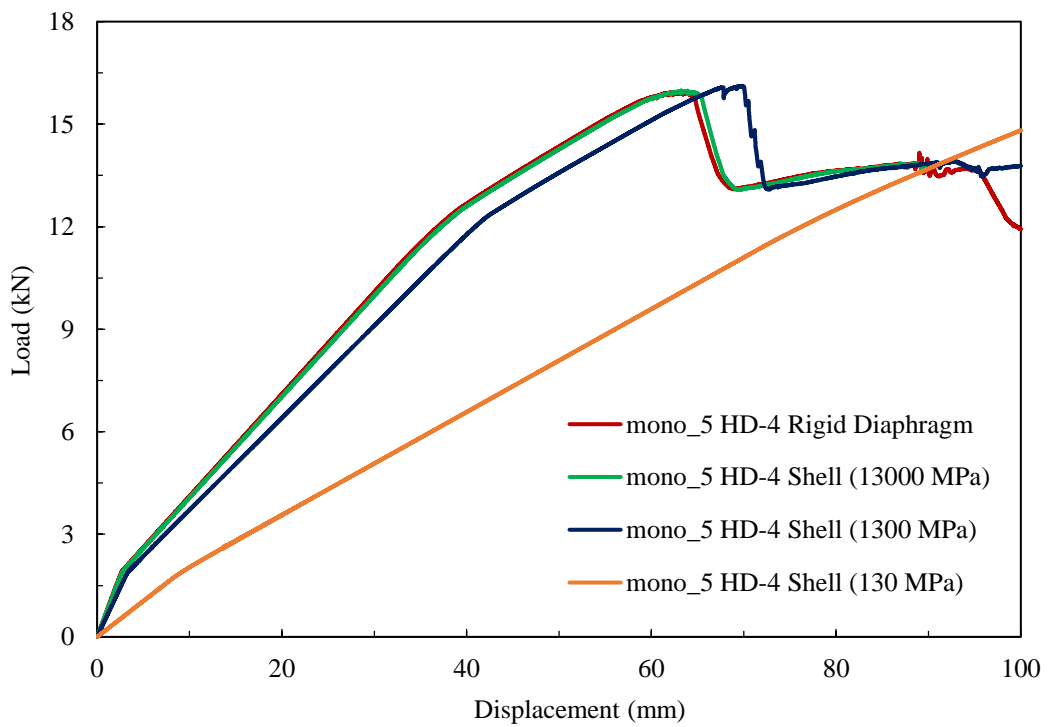


Figure 7.12 Load-displacement response of wall models having various OSB sheathing stiffnesses

CHAPTER 8

SEISMIC EVALUATION OF CFS SHEAR WALLS

8.1. Conceptual Background and Definitions

Up to recently seismic design codes and guidelines have specified force-based analysis rather than displacement-based analysis methods. Elastic behavior assumption is a generally accepted approach in force-based analysis. However, structural systems usually do not remain elastic under lateral loading and they undergo inelastic deformations. In other words, structures dissipate a considerable amount of energy by ductile behavior. In that case, a design based on elastic forces would not be realistic and economical. In order to incorporate nonlinear behavior into an elastic analysis, seismic force modification factor (R) is used. It can be simply defined as the ratio of the maximum elastic lateral force (V_e) to the design lateral force (V_d).

$$R = \frac{V_e}{V_d} \quad [8.1]$$

Seismic force modification is used to reduce the elastic response spectrum to the inelastic design spectrum. Seismic design codes propose appropriate R factors for different structural systems. Seismic response modification factor is expressed as a function of some structural parameters including ductility, over-strength, damping and redundancy. There are slight differences in the formulation of R factor among different design codes.

In this study, in order to evaluate seismic response of CFS shear walls, seismic force modification factors were calculated based on analysis results from wall numerical models. R factors were obtained by multiplying the ductility related force modification factor R_μ and overstrength related force modification factor R_Ω (Equation 8.2).

Relation between these factors and elastic demand, nominal strength and design strength is shown in Figure 8.1.

$$R = R_{\mu} \times R_{\Omega} \quad [8.2]$$

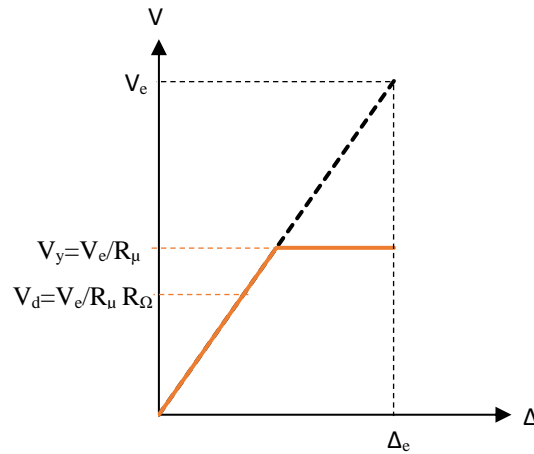


Figure 8.1 Determination of design force by using ductility and overstrength factors

The use of factored design loads, minimum code requirements, discrete member selection, neglected structural and non-structural members are the main causes of overstrength at local and global levels. In order to consider this capacity difference, R_{Ω} is incorporated in the seismic response modification factor. It can be expressed as a combination of various sources overstrength as follows (Boudreault, 2005):

$$R_{\Omega} = R_{size} \times R_{\phi} \times R_{yield} \times R_{sh} \times R_{mech} \quad [8.3]$$

R_{size} , R_{sh} and R_{mech} are overstrength factors due to standardized member sections, ability of materials to undergo strain hardening and yielding sequence in a structural system respectively. Overstrength provided due to these three effects are relatively minor, therefore the values of R_{size} , R_{sh} and R_{mech} were taken as 1.0 in this study. R_{ϕ} is

related with the overstrength due to difference between nominal and factored resistances. Considering that a resistance factor of 0.6 is specified in AISI 100-16 Standard for lateral design of OSB sheathed CFS shear wall systems, the R_ϕ was taken as $1/0.6=1.67$. R_{yield} reflects the fact that the actual strength is usually higher than the minimum specified yield strength. The values of R_{yield} were determined based on the load capacities determined from the wall numerical model by using Equation 8.4.

$$R_{yield} = \frac{P_{peak}}{P_{yield}} \quad [8.4]$$

Ductility ratio, μ is defined as the ratio of maximum displacement from nonlinear analysis Δ_u to the yield displacement Δ_y . Ductility related force modification factor R_μ depends on the natural period of the structure. Because of their light weight, cold-formed structures are likely to have short natural period and R_μ can be calculated with Equation 8.6. Similar studies conducted by Boudreault (2005) and Karabulut (2015) used the same approach for the calculation of R_μ .

$$\mu = \frac{\Delta_u}{\Delta_y} \quad [8.5]$$

$$R_\mu = \sqrt{2\mu - 1} \quad [8.6]$$

8.2. Idealization of Capacity Curve

Although yield force, P_{yield} , is the key part of the seismic response modification parameters, in majority of the cases the structural response lacks a well defined yield point. In these cases it is not easy to determine P_{yield} from a nonlinear load displacement curve. An idealized bilinear curve was utilized in this study in order to obtain P_{yield} and other essential seismic response parameters mentioned above.

Equivalent energy elastic plastic (EEEP) curve approach was adopted to obtain an idealized bilinear load-displacement response from the cyclic pushover curve of wall

models. EEEP curve can be obtained directly from monotonic wall model response. For the cyclic numerical models, firstly the cyclic backbone curve should be obtained as shown in Figure 8.2. From the cyclic backbone curve, P_{yield} value can be obtained easily by using Equation 8.7.

$$P_{yield} = \left(\Delta_u - \sqrt{\Delta_u^2 - \frac{2A}{K_e}} \right) \times K_e \quad [8.7]$$

where Δ_u is the maximum displacement reached from nonlinear analysis, A is the area under the cyclic backbone curve and K_e is the elastic stiffness. Elastic stiffness value is calculated considering the point where load is 40% percent of the peak load. Same stiffness value is used for the stiffness of first segment of EEEP curve. Figure 8.3 shows determination of EEEP curve based on the positive displacement segment of cyclic backbone curve of Wall Model 6. According to this approach, amount of absorbed energy is conserved. In other words, the areas under the cyclic backbone curve and idealized bilinear EEEP curve are equal.

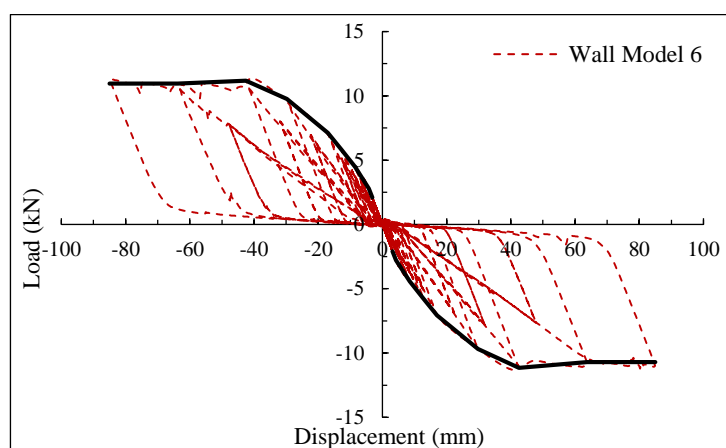


Figure 8.2 Backbone pushover curve of a cyclic model response

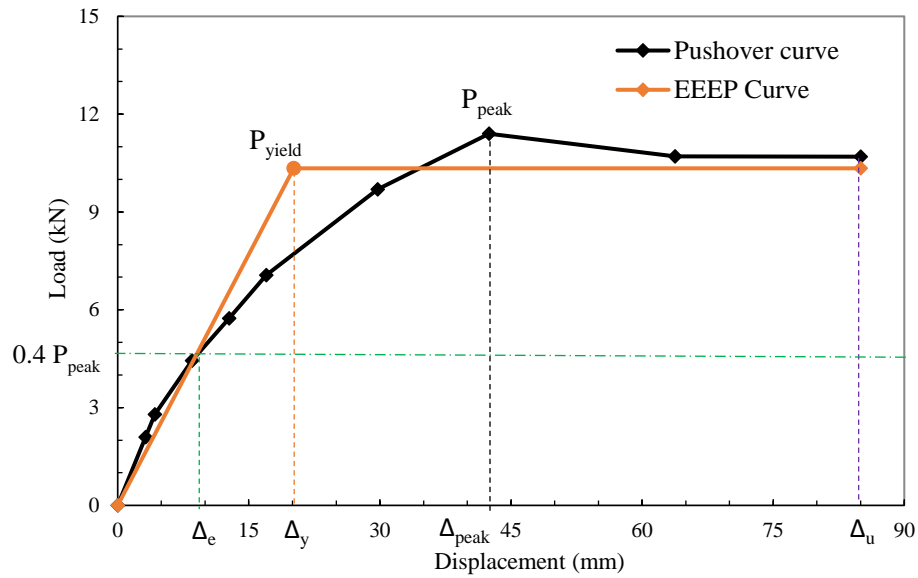


Figure 8.3 EEEP curve obtained from pushover curve of Wall Model 6

8.3. Determination of Seismic Response Modification Factor

EEEEP curves obtained based on the cyclic load-displacement hysteretic response from wall numerical models were used to determine the seismic response modification factors. Various response parameters determined this way are summarized in Table 8.1. As mentioned in the previous section ductility related force modification factor R_{μ} was determined with Equation 8.6 by using the maximum displacement Δ_u and yield displacement Δ_y determined from EEEP curve. Similarly, R_{yield} value was calculated with Equation 8.4 by using the experimentally determined P_{peak} and P_{yield} values. R_{yield} and R_{ϕ} values were then used to obtain the overstrength related force modification factor R_{Ω} . Finally, the overall seismic force modification factor R was determined as $R_{\mu} \times R_{\Omega}$.

Values presented in Table 8.1 show that walls having 50 mm fastener spacing usually have lower R_{μ} values compared to those having 150 mm fastener spacing. Table 8.2 presents the statistical properties for the calculated R , R_{μ} and R_{Ω} values. There is no significant change in R_{Ω} values among the investigated wall models. Average value is

found as 1.82 with the coefficient of variation of 7.1%. Mean of R_{μ} values is found as 2.83 with a greater coefficient of variation value of 16.5%.

Table 8.1 Response modification factors for wall models

Wall model	Size (cm)	Sheathing type	Fastener spacing (mm)	P_{peak} (kN)	P_{yield} (kN)	K_e (kN/mm)	R_{μ}	R_{yield}	R_{Ω}	R
3	122x244	Single	150	11.40	8.97	0.54	3.13	1.27	2.12	6.64
4	122x244	Single	150	11.43	10.43	0.77	3.27	1.09	1.82	5.95
6	122x244	Single	150	11.14	10.23	0.52	2.77	1.09	1.82	5.04
8	122x244	Single	50	30.80	29.11	0.89	2.27	1.06	1.77	4.02
10	122x244	Single	50	30.90	29.22	1.18	2.66	1.06	1.77	4.71
18	122x244	Double	50	58.46	54.49	1.54	2.09	1.07	1.79	3.73
24	244x244	Single	150	21.90	20.57	1.26	3.36	1.06	1.77	5.95
37	488x244	Single	150	36.69	36.21	1.93	3.10	1.01	1.69	5.23

Table 8.2 Statistical properties of response modification factors

	R_{μ}	R_{Ω}	R
Mean	2.83	1.82	5.16
Standard Deviation	0.47	0.13	1.0
Coefficient of Var. (%)	16.5	7.1	19.4

Within the scope of a similar study conducted by Boudreault (2005), modification factors were calculated based on a series of OSB sheathed CFS shear wall experiments. In that study, average R_{μ} and R_{Ω} values were reported to be 2.93 and 1.83, respectively. These values are in close agreement with the mean R_{μ} and R_{Ω} values of 2.83 and 1.82 determined in the current study. A comparison of the seismic force modification factor determined in this study with the values provided by various building codes for seismic force resisting systems comprised of OSB sheathed CFS shear walls is presented in Table 8.3. R factors provided in the North American

building codes are slightly different from each other and they are consistently higher than the value computed in this study. On the other hand, the R value provided in the latest Turkish Earthquake Building Code is even lower than the value computed in this study. It should be noted that the R factor calculation was based on only a CFS shear wall in this study while building codes propose R factors for a structural system. Although shear walls are the main energy dissipating elements under lateral loads, contribution of other structural members on the overall seismic behavior can't be neglected. Therefore, a direct comparison of R values between the building codes and this study is questionable.

Table 8.3 R factor values proposed by different building codes

	This study	ASCE 7-10	UBC 1997	NBCC 2005	TEBC 2018
R	5.16	6.5	5.5	5.4	4

CHAPTER 9

CONCLUSION

In this study, a fastener-based numerical model was developed to predict the lateral load response of shear walls that are framed by CFS profiles and sheathed with OSB panels. OpenSees platform was used for numerical modeling. A special hysteretic material model, Pinching4, capable of softening, strength degradation, and cyclic pinching was utilized for modeling of fasteners providing the connection between CFS framing members and OSB sheathing panel. In order to define parameters of this hysteretic model, a series of monotonic and cyclic loading tests were conducted on OSB-to-CFS screw connections.

Additionally, a complementary test program was conducted on OSB specimens to determine the in-plane shear strength and shear modulus. It was seen that there is a high level of variation in both shear strength and shear modulus values among specimens due to inherent nature of wood material. Experimentally determined shear properties were compared with the values available in the literature in an attempt to assess how close the locally available OSB panels represent the material utilized in international studies.

Cyclic hysteresis responses of wall panels predicted by numerical models are in a good agreement with the experimentally measured wall response in terms of strength, stiffness, and pinching characteristics. Wall numerical model verified with experimental results was then used for a parametric study in order to understand the influence of various parameters such as local fastener behavior, fastener spacing, rigidity of stud-track connection, stiffness of CFS framing members, stiffness of hold-down members and the level of gravity loading on overall wall response. These

analyses were conducted under monotonic loading in order to avoid the additional complexity associated with reversed cyclic loading.

Numerical modeling with fastener-based approach was found adequate for this type of structures. Modeling assumptions such as rigid diaphragm for OSB sheathing and linear elastic material for CFS frame elements gave satisfactory results. It is worth to note that the numerical models used in the study do not consider material yielding and buckling failure modes of CFS members. For this reason, use of the developed numerical model wouldn't be appropriate for walls under excessive gravity loading, where the response is expected to be governed by inelastic deformation of wall studs.

In order to evaluate seismic performance of wall panels, seismic force modification (R) factors were calculated by using the bilinear force-displacement responses determined following the Equivalent Energy Elastic-Plastic (EEEP) approach. Mean values of the ductility related force modification factor (R_{μ}) and overstrength related force modification factor (R_{Ω}) were determined respectively as 2.83 and 1.82, producing a seismic force modification factor of 5.16. The seismic force modification factor that was determined for the OSB sheathed CFS shear walls analyzed as part of this study is in general agreement with the values provided by various building codes for seismic force resisting systems comprised of OSB sheathed CFS shear walls.

REFERENCES

American Iron and Steel Institute (2016). Specification for the Design of Cold Formed Steel Structural members. *Washington DC, USA*

American Society for Testing and Materials (ASTM) D1037 (1999). Standard Test Method for Evaluating Properties of Wood-Base Fiber and Particle Panel Materials. *West Conshohocken, PA, USA*

American Society of Civil Engineers (2010). Minimum Design Loads for Buildings and Other Structures.

Bian, G., Buonopane, S.G., Ngo, H.H., & Schafer, B.W. (2014). Fastener-Based Computational Models with Application to Cold-Formed Steel Shear Walls. *International Specialty Conference on Cold-Formed Steel Structures*.

Bian, G., Padilla-Llano, D.A., Leng, J., Buonopane, S.G., Moen, C.D., & Schafer, B.W. (2015). Opensees Modeling of Cold-Formed Steel Framed Wall System. *International Conference on Behavior of Steel Structures in Seismic Areas*

Bian, G., Padilla-Llano, D.A., Buonopane, S.G., Moen, C.D., & Schafer, B.W. (2015). OpenSees modeling of wood sheathed cold-formed steel framed shear walls. *Proceedings of the Annual Stability Conference Structural Stability Research Council Nashville, Tennessee, March 24-27, 2015*.

Bouc, R. (1967). Forced Vibrations of a Mechanical System with Hysteresis. In *Proceedings of the 4th Conference on Non-linear Oscillations* (pp. 315–321).

Boudreault, F. (2005). *Seismic analysis of steel frame / wood panel shear walls*. M.Sc. Thesis, McGill University.

Buonopane, S.G., Tun, T., & Schafer, B.W. (2014). Fastener-based computational models for prediction of seismic behavior of CFS shear walls. *Proceedings of the 10th National Conference in Earthquake Engineering*, Earthquake Engineering Research Institute, Anchorage, AK, 2014.

Buonopane, S., Bian, G., Tun, T., & Schafer, B. (2015). Computationally efficient fastener-based models of cold-formed steel shear walls with wood sheathing. *Journal of Constructional Steel Research*, 110, 137-148. doi:10.1016/j.jcsr.2015.03.008

Chui, Y. H., Ni, C., & Jiang, L. (1998). Finite-Element Model for Nailed Wood Joints under Reversed Cyclic Load. *Journal of Structural Engineering*, 124(1), 96-103. doi:10.1061/(asce)0733-9445(1998)124:1(96)

Della Corte, G., Fiorino, L., & Landolfo, R. (2006). Seismic Behavior of Sheathed Cold-Formed Structures: Numerical Study. *Journal of Structural Engineering*, 132(4), 558-569. doi:10.1061/(asce)0733-9445(2006)132:4(558)

- Dolan, J. D. (1989). *The Dynamic Responses of Timber Shear Walls*. Ph.D. Thesis, The University of British Columbia
- Dubina, D. (2008). Behavior and performance of cold-formed steel-framed houses under seismic action. *Journal of Constructional Steel Research*, 64(7-8), 896–913. doi: 10.1016/j.jcsr.2008.01.029
- Fiorino, L., Corte, G. D., & Landolfo, R. (2007). Experimental tests on typical screw connections for cold-formed steel housing. *Engineering Structures*, 29(8), 1761-1773. doi:10.1016/j.engstruct.2006.09.006
- Fiorino, L., Iuorio, O., & Landolfo, R. (2008). Experimental response of connections between cold-formed steel profile and cement-based panel. *International Specialty Conference on Cold-Formed Steel Structures*.
- Foliente, G. C. (1995). Hysteresis Modeling of Wood Joints and Structural Systems. *Journal of Structural Engineering*, 121(6), 1013-1022. doi:10.1061/(asce)0733-9445(1995)121:6(1013)
- Folz, B., & Filiatrault, A. (2001). Cyclic Analysis of Wood Shear Walls. *Journal of Structural Engineering*, 127(4), 433–441. doi: 10.1061/(asce)0733-9445(2001)127:4(433)
- Fulop, L., & Dubina, D. (2002). Seismic Performance of Wall-stud Shear Walls. In *Proceedings of the Sixteenth Specialty Conference on Cold-Formed Steel Structures* (pp. 483–500).
- Fülöp, L., & Dubina, D. (2004). Performance of wall-stud cold-formed shear panels under monotonic and cyclic loading. *Thin-Walled Structures*, 42(2), 339-349. doi:10.1016/s0263-8231(03)00064-8
- Fülöp, L., & Dubina, D. (2004). Performance of wall-stud cold-formed shear panels under monotonic and cyclic loading Part II: Numerical modelling and performance analysis. *Thin-Walled Structures*, 42(2), 339-349. doi:10.1016/s0263-8231(03)00063-6
- Gao, W., & Xiao, Y. (2017). Seismic behavior of cold-formed steel frame shear walls sheathed with ply-bamboo panels. *Journal of Constructional Steel Research*, 132, 217-229. doi:10.1016/j.jcsr.2017.01.020
- Henriques, J., Rosa, N., Gervasio, H., Santos, P., & Silva, L. S. (2017). Structural performance of light steel framing panels using screw connections subjected to lateral loading. *Thin-Walled Structures*, 121, 67-88. doi:10.1016/j.tws.2017.09.024
- Iuorio, O., Fiorino, L., & Landolfo, R. (2014). Testing CFS structures: The new school BFS in Naples. *Thin-Walled Structures*, 84, 275–288. doi: 10.1016/j.tws.2014.06.006

- Kim, T., Wilcoski, J., & Foutch, D. A. (2007). Analysis of Measured and Calculated Response of a Cold-formed Steel Shear Panel Structure. *Journal of Earthquake Engineering*, *11*(1), 67-85. doi:10.1080/13632460601031862
- Krawinkler, H., Parisi, F., Ibarra, L., Ayoub, A., & Medina, R. (2000). Development of a testing protocol for woodframe structures. Report W-02 covering task 1.3.2, CUREE/Caltech woodframe project.
- Landolfo, R., Fiorino, L., & Corte, G. D. (2006). Seismic Behavior of Sheathed Cold-Formed Structures: Physical Tests. *Journal of Structural Engineering*, *132*(4), 570-581. doi:10.1061/(asce)0733-9445(2006)132:4(570)
- Lee, M., & Foutch, D. A. (2010). Performance evaluation of cold-formed steel braced frames designed under current U.S. seismic design code. *International Journal of Steel Structures*, *10*(3), 305-316. doi:10.1007/bf03215839
- Leng, J., Schafer, B.W., & Buonopane, S.G. (2012). Seismic Computational Analysis of CFS-NEES Building. *International Specialty Conference on Cold-Formed Steel Structures*.
- Leng, J., Schafer, B.W., & Buonopane, S.G. (2013). Modeling the seismic response of cold-formed steel framed buildings: model development for the CFS-NEES building. *Proceedings of the Annual Stability Conference Structural Stability Research Council St. Louis, Missouri, April 16-20, 2013*.
- Leng, J. (2015). *Simulation of Cold-Formed Steel Structures*. Ph.D. Thesis, Johns Hopkins University
- Leng, J., Peterman, K. D., Bian, G., Buonopane, S. G., & Schafer, B. W. (2017). Modeling seismic response of a full-scale cold-formed steel-framed building. *Engineering Structures*, *153*, 146-165. doi:10.1016/j.engstruct.2017.10.008
- Liu, P., Peterman, K., & Schafer, B. (2014). Impact of construction details on OSB-sheathed cold-formed steel framed shear walls. *Journal of Constructional Steel Research*, *101*, 114-123. doi:10.1016/j.jcsr.2014.05.003
- Mccutcheon, W. J. (1985). Racking Deformations in Wood Shear Walls. *Journal of Structural Engineering*, *111*(2), 257-269. doi:10.1061/(asce)0733-9445(1985)111:2(257)
- McKenna, F., Fenves, G. L., Scott, M. H., & Jeremić, B. (2000). Open system for earthquake engineering simulation (<http://opensees.berkeley.edu>).
- Miller, T. H., & Pekoz, T. (1994). Behavior of Gypsum-Sheathed Cold-Formed Steel Wall Studs. *Journal of Structural Engineering*, *120*(5), 1644-1650. doi:10.1061/(asce)0733-9445(1994)120:5(1644)

NRCC National Research Council of Canada (2004). National Building Code of Canada 2005 (NBCC). *Institute for Research in Construction, Ottawa, Ontario, Canada*

Padilla-Llano, D.A. (2015). *A Framework for Cyclic Simulation of Thin-Walled Cold-Formed Steel Members in Structural Systems*. Ph.D. Thesis, Virginia Polytechnic Institute and State University.

Pehlivan, B. M., Baran, E., & Topkaya, C. (2018). Testing and analysis of different hold down devices for CFS construction. *Journal of Constructional Steel Research*, 145, 97-115. doi:10.1016/j.jcsr.2018.02.007

Peterman, K.D., & Schafer, B.W. (2013). Hysteretic shear response of fasteners connecting sheathing to cold-formed steel studs. Research report, CFS-NEES, RR04.

Salenikovich, A. J. (2000). *The racking performance of light-frame shear walls*. Ph.D. Thesis, Virginia Polytechnic Institute and State University.

Schafer, B., Ayhan, D., Leng, J., Liu, P., Padilla-Llano, D., Peterman, K., Yu, C. (2016). Seismic Response and Engineering of Cold-formed Steel Framed Buildings. *Structures*, 8, 197–212. doi: 10.1016/j.istruc.2016.05.009

Shamim, I., & Rogers, C.A. (2012). Numerical Modelling and Calibration of CFS Framed Shear Walls under Dynamic Loading. *International Specialty Conference on Cold-Formed Steel Structures*.

Shamim, I. (2012). *Seismic Design of Lateral Force Resisting Cold-Formed Steel Framed (CFS) Structures*. Ph.D. Thesis, McGill University.

Shamim, I., Dabreo, J., & Rogers, C. A. (2013). Dynamic Testing of Single- and Double-Story Steel-Sheathed Cold-Formed Steel-Framed Shear Walls. *Journal of Structural Engineering*, 139(5), 807–817. doi: 10.1061/(asce)st.1943-541x.0000594

Stewart, W. G. (1987). *The Seismic Design of Plywood Sheathed Shear Walls*. Ph.D. Thesis, University of Canterbury.

Okasha, A. F. (2004). *Performance of Steel Frame / Wood Sheathing Screw Connections Subjected to Monotonic and Cyclic Loading*. M.Sc. thesis, McGill University.

Tun, T. H. (2014). *Fastener-Based Computational Models of Cold-Formed Steel Shear Walls*. M.Sc. thesis, Bucknell University.

Tuomi, R. L., & McCutcheon, W. J. (1978). Racking Strength of Light-Frame Nailed Walls. *Journal of the Structural Division*, 104(7), 1131–1140.

Turkish Building Earthquake Code (2018). *Ankara, Turkey*

Uniform Building Code UBC (1997). *California, USA*

Usefi, N., Sharafi, P., & Ronagh, H. (2019). Numerical models for lateral behaviour analysis of cold-formed steel framed walls: State of the art, evaluation and challenges. *Thin-Walled Structures*, 138, 252-285. doi:10.1016/j.tws.2019.02.019

Vieira, L.C.M., & Schafer, B.W. (2009). Experimental Results for Translational Stiffness of Stud-to- Sheathing Assemblies. AISI-COFS Supplemental Report.